University of Alberta

Prediction of Rainfall Runoff for Soil Cover Modelling

by

Sarah Kristine Jubinville

A thesis submitted to the Faculty of Graduate Studies and Research
in partial fulfillment of the requirements for the degree of

Master of Science
in
Geotechnical Engineering

Department of Civil and Environmental Engineering

Spring 2013
Edmonton, Alberta

ABSTRACT

Surface runoff can be the largest component of the surface water budget that controls the quantity of precipitation that could infiltrate through a soil cover into underlying waste material. Site-specific models are routinely used to predict infiltration; however, the direct measurement of runoff that is required to properly calibrate the model is almost never performed. To date, there does not appear to be a proven reliable procedure for predicting surface runoff based on measurable properties at the soil surface.

This thesis presents a field and laboratory program to characterize the hydraulic properties of a compacted waste rock and overburden soil cover at the Savage River Mine in Australia. A physically based one-dimensional model was developed for predicting surface runoff using the measured rainfall intensity and surface saturated hydraulic conductivity. Runoff predictions from the proposed Savage River Runoff Model (SRR Model) and the SoilCover computer model are compared to measured runoff quantities. Both models are shown to be sensitive to the resolution of the rainfall data used as input. Runoff predictions from both models were also found to vary considerably within the natural variability of surface saturated hydraulic conductivity. In summary, it was concluded that both models are capable of predicting surface runoff volumes within 4%, provided engineering judgment is used when inputting rainfall and measured soil properties.

ACKNOWLEDGEMENTS

I am incredibly grateful to a number of individuals who have encouraged and supported me throughout this program.

I am exceedingly thankful to my supervisor, Dr. Ward Wilson. He was and is a constant inspiration to me, and I never once left his office without feeling like I could tackle anything that came my way. I am grateful for his limitless energy and enthusiasm for life, family, and academics, and I only hope I can infuse the same in my own life and the lives those around me. I would also like to thank my mentor and friend, Dr. Kevin Biggar, for his confidence, encouragement, and advice that led me to pursue this graduate degree in the first place.

The support provided by Bruce Hutchison and the staff at the Savage River Mine was crucial to the success of this project. Extra thanks to Matt Phillips and Todd Hodgsen for their on-site support, the ongoing data supply, and for their time and effort in setting up the Old Tailings Dam. A special thanks again to Bruce Hutchison and his wife, Susie, for their generous hospitality in my final evening in Tasmania.

Thank you to Louis Kabwe and Christine Hereygers at the University of Alberta for their help in organizing my field supplies and ongoing assistance during the laboratory program.

I extend an enormous thank you to my Mom and Brian, and my Dad, for their love and guidance. I would be lost without their unwavering support and encouragement these last two years. Thank you to my brother and sister, Tom and Sydney, for the love and laughs along the way. To my friends, I truly appreciate your support and understanding both of when I needed a break and when I needed to buckle down.

Finally, but most importantly, I thank my husband, Rob. I cannot adequately express my appreciation for all the support that you have provided these last two years. You are my everything and I could not have completed this thesis without your constant encouragement, love, and understanding. Thank you.

TABLE OF CONTENTS

LIST OF TABLES

LIST OF FIGURES

Chapter 1. INTRODUCTION

1.1 General

Soil covers are used to protect receiving environments from the products stored in mine waste repositories and landfills. The design of an engineered soil cover is often governed by the net infiltration of water. Any water that infiltrates through the soil cover is generally the quantity of water that will percolate into the underlying waste and cause long term liabilities such as acid rock drainage (ARD), heavy metal leaching, and poor quality seepage that must be treated. Surface runoff can be the largest component that immediately controls the quantity of precipitation that may produce infiltration.

Little attention has been given to the prediction of runoff under different climatic conditions, rainfall intensities, storm events, surface characteristics, soil types, slopes and topographies, and vegetation. Conversely, the prediction of infiltration for cover systems is a topic of abundant research and the mechanisms governing infiltration are well understood. However, infiltration models are typically site specific and often depend upon direct measurements of the quantity of runoff. Generally, it would be useful if a simple test procedure could be performed on a soil cover that would provide accurate runoff predictions and thus more reliable estimates of infiltration provided to the soil cover model.

1.2 Background

The Savage River Mine is an open-cut magnetite mine situated in north-western Tasmania, Australia, approximately 100 km south west of Burnie. It is located at 100-350 m elevation in rugged and mountainous terrain that is densely covered in rain forest. The climate is cool with high and consistent annual rainfall (Grange Resources 2012a).

The mine and processing plant are currently owned (90%) and operated by Grange Resources Ltd. Approximately 15.6 million bulk cubic meters (BCM) of ore and waste was mined in 2011, which produced 1.98 million tonnes of magnetite pellets (Grange Resources 2012c).

Savage River Mine was acquired from the original leaseholders and operators in 1997 by Australian Bulk Minerals. An agreement with the Tasmanian government limited the liability of remediation of contamination to that caused by the company's operations. Thus, contamination caused by previous operators is not the legal responsibility of current operators. However, Grange Resources operates at "Best Practice Environmental Management" and has integrated its efforts with the government's Savage River Rehabilitation Programme (SRRP). (Grange Resources 2012b).

The SRRP is a jointly managed initiative between the Tasmanian government and Grange Resources, which focuses on rehabilitating the historic ARD problem from the waste rock and tailings stored at the Savage River Mine. The design and construction of a water-shedding cover for a waste rock dump, called B-Dump, and the investigation of options to address the long term management of acid drainage from the Old Tailings Dam (OTD) are projects that are part of the SRRP.

1.3 Scope and Objectives

The general objective of this thesis was to develop a rational approach and conceptual model for predicting runoff using real-time rainfall intensities and measureable soil properties. A field and laboratory investigation was completed as part of this research, and a one-dimensional computer model was developed to predict runoff based on the measured soil properties and real-time rainfall intensities.

The field testing and sampling program was conducted at the Savage River Mine. The field program and subsequent laboratory testing characterized the surficial hydraulic properties of the water-shedding soil cover on B-Dump and the exposed tailings at the OTD. Rainfall-runoff data recorded at site was used in conjunction with the material properties of the soil cover on B-Dump to develop and propose a one-dimensional model for runoff prediction. Runoff was also predicted using the SoilCover computer model (Unsaturated Soils Group 2000), which is a common program used in the industry. The predictions from both the proposed Savage River Runoff Model (SRR Model) and SoilCover were then compared to measured runoff quantities from the B-Dump location.

The parameters obtained from the OTD characterization were then input into the proposed and SoilCover models and the rainfall-runoff response of the tailings was examined. Corresponding rainfall-runoff measurements were not available for comparison to OTD runoff predictions; however, the results of the B-Dump analyses were used to establish a reasonable estimate of actual OTD runoff.

The specific goals of the research were as follows:

1. Design and complete a field and laboratory investigation to characterize the hydraulic properties of the materials comprising the B-Dump water-shedding soil cover and the exposed OTD tailings at the Savage River Mine.

2. Propose and develop a computer model that is rational and physically consistent with runoff mechanisms that will predict runoff based on only rainfall intensity and simple soil properties as input. Then, compare runoff predictions to the measured runoff quanitites.

3. Predict runoff using the industry accepted SoilCover software and compare results to measured runoff quantities and to the predictions from the proposed SRR Model.

4. Provide objective discussion for the comparison between the modelled scenarios, predictions, and measured rainfall-runoff response, including:
    a. The impact of the resolution of rainfall data input in the models on prediction accuracy.
    b. The variation of runoff predicted within the natural variability of the saturated hydraulic conductivity of the soil cover surface.
    c. The limitations of one-dimensional modelling in representing the four dimensional (X, Y, Z, time) runoff process and the use of engineering judgement when selecting model input parameters.

1.4 Thesis Outline

This thesis is comprised of six chapters. The research is introduced in Chapter One and includes a description of the general site background, the scope and objectives of the research, and the overall outline of this thesis. Chapter Two provides a review of the literature pertinent to this research. In particular, the mechanisms of rainfall-runoff and the challenges associated with runoff prediction are discussed; recent research supporting the development of this thesis is presented; and detailed site background is provided, including previous research completed. The scope and methods of the field and laboratory program are described in detail in Chapter Three. Chapter Four presents a summary of the results of the field and laboratory investigation. Chapter Five presents the rainfall-runoff analyses completed in this research. Chapter Five also includes a detailed discussion of the basis and development of the proposed SRR Model; a summary of the input required and used in the SoilCover model; then presents and discusses the runoff predictions resulting from the models. Finally, Chapter Six offers the research conclusions and provides recommendations for further study.

Chapter 2. LITERATURE REVIEW AND BACKGROUND INFORMATION

2.1 Introduction

The following section describes the engineering applications of soil covers, the types of soil covers, and their design objectives. Important factors that must be considered through the design, construction, and operation phases of the soil covers are also discussed.

2.1.1 Soil Cover Types and Design Objectives

Soil covers are used to protect receiving environments from the products stored in mine waste repositories and landfills. O'Kane and Wels (2003) and the GARD Guide (The International Network for Acid Prevention (INAP) 2009) provide excellent overviews of the types of soil covers and the factors to be considered in their design. The type and design objective of each soil cover will vary according to the properties of the waste being stored, the climate, the materials available for constructing the cover, and ultimate target landscape for closure of the facility. The objectives of a particular cover system often fall under one or more of the following categories:

- Dust and erosion control,
- Chemical stabilization of acid-forming mine waste, through control of oxygen ingress,
- Contaminant release control, through control of water infiltration, and
- Provide a growth medium for vegetation.

Two basic types of cover systems can be used to satisfy these criteria:

- Barrier covers, and
- Store and release covers.

Soil barrier covers are typically low in hydraulic conductivity to limit both oxygen diffusion and water infiltration into underlying waste. Barrier covers are designed to remain above 85% saturation, and thus inhibit oxygen diffusion and acid generation in the waste material. These covers also limit the seepage load from the waste that must be treated prior to release into the environment, if the waste is potentially acid forming. An important design consideration for low hydraulic conductivity covers is the climate. For example, an oxygen limiting saturated barrier theoretically works for an environment with greater precipitation than evapotranspiration; however, if the climate is characterized by a wet season followed by an extended dry season, it may not be possible to maintain high saturation, and a different cover type would be more appropriate. Other design considerations include system layering and availability of materials, long term erosion, weathering, and evolution of the cover and those impacts on performance.

Store and release systems are also referred to as evapotranspiration covers and water balance systems. These covers are designed to reduce water infiltration in climates where saturation cannot be maintained. These covers function by accepting and storing water from precipitation in wet periods, then releasing the stored water by evapotranspiration during dry periods. Store and release covers can achieve water infiltration values approaching zero but do not prevent oxygen ingress. A primary consideration is the establishment of sustainable vegetation, which is a critical component for adequate performance of store and release covers.

2.2 Rainfall Runoff

The following sections: 1) describe the basic mechanisms governing rainfall runoff, 2) summarize the principles of predicting runoff, 3) illustrate the variability of runoff observed and measured in the field, and 4) discuss sensitivities and calibration of models that simulate field response.

2.2.1 Runoff Mechanisms

Three primary mechanisms describing the generation of surface runoff are used. The first is known as Hortonian Overland Flow, after Horton (1933), and is called infiltration-excess runoff. The second is Saturation Overland Flow, and is called saturation-excess runoff after Dunne and Black (1970). The third is lateral Subsurface Flow, after Hursh (1944) and Hewlett and Hibbert (1967). A single mechanism or a combination of these mechanisms may occur for a particular soil type and rainfall event, and together are termed "direct runoff" (USDA 2004).

The maximum rate at which a soil can absorb precipitation as it falls is defined by Horton (1933) as the "infiltration capacity". He proposed that the infiltration-capacity is controlled chiefly by conditions at and close to the soil surface, as opposed to being governed by the moisture conditions within the soil mass (Horton 1940). The infiltration capacity function describes the exponential decay of the rate of rain infiltration into a soil with time down to a minimum non-zero infiltration capacity for a particular rainfall event and soil combination.

The rain intensity at the beginning of a rainfall event is typically less than the infiltration capacity. Horton (1933, 1940) states that all the rainfall is absorbed by the soil at this time and no runoff or surface detention occurs. Infiltration capacity begins to decrease and, eventually, the infiltration capacity decreases to the point where it is less than the rainfall intensity. Surface depressions begin to fill but no runoff is yet generated. Runoff is only generated once the rainfall intensity exceeds the infiltration capacity and all surface depressions are filled. Figure 2-1a) illustrates this runoff mechanism.

Near the end of a storm event, the intensity of rainfall typically decreases to a rate that is once again lower than the infiltration capacity. After this time, portions of the remaining rainfall and water retained in the surface depressions will run off and portions begin to infiltrate into the soil profile. Neither portion contributes significantly to the total rainfall runoff volume or the total water infiltration volume. Therefore, Horton (1940) proposed that the total surface runoff volume is not greatly different from the total rain volume that fell at intensities in excess of the infiltration capacity.

Dunne and Black (1970) investigated soils having infiltration capacities well in excess of rainfall intensity. They found that Hortonian Overland Flow did not occur on their research catchment; however, another type of runoff made a significant contribution to the storm flow measured in their experiment. Similar to Hortonian Overland Flow, the runoff was sensitive to changes in rainfall intensity and storm duration. The runoff observed by Dunne and Black (1970) was generated by direct precipitation onto areas where the water table reached the ground surface or within areas that were already saturated. Therefore, this type of runoff is called saturation-excess runoff, and is shown in Figure 2-1b). Rain falling at intensities in excess of the field saturated hydraulic conductivity of the soil will produce runoff once the storage capacity and surface depressions of the soil are filled.

Subsurface flow is characterized by shallow penetration into a porous soil horizon, followed by rapid lateral flow with the slope toward natural outlets, such as streams or depressions, during the runoff period (Hursh 1944, Hewlett and Hibbert 1967). The percolated rain water may encounter an impermeable layer or the water table at a certain depth. This water then flows within the slope and contributes a somewhat delayed yet marked increase in the runoff hydrograph measured for the storm (Hewlett and Hibbert 1967, Weyman 1970). The processes where percolated water encounters the water table or a less permeable layer are illustrated in Figure 2-1c) and d), respectively.

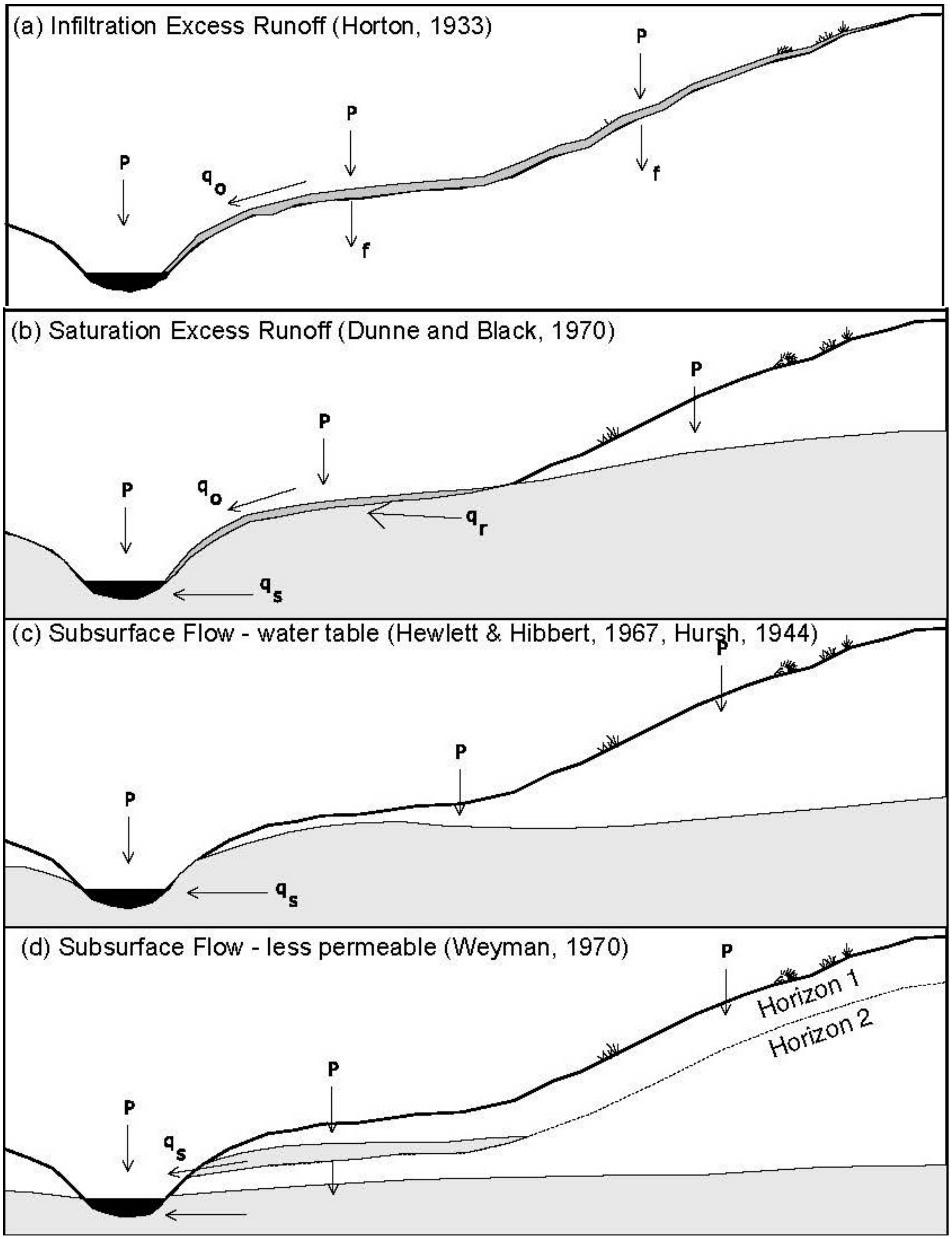

Figure 2-1: Schematic of runoff mechanisms – adapted from Beven (2012)

2.2.2 Methods of Runoff Prediction

The rainfall-runoff relationship has been widely studied at scales ranging from the point scale; to the field, plot, and hillslope scale; and to the watershed scale. Empirical models (Horton 1940) and conceptual models (Philip 1957, Mein and

Larson 1973) are derived for point scale infiltration. The SCS Curve Number (USDA 2004) and the unit hydrograph (Sherman 1932) are common methods of predicting runoff at the watershed scale. Accepted methodologies for the rainfall runoff process at the field or hillslope scale are rare, since the field scale appears to be a transition area between the highly non-linear infiltration at the point scale and the potentially linear representation of runoff at the watershed scale (Stone et al. 1996). The significant influence of spatial and temporal variability in the characteristics controlling rainfall runoff response, such as hydraulic properties of the soil, vegetation, topography, and rainfall variability (Yin 2008, Sajid 2009) is attributed to the lack of predictive methods at the field/hillslope scale (Stone et al. 1996).

Many runoff predictions deal with classifying the watershed or hillslope by measuring some portion of its response to rainfall, then applying this index to climate models and historic rainfall events to predict runoff in the future. Swanson et al. (2003) describes several soil-atmosphere coupling models that all agree that model calibration significantly improves the accuracy of predicted compared to measured values. However, the need for uncalibrated rainfall runoff models has been widely identified, for example Schmocker-Fackel et al. (2007).

2.2.3 Observed Runoff Variation

Large differences in hillslope hydrology may not be apparent upon visual inspection of the slope surfaces, and may only become apparent during rainfall events or simulations (Scherrer et al. 2007). Beven (2012) suggests that there may still be much to learn from direct observations of runoff processes in a location of interest. Current hydrological models are all very similar, but most do not incorporate the processes and flows that have been observed in the field (Weiler 2011). Process decision schemes, as shown in Figure 2-2, have been developed for determining the dominant runoff process based on the characteristics of the soil profile (Scherrer and Naef 2003, Schmocker-Fackel et al. 2007). The dominant runoff mechanism may be classified by observing the response of the slope to rainfall (Scherrer et al. 2007), such that an appropriate method of runoff prediction may be selected.

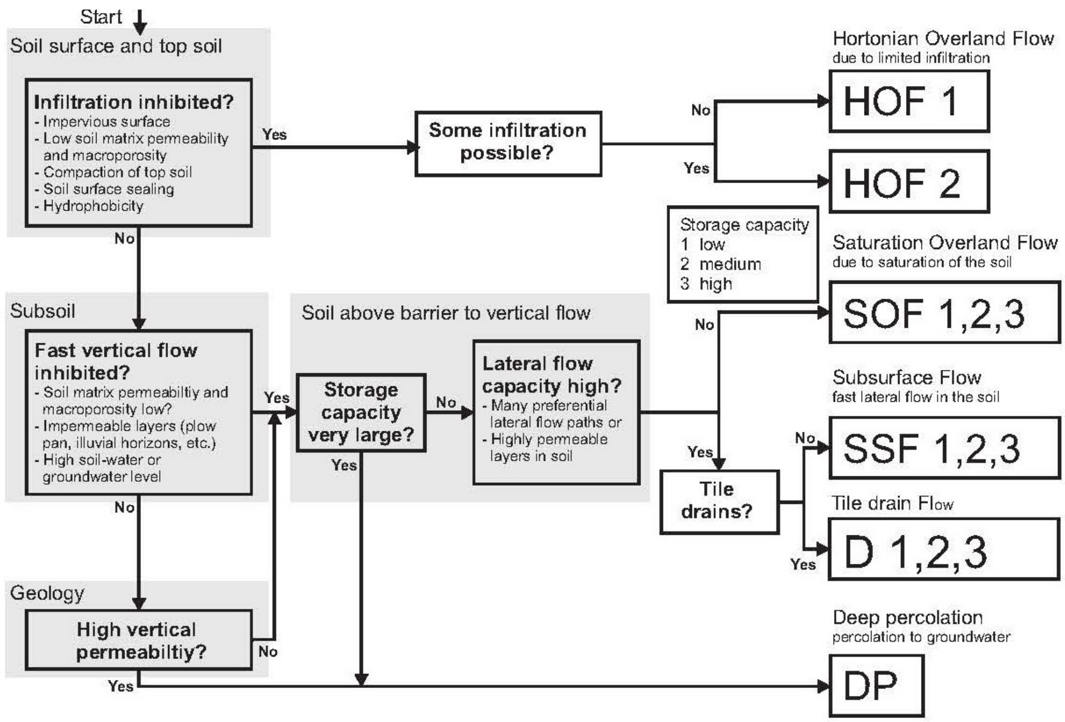

Figure 2-2: Selection of the dominant runoff process for a soil profile, from Schmocker-Fackel et al. (2007)

Significant differences in the runoff quantities generated from soil covers under different climates, rainfall intensities, surface soil characteristics, and vegetation have been observed in several recent studies. Albright et al. (2004) measured runoff on 24 test sections at 11 landfill cover systems in the United States in climates ranging from arid to humid and on slopes of 5% to 25%. They found that direct surface runoff measurements accounted for between zero and 10% of total annual precipitation. In addition, they found that direct surface runoff measurements were statistically independent of the slope of the cover, regardless of whether the cover was a conventional barrier type or alternative water balance type.

The runoff on a residual slope in response to rainfall was investigated by Rahardjo et al. (2005) under both simulated and natural rainfall events of varying intensity and duration. Runoff quantities accounted for between zero to 45% of total rainfall for simulated events and 26% to 60% of total rainfall for natural rainfall events. This study concluded that runoff volumes were influenced by total rainfall, duration of rainfall, and antecedent moisture conditions.

An expansive soil slope with a profile rich in cracks and fissures was studied (Zhan et al. 2007). The percentage of runoff was found to vary from zero to 45% of rainfall. It was hypothesized that the surface runoff increased due to swelling and closure of the cracks and fissures upon wetting.

Studies performed by Wilson et al. (2006) and Miskolczi (2007) on soil covers constructed by blending tailings and waste rock measured corresponding quantities of runoff and infiltration. They concluded that the net infiltration quantities were reduced by approximately two orders of magnitude due to increased surface runoff. The above mentioned studies are examples of the significant variation in surface runoff that can be generated from a soil cover and illustrate the importance of quantifying surface runoff.

None of the studies discussed above make any attempt to predict the measured runoff quantities based on the hydraulic properties of the soil surface and measured rainfall intensities. The primary focus of the present study will be directed at this apparent knowledge gap.

2.2.4 Model Comparisons with Observed Field Response

Several recent studies have attempted to reproduce field measurements of water balance parameters in soil covers using different software programs common in the industry (Scanlon et al. 2002, Swanson et al. 2003, Benson et al. 2004, Benson et al. 2005, Scanlon et al. 2005, Ogorzalek et al. 2008, Bohnhoff et al. 2009). Many recent studies have confirmed the importance of runoff predictions in water balance modelling. These studies all demonstrate that the accuracy of predicted water balance components, such as infiltration and storage, are highly dependent on the accuracy of runoff predictions (Roesler et al. 2002, Scanlon et al. 2002, Benson et al. 2005).

Water balance predictions are sensitive to the resolution of precipitation input, hysteresis, the equations used to represent soil hydraulic properties, liquid and vapour flow, soil depth and texture, and the actual coding and input required or allowed by the model (Fayer et al. 1992, Stothoff 1997, Scanlon et al. 2002, Hearman and Hinz 2007, Benson 2010).

For example, Scanlon et al. (2002) compared seven different codes (HELP, HYDRUS-1D, SHAW, SoilCover, SWIM, UNSAT-H, and VS2DTI) with water balance measurements from non-vegetated engineered covers in Idaho and Texas. The reliability of the coding, i.e. how closely the model output matched measured data, was examined for various portions of the water balance equation, including surface runoff. In general, all codes under-predicted surface runoff when daily precipitation data was used and similarly low results were produced even when hourly precipitation data was used. Runoff predictions have also proven sensitive to the resolution of precipitation rate input by Wainwright and Parsons (2002), Bronstert and Bardossy (2003), Benson et al. (2004), Benson et al. (2005), and Bohnhoff et al. (2009).

Surface runoff predictions were also found to be very sensitive to the hydraulic properties of the surface layer (Roesler et al. 2002). Swanson et al. (2003) noted that the hydraulic conductivity of the surface layer is the most sensitive parameter to be fitted in a model. In fact, knowledge of the distribution of the soil hydraulic property data appears more important than that of rainfall data in simulating surface runoff generation at the hillslope scale (Loague 1988). Many models require calibration to successfully reproduce measured field response, as previously discussed in Section 2.2.2.

Furthermore, in many studies the adjustment of the surface hydraulic conductivity to achieve output matching observations was neither insignificant nor consistent. The hydraulic conductivity of the topsoil had to be decreased by an order of magnitude to increase the runoff output by the model that simulated field measurements in the study by Scanlon et al. (2002). A factor of 0.5 to 1.4 was applied to K_{sat} by Fayer et al. (1992) to improve the comparison between their model and observations. Bohnhoff et al. (2009) found better agreement in water balance predictions after increasing the saturated hydraulic conductivity of the soil cover by a factor of 5 to 10. Simulations performed by Roesler et al. (2002) increased the surface K_{sat} by up to two orders of magnitude to achieve runoff predictions matching field observations.

Though the uncertainty surrounding the soil properties is often removed for an engineered soil cover, the changes in the characteristics of the soil cover over time may cause significant changes in the cover response to rainfall. Changes in the soil cover due to weathering and the ongoing adjustments in the vegetation and biota supported by the cover may cause significant changes in the structure, texture, and hydraulic properties of the soil after the cover is constructed (Albright et al. 2006, Fredlund and Wilson 2006, Benson et al. 2007). It has been shown that using in-service hydraulic properties of the soil cover yields far more accurate results from a model compared to using as-built hydraulic properties (Roesler et al. 2002, Albright et al. 2012). Roesler et al. (2002) found that the initial constructed permeabilities of the materials (measured in the lab) were too low and overpredicted runoff in all the models. When the permeabilities were calibrated to a higher value to represent weathering and changes occurring in the soil cover, runoff predictions more accurately represented measured values.

Modelling of these changes is site specific, complex, and the degree of accuracy of modelled changes is uncertain, as discussed in the previous paragraphs. Therefore, it would be useful if a simple testing procedure could be performed on the soil cover that would provide accurate runoff predictions and more reliable estimates of infiltration from the soil cover model. This simple testing could be undertaken periodically to continually update soil cover characteristics, performance, and rainfall runoff models. For example, Hopp et al. (2011) used field and laboratory measurements that were between 7 to 10 years old to successfully model the water balance of an engineered cover in a humid environment. Thus, additional field measurements of in-service material properties may only need to be re-established once per decade for highly engineered covers.

Only recently has there been success in modelling subsurface runoff in a water balance cover using field and laboratory measurements to predict observed response (Hopp et al. 2011). The experiment by Hopp et al. (2011) tested a planar cover with a slope of 3H:1V that was designed to restrict oxygen and water ingress into underlying waste by conveying infiltrating water laterally downslope within the cover. A trench was excavated at the base of the slope to capture all water moving laterally within each layer of the cover system. The subsurface flow was measured directly by a gutter system within the trench and tipping buckets. The cover was studied using both natural rainfall events and controlled sprinkler trials.

Hopp et al. (2011) input field and laboratory measurements of saturated hydraulic conductivity and Soil-water characteristic curves (SWCC) directly into their finite element model (HYDRUS 2-D), along with data from measured rainfall events. The model produced results that closely followed field observations, suggesting the potential for uncalibrated models (i.e. models for which actual measurements do not need to be modified to produce results that match field observations) to yield accurate predictions of water balance components. Hopp et al. (2011) suggested that the success of the model without calibration reflects the highly engineered nature of the system, where the materials were well characterized during design and construction. These conclusions point to the potential for success in the use of uncalibrated methods to accurately predict field conditions.

2.3 Justification for Further Research

Section 2.2 summarized runoff mechanisms, methods of runoff prediction, observed runoff variation, and previous model comparisons with observed field response. The current methods of runoff prediction require either complex one or two-dimensional modelling of infiltration at the point scale; or estimates based on necessary generalizations of soil properties and rainfall events made for the watershed scale. Direct measurements have demonstrated significant variability in runoff generated from slopes with differing characteristics and the significance of runoff in controlling the quantity of infiltration. Field observations of the runoff process have proved important and useful for identifying dominant runoff mechanisms and selecting appropriate prediction techniques. The most accurate methods for runoff prediction require model calibration with direct measurements of runoff during actual or simulated rainfall events on field slopes and surfaces. Only limited success has been achieved using an uncalibrated model in predicting one component of direct runoff, that of lateral subsurface runoff. From these summaries, it can be concluded that there does not appear to be any proven reliable procedure for predicting surface runoff based on measurable properties at the soil surface.

Surface runoff predictions have proven to be primarily sensitive to the hydraulic properties of the surface soil layer and to rainfall intensity. Langhans et al. (2011) have re-examined the concept of infiltration capacity by defining two parameters:

1. Effective hydraulic conductivity (K_e) – the spatially-averaged hydraulic conductivity when the soil is field saturated and steady state is reached.

2. Apparent infiltration rate at steady state (f_s) - the infiltration rate of which a certain fraction contributes to infiltration-excess (Hortonian) runoff production.

Langhans et al. (2011) show that K_e is dynamic, dependant on the rainfall intensity, and equivalent to the apparent infiltration rate (f_s). Easily measured variables, such as rainfall intensity, can then be linked to K_e and account for the effects of a heterogeneous soil on infiltration rates. Benson et al. (2005), for example, attributed the over-prediction of surface runoff to the precipitation intensity used in the model, rather than the field-representative saturated hydraulic conductivity (K_{sat}). Stone et al. (2008) modelled observed plot-scale runoff using an infiltration rate that was dependant on rainfall intensity and found that when the rate quickly approached a constant value, modelled runoff hydrographs matched the observations. It has been suggested that the infiltration-intensity relationship approaches a constant value faster when vegetation cover is limited (Hawkins 1982, Dunne et al. 1991, Janeau et al. 1999, Stone et al. 2008). These studies clearly identify the interdependency of surface hydraulic properties, rainfall intensity, and resulting runoff.

In this thesis, the relationship between rainfall intensity, hydraulic properties of the soil surface, and resulting runoff was examined. The surfaces of B-Dump and tailings at the OTD are primarily non-vegetated and the rainfall-runoff relationship was measured along with material hydraulic properties. The catchments on B-Dump differ in size, topography, and surface soil characteristics, whereas the OTD catchments differ mainly in surface soil characteristics. These physical differences form the basis for the comparison and analysis of the measured and modelled rainfall-runoff relationships described and discussed in the following chapters.

2.4 Savage River Mine

The Savage River Mine in northwestern Tasmania, Australia, uses a non-vegetated low hydraulic conductivity cover to limit water infiltration into potentially acid forming waste rock stored in B-Dump. The design and construction of this water shedding cover on B-Dump is reported by ABM (2006) and is summarized below in Section 2.4.1. Tailings stored in the Old Tailings Dam at Savage River Mine are currently unprotected by a soil cover and are forming acid, as discussed below in Section 2.4.2. The climatic conditions present at Savage River Mine are discussed in Section 2.4.3. Previous testing undertaken on the B-Dump soil cover is described in Sections 2.4.4, and 2.4.4.2.

2.4.1 B-Dump Water Shedding Cover

The design of the B-Dump waste rock stockpile began in 2002 and evolved throughout construction due to changes in the mine plan and the availability of preferred construction materials. The original concept was to construct a compacted clay cover over waste rock from the original mine plan, however it was realized that sufficient compaction of the clay overburden could not be achieved. During the development of the South Deposit at the mine, larger volumes of competent alkaline waste rock were discovered. This ultimately led to the design of a compacted waste rock water-shedding cover.

The water-shedding cover is comprised of alkaline calcite chlorite schist (A-Type) waste rock and clay overburden removed from the South Deposit. These materials were placed over neutral to low potentially-acid-generating (B-Type) waste rock and clayey weathered rock. A-Type waste was used to sheet across the dump surface to improve trafficability during construction, so layers of A-Type are within the B-Dump waste as well. Material was hauled and compacted using 100 tonne and 150 tonne trucks. A portion of B-Dump was designed as an alkaline side-hill cover, which allows water to percolate through alkaline material to increase acid neutralization and associated precipitates that would eventually seal the dump. To date, B-Dump is predominately non-vegetated.

The surface topography of B-Dump is such that five main catchment basins are well defined. Catchments 1 and 2 direct surface runoff south off the dump into an alkaline soakage area and then into Main Creek. Runoff from catchments 3, 4, and 5 flows north through pipes and then west, joining natural drainage into the mine's Center Pit South. The five catchments and runoff directions of B-Dump are illustrated in Figure 2-3. The total surface area of B-Dump is approximately 22.6 ha.

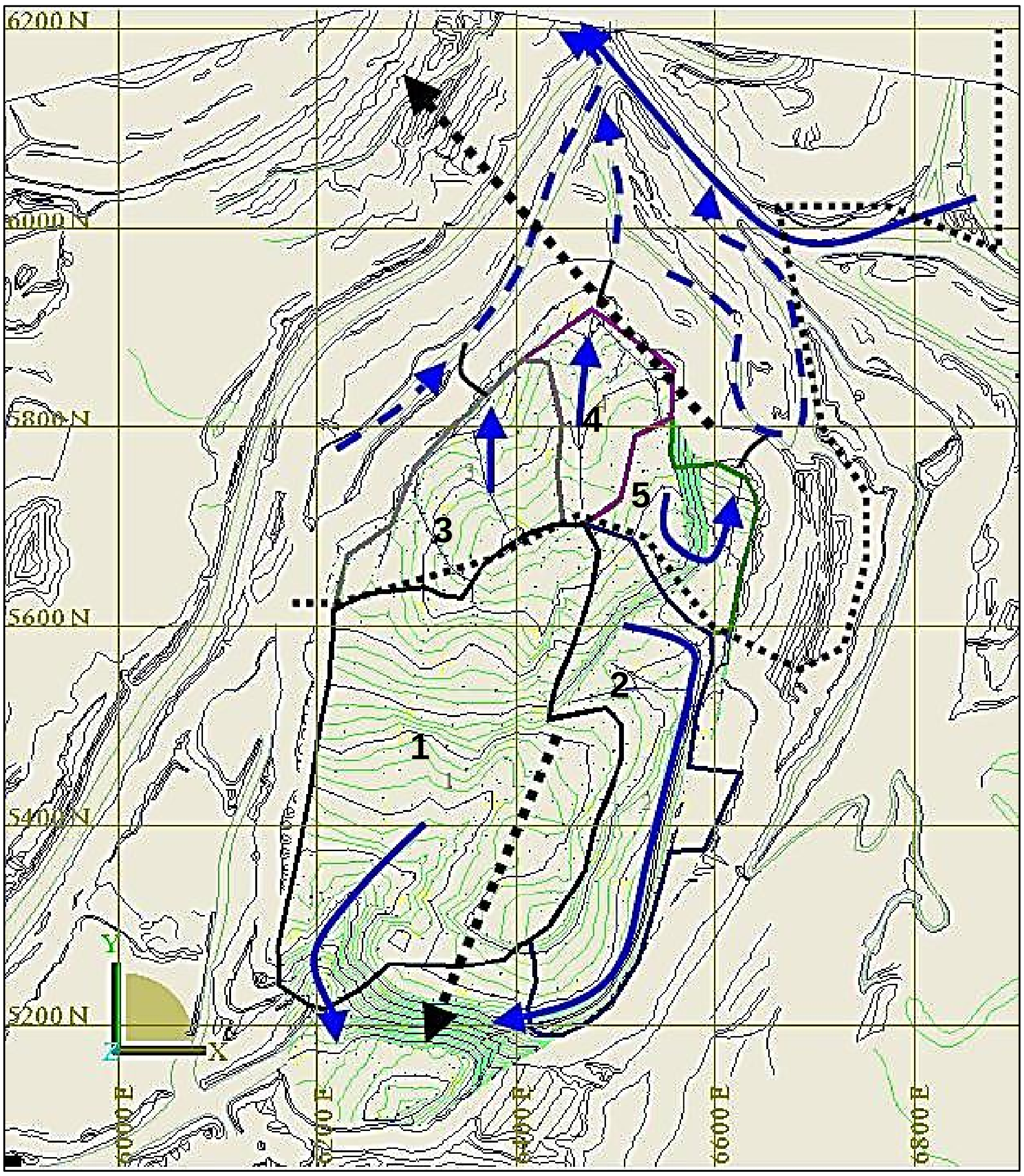

Figure 2-3: B-Dump catchments and runoff directions (ABM 2006)

2.4.2 Old Tailings Dam

A geochemical assessment of the near surface tailings was performed in 2010 (SRK Consulting 2010). Pertinent information regarding OTD was gathered from this report and is summarized here. The OTD contains approximately 14×10^6 m^3 of uncapped, pyrite rich tailings over roughly 60 ha. Prior to decommissioning in 1983, a significant amount of coarse tailings was placed in the south west corner of the existing beach. Except for the area where coarse tailings were placed, the tailings were generally observed to be fine grained and may or may not be overlain by a crust of iron stained weathered tailings approximately 5 mm thick. The tailings are predominately non-vegetated. The depth of the water table decreases from 3 m to 1 m as the distance from the south dam face increased. Acid drainage has been occurring from the southern wall of the dam since the late 1970's. SRK (2010) concluded that acid drainage is being produced from the upper 1 m of unsaturated tailings.

No instrumentation was previously installed to measure rainfall or runoff from any areas of the OTD. During this research, two catchments were defined and instrumented, as discussed further in Section 3.2.2.

2.4.3 Climate

Savage River Mine is located in a cool, temperate climate with an average annual rainfall and evaporation of 1938 mm and 902 mm, respectively. Summer months are from December through March, and winter runs from May through August. The average monthly rainfall peaks in July, exceeding 234 mm, and is lowest in January at 78 mm. Average monthly evaporation is 146 mm in January and 27 mm in June. In general, rainfall amounts exceed evaporation from March to November. Mean temperatures reach daily maximum (minimum) values of 20.1°C (9.9°C) in February and drop to 9.4°C (3.3°C) in July. The average annual trends of monthly rainfall, evaporation, and daily temperatures for Savage River Mine are shown in Figure 2-4.

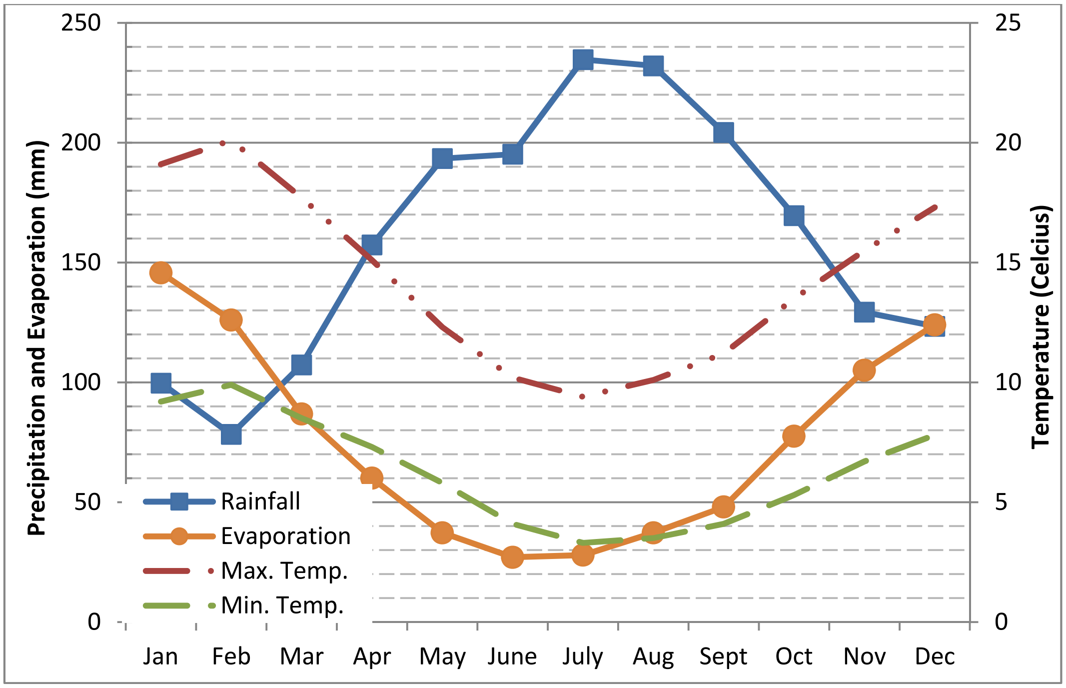

Figure 2-4: Average monthly rainfall, monthly evaporation, and daily temperature for Savage River Mine (1966 ~ 2011)

The above climate information for Savage River Mine was summarized from data obtained from the Australian Bureau of Meteorology website (2012).

2.4.4 Previous Studies at Savage River Mine

Two studies that are relevant to this research were completed at the Savage River Mine. An initial comparison between measured rainfall and corresponding runoff was completed by GHD in 2009 for Catchment 1 and 2 on B-Dump. In addition, the material characterization was completed for the clay overburden material used as part of the soil cover on B-Dump. These studies are described in further detail in the sections below.

2.4.4.1 Rainfall-Runoff Comparison

Catchments 1 and 2 on B-Dump were instrumented with tipping-bucket rain gauges and V-notch weirs to measure corresponding rainfall and runoff in real time. Preliminary analyses of the rainfall runoff data from B-Dump was conducted by GHD (2009) for the periods of March 29, 2007 to June 20, 2007 and again from August 27, 2007 to September 30, 2007. The analyses indicated that up to 97% of precipitation became surface runoff in Catchment 1, while only 33% of precipitation became runoff in Catchment 2. The quantity of measured runoff compared to the measured rainfall was very close for Catchment 1 but a significant difference was noted for Catchment 2, despite the materials and construction of both catchments being similar. GHD (2009) reported that when evaporation and infiltration losses were considered, runoff correlation with rainfall improved. The infiltration loss rate assigned for Catchment 1 and Catchment 2 was 5 x10^{-9} m/s and 1.5 x10^{-7} m/s, respectively. The report concluded that the most likely reason for higher losses in Catchment 2 was the presence of the flat alkaline side-hill cover, which was designed to promote infiltration to add alkalinity to underlying waste materials.

An error in the flow rate calculation of runoff in Catchment 1 was discovered upon review of the rainfall-runoff data provided by GHD (2009). A sharp discontinuity in the relationship between measured water level (H) in the weir and the corresponding flow rate (Q) was observed in Catchment 1 as water levels reached 0.46 m (shown in Figure 2-5). This water level corresponded to the height at which water began to flow through the rectangular portion of the weir box above the open V-notch portion.

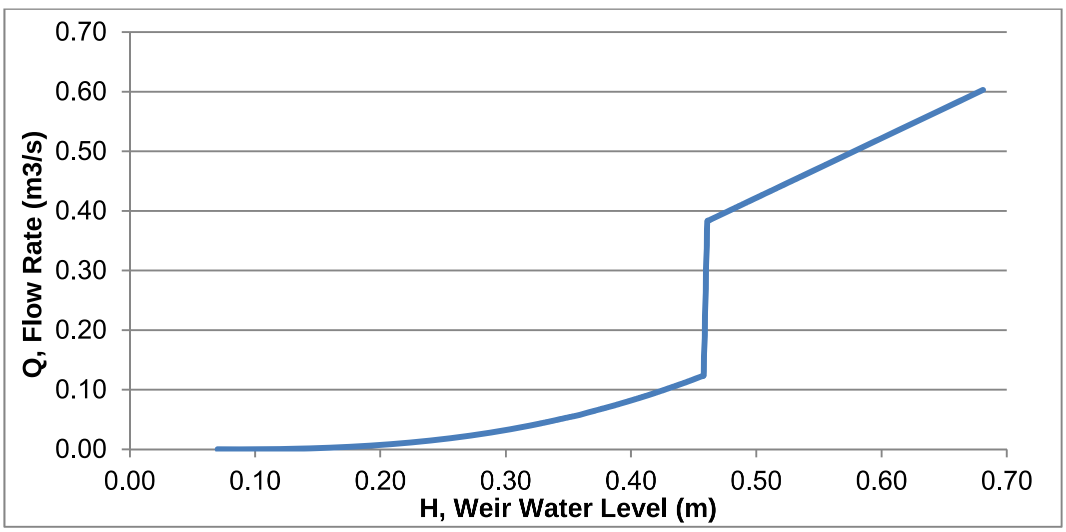

Figure 2-5: Relationship between Catchment 1 measured weir water levels and corresponding flow rates (reported by GHD (2009))

For a triangular shaped channel such as the V-notch weir for water levels below 0.46 m, Q is a function of H^2, so the resulting H-Q relationship is parabolic. For flow through a rectangular shaped channel such as the weir box above the V-notch for water levels greater than 0.46 m, Q is a function of H, so the resulting H-Q relationship is linear. The formulae for converting weir measurements to flow rate were unavailable for review, but it appears that flow rates for water levels above 0.46 m were calculated as if the water were flowing through an entirely rectangular channel.

The H-Q relationship should transition smoothly between the parabolic (V-notch flow) and the linear (rectangular weir box flow). The H-Q relationship adopted for this research is shown in Figure 2-6. The parabolic V-notch portion of the curve is unchanged from the original data-set, while the revised linear portion is parallel to the original data-set for weir levels above 0.46 m.

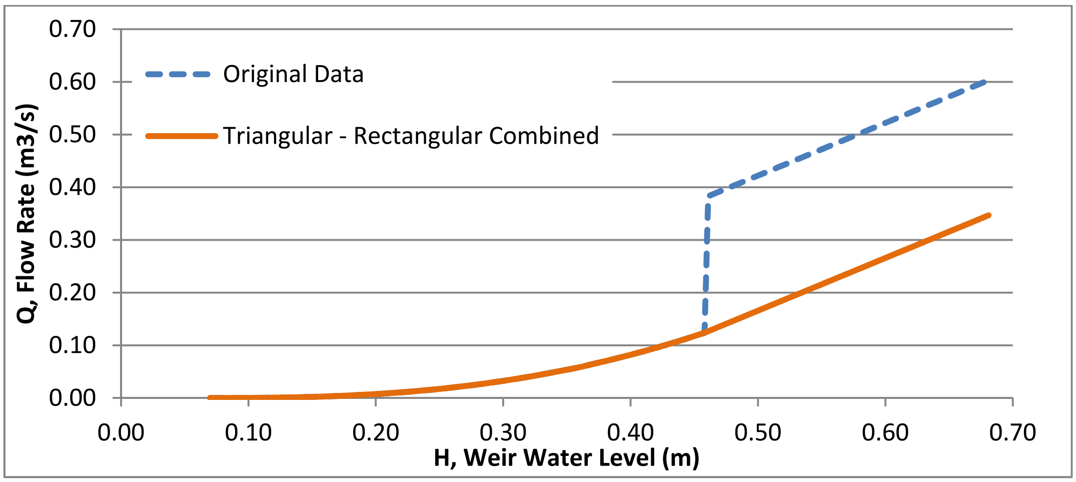

Figure 2-6: Revised relationship between Catchment 1 measured weir levels and corresponding flow rates

This revised relationship is used to amend the cumulative runoff volumes for Catchment 1. Runoff volumes predicted from this research are compared to these amended values in Section 5.3. The revised relationship indicates approximately 69% of precipitation is converted to surface runoff in Catchment 1, compared to the 97% originally reported by GHD (2009).

Catchment 2 typically produced less runoff than Catchment 1. The water levels did not reach a height that would overtop the V-notch and begin to flow in the rectangular portion of the Catchment 2 weir box. No error in the Catchment 2 runoff calculations was observed, therefore the Catchment 2 runoff volumes have not been changed from those provided by GHD (2009).

The original and amended runoff data is provided in digital format in the Appendix.

2.4.4.2 Clay Overburden Testing

In 2002, the waste management concept for B-Dump included a compacted clay cover encapsulating the potentially acid forming waste rock (ABM 2006). The as-built permeability of the field compacted clay was investigated by Thompson and Brett (2002) to verify the design parameters. The following summarizes the study conducted by Thompson and Brett (2002).

A series of permeameter and nuclear densometer tests were performed on clay test plots constructed with differing placement techniques and compaction. Samples were removed at each site for laboratory permeability, gradation, and compaction analysis. The range of permeability for the field and laboratory tests was virtually equivalent, from 1.3×10^{-6} m/s to 3.0×10^{-8} m/s. Nuclear densometer tests showed the material could be compacted to densities in excess of 100% maximum dry density, with an average in-situ density of 1.84 g/cm^3. Grain size analysis showed the material to be silty sand to silty gravel with fines content ranging from 11% to 28% passing 75 µm. These results are subsequently compared in Section 4.1.2.2 to the results obtained for the clay materials tested during this research.

Chapter 3. MATERIALS AND METHODS

A critical objective of the research was to obtain an adequate data set to fully characterize the materials on B-Dump and the OTD. This objective was accomplished using three steps.

The first step was to develop and execute a field investigation of the surface materials present on B-Dump and the OTD. This process is described in detail in Section 3.1. In summary, full characterization of the materials required detailed areal mapping of material types followed by in-situ testing of each material, including infiltration tests, density measurements, soil suction and moisture content determinations, and representative sampling for further laboratory testing.

The second step included defining the response of the surface material to rainfall, and is discussed in Section 3.2. Several rainfall events occurred during the field program, which allowed first-hand observation and recording of the direct response of each material to rainfall.

For the third step, samples collected during the field program were taken to the University of Alberta for laboratory analysis. Preliminary testing was conducted to classify all material samples into a specific soil group, and then representative samples were selected for further analysis. Laboratory testing on the selected representative samples included detailed soil classification, specific gravity analysis, and soil water characteristic curve determination. The laboratory tests conducted on B-Dump and OTD materials are detailed in Section 3.3.

The direct results of the field and laboratory program are summarized in Chapter 4.

3.1 Field Program

The field testing and sampling program was conducted between November 16 and December 3, 2011, at the Savage River Mine. Dr. G. Ward Wilson from the University of Alberta was on site from November 16 to 19, to initiate the field program and provide guidance to the researcher for finalizing testing locations.

The first and final day of the program were reserved for miscellaneous related activities, including site orientation, equipment organization, and sample shipping. Eleven days, from November 17 to 27, were dedicated to B-Dump in order to fully characterize the soil cover material where detailed rainfall and runoff measurements were previously recorded. Five days, from November 28 to December 2, were dedicated to testing and sampling the tailings at the OTD.

3.1.1 Test Site Selection

The test sites were spread over as much of the B-Dump and OTD surface area as possible in order to obtain an accurate representation of the materials under investigation. Site selection was predominantly based on the visual classification of the materials during dry conditions. Other factors considered in site selection included the objective to conduct a minimum of two tests on similar materials as well as considering observed response to rainfall events, the local topography, and ease of access to the location.

3.1.1.1 B-Dump

General test areas were outlined for Catchment 1 and Catchment 2 prior to visiting the site based on construction reports and maps provided by Grange Resources. Potential test sites were selected based on drive-by observations of the soil cover during dry conditions on November 17, as well as observations of runoff response to a rainstorm event on November 18. Detailed mapping of the areal extent of each material type comprising the soil cover on B-Dump was undertaken (discussed further in Section 4.1.1)and it was during this time that test locations were finalized.

Material types were identified visually by walking around on B-Dump, ensuring the entire area was observed, and regularly checking material consistency by excavating a small amount using a handheld pick. Four different material types were ultimately identified based on their texture and their source (in brackets), as follows:

- Fine waste rock (run of mine),
- Coarse waste rock (run of mine),

- Fine clay[1] (overburden), and
- Coarse clay (overburden).

Photographs of the fine and coarse textured run-of-mine waste rock are shown in Figure 3-1, a) and b), respectively; note the utility knife for scale. Photographs of the fine and coarse clay overburden are shown in in Figure 3-2 a) and b), respectively; note the bucket for scale. Investigation of these four materials formed the basis for the B-Dump field program.

Figure 3-1: Texture of B-Dump run-of-mine waste rock material - a) fine, b) coarse

Figure 3-2: Texture of B-Dump clay overburden material - a) fine, b) coarse

A total of nine test sites were located on B-Dump. The test sites, with corresponding catchment and material tested, are listed in Table 3-1. Test

[1] The term "clay" is used for consistency with nomenclature used in previous reports on B-Dump (Thompson and Brett Pty Ltd. 2002, ABM 2006, GHD 2009). The classic description of the material is silty or gravelly sand, as discussed in Section 4.1.2.2.

locations on B-Dump are shown in Figure 3-3, along with catchment outlines and material areas.

Table 3-1: B-Dump Testing Locations

Test Site Label*	Catchment	Material Tested
BD1-C-1	1	Fine waste rock
BD1-C-2	1	Fine waste rock
BD1-C-3	1	Fine clay overburden
BD1-C-4	1	Coarse clay overburden
BD1-C-5	1	Fine clay overburden
BD2-C-1	2	Coarse clay overburden
BD2-C-2	2	Fine waste rock
BD2-C-3	2	Coarse waste rock
BD2-C-4	2	Coarse waste rock

*Note regarding test site labels: the initial three characters, BD1 and BD2, represent test sites in B-Dump catchments 1 and 2, respectively. The final number is a unique identifier for that test location.

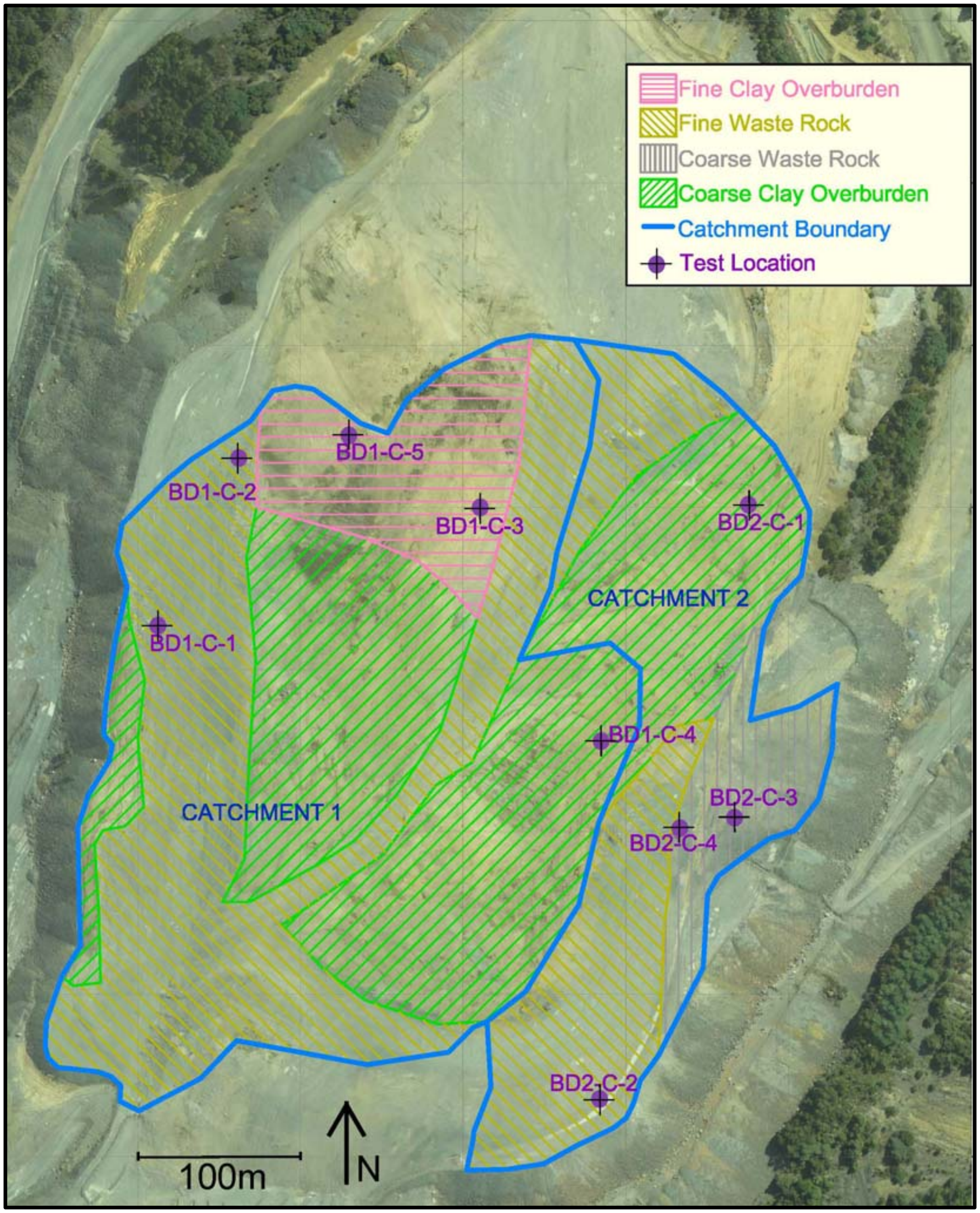

Figure 3-3: B-Dump catchments, material areas, and test locations

3.1.1.2 Old Tailings Dam

Potential test sites at the OTD were selected based on visual observation of the tailings surface during a walk-around inspection on November 16, 2012. Three distinct materials were identified based on their observable surface properties, as follows:

- Fine tailings,
- Coarse tailings, and
- Hardpan.

Photographs of the three tailings types are shown in Figure 3-4 a), b), and c); note the inner width of the wooden frame is 30 cm.

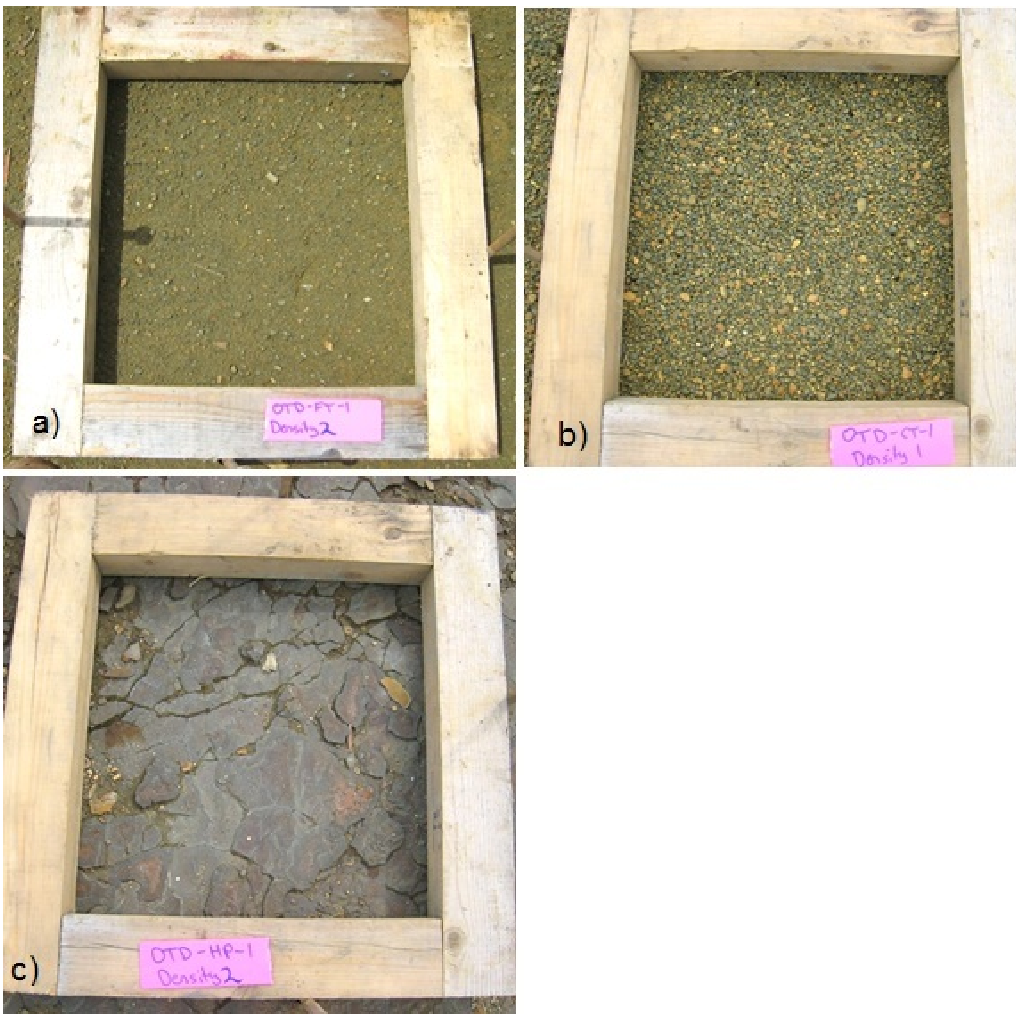

Figure 3-4: Texture of Old Tailings Dam tailings - a) fine, b) coarse, c) hardpan

A total of six test sites were located on the OTD, with two sites dedicated to each of the material types. The test sites, with corresponding catchment and material tested, are listed in Table 3-2 and illustrated in Figure 3-5.

Table 3-2: Old Tailings Dam Testing Locations

Test Site Label	Catchment	Material Tested
OTD-FT-1	B	Fine tailings
OTD-FT-2	A	Fine tailings
OTD-CT-1	Not applicable	Coarse tailings
OTD-CT-2	Not applicable	Coarse tailings
OTD-HP-1	A	Hardpan
OTD-HP-2	A	Hardpan

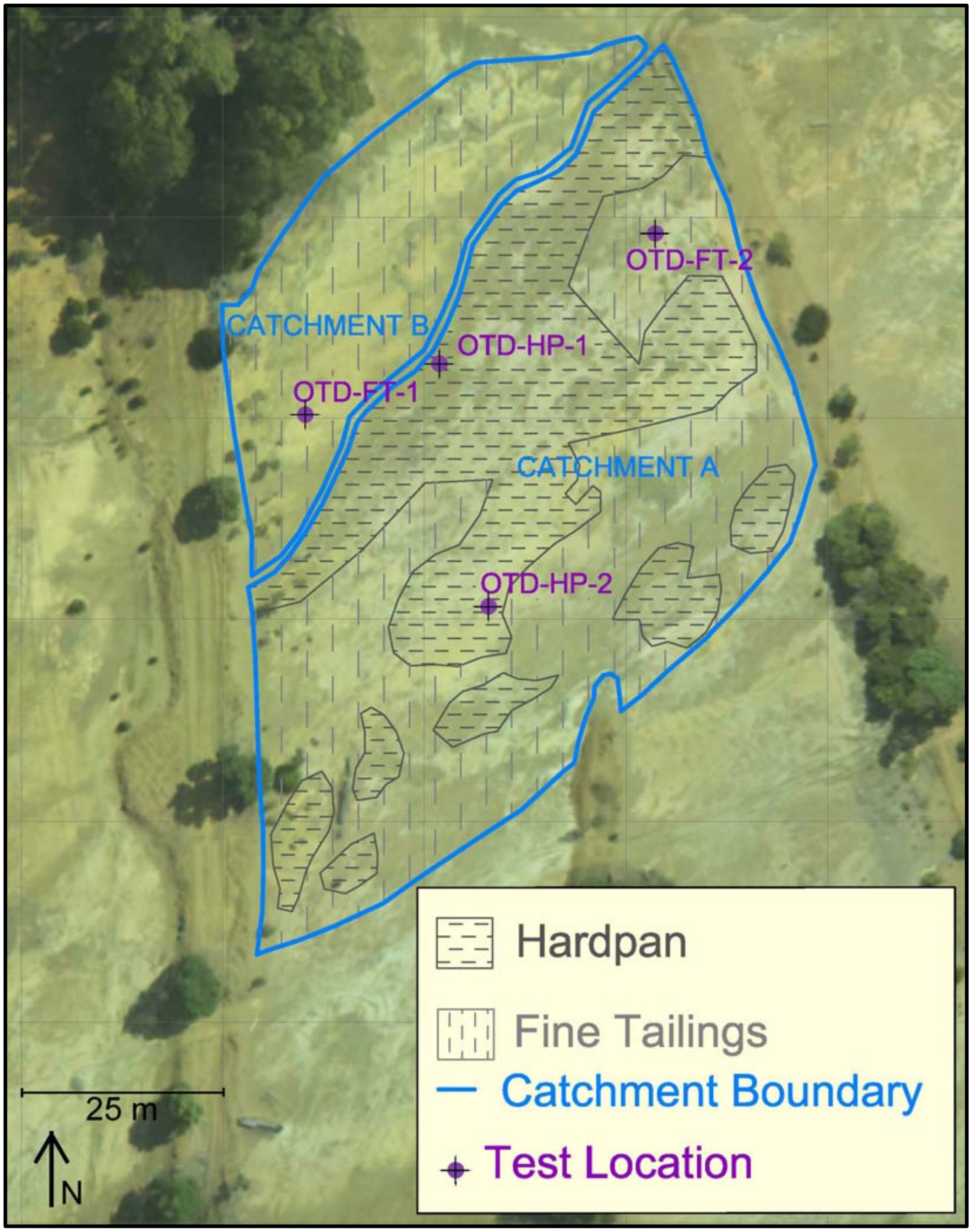

Figure 3-5: Old Tailings Dam catchments, material areas, and test locations

3.1.2 Field Tests Performed

A number of field tests were conducted to fully characterize the in-situ soil hydraulic properties on the B-Dump soil cover and the exposed tailings at the OTD. Combinations of the following tests were performed at each test site, as follows:

- Hand augering or digging to generally classify materials and establish a soil profile,
- Infiltration testing for saturated hydraulic conductivity measurements at the surface and at depth,
- Density measurements of the surface soil,
- Soil suction and temperature profile,
- Moisture content sampling at each soil suction and density measurement, and
- Representative sampling for further lab testing.

The following sections discuss the tests performed on each material comprising the B-Dump soil cover and the tailings at the OTD. The details concerning the installation of equipment and any issues encountered while the tests were performed are noted. Results of the tests are discussed in Chapter 4.

3.1.2.1 B-Dump

Prior to beginning any field tests, an area for each individual field test was outlined and cordoned off to avoid disturbing the material with foot traffic (for example, Figure 3-6). The soil profile was established in conjunction with digging the in-situ density test pits, since the materials on B-Dump were too coarse or too dense to use a hand auger. No layering of materials was observed, therefore the profile was considered uniform near the surface for the B-Dump soil cover materials.

Figure 3-6: Example of test site outline for avoiding material disturbance

3.1.2.1.1 Saturated Hydraulic Conductivity

The saturated hydraulic conductivity at the surface of B-Dump materials was determined using a ring infiltrometer set-up, as described below. Guelph Permeameter testing was not performed on B-Dump materials.

Ring Infiltrometer

Double or single-ring infiltrometer tests were conducted at each test site to obtain the rate of infiltration and saturated hydraulic conductivity, K_{sat}, at the surface. The tests were performed in accordance with the practice ASTM D3385 (2009a), with limited modifications. In summary, two open steel cylinders 30 cm and 60 cm in diameter were installed, one inside the other, into the ground. The cylinders were partially filled with water, which was then maintained at a constant level. The volume of water required to maintain the constant water level in the rings is equivalent to the volume of water that infiltrates into the soil. This volume was measured over time and converted into an incremental infiltration velocity that, at its maximum steady-state rate, is equivalent to the saturated hydraulic conductivity, K_{sat}, at the surface (ASTM 2009a).

ASTM (2009a) calls for the outer ring and inner ring to be installed in the soil to a depth of approximately 150 mm and 50 to 100 mm, respectively. In most cases on B-Dump, these depths could not be achieved due to the density and coarse texture of the materials. However, the purpose of the greater depth of installation is to minimize disturbance and to prevent water leakage from within the rings to the ground surface surrounding the ring (ASTM 2009a). These objectives were accommodated by alternate means.

Disturbance of the fine waste rock and coarse clay overburden materials was minimized by hand excavation of the outer ring perimeter, digging down and outward to leave the inner material intact (Figure 3-7: a). The inner ring was driven to a shallower depth to gain marginal embedment and avoid fracturing the surface. The disturbance around the inside and outside of both rings was then patched with a mixture of fines from the local material and bentonite, moistened with water, and tamped into place. Figure 3-7: b) shows the typical minor disturbance created outside of the inner ring, which was subsequently patched with the bentonite and fines mixture, as seen on the inside of the outer ring. Hand excavation in the fine clay material was unnecessary, as inner and outer rings could be easily driven into the soil. Minor disturbance in the fine clay was similarly patched with a fines-bentonite mixture. In all cases, disturbance of this mixture was carefully avoided when filling the rings (Figure 3-7: c) to prevent the bentonite from spreading over the surface and impacting results. During all tests, no leakage out of the rings was observed with the fines-bentonite seal in place.

A constant water level was maintained using a Mariotte tube setup. On hot days, these tubes were sheltered during the test to prevent air expansion that could affect test results. The rings were sheltered with plastic to prevent precipitation and evaporation from affecting the water levels (Figure 3-7: d) during times of inclement weather and when tests ran for extended periods of time.

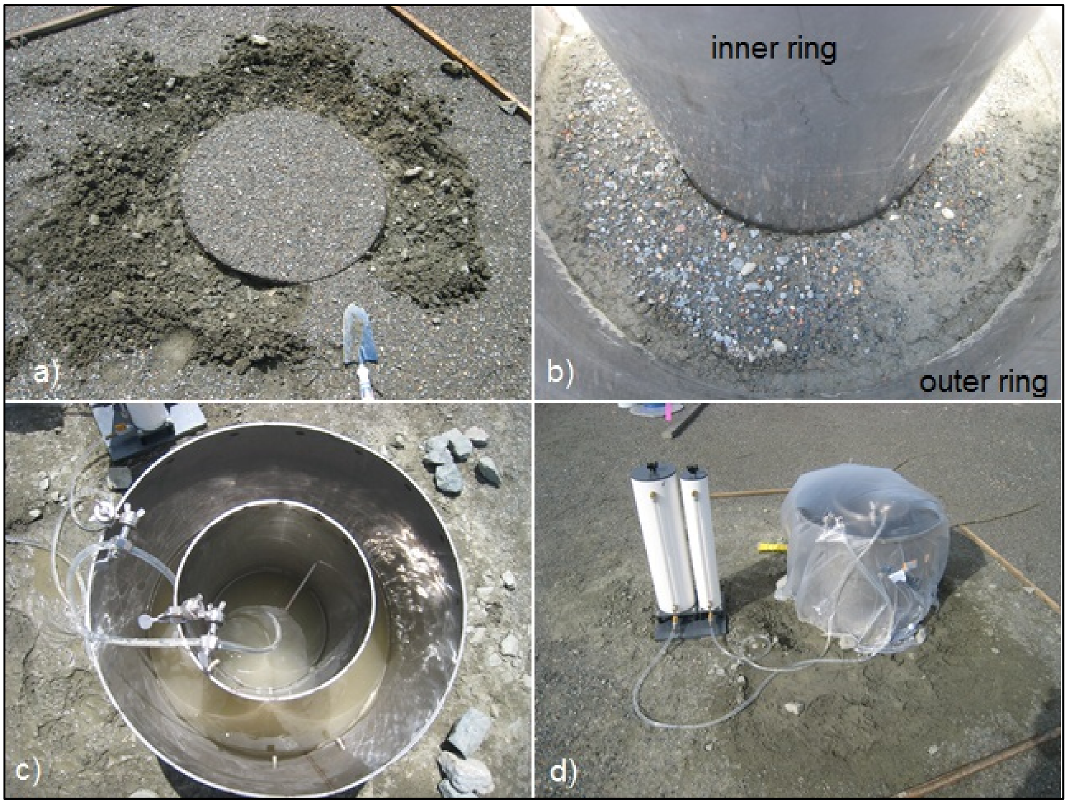

Figure 3-7: Double-ring infiltrometer test in fine waste rock - a) pre-excavation of outer perimeter, b) example of disturbance and patching, c) rings filled with water, d) Mariotte tube setup and ring shelter

The installation of both an inner and outer ring was impossible for the coarse waste rock tests, due to the cobbly nature of the material. It was determined that only a single outer ring be installed and the test necessarily reverted to a falling head analysis. Many coarse particles extended from the ring perimeter into the inner testing surface during manual excavation. For example, Figure 3-8: a) shows the intended test surface and Figure 3-8: b) shows the test surface achieved once coarse particles were removed from the ring perimeter. An adequate seal could not be achieved using a fines-bentonite mixture in this case, so a sand-cement-bentonite mixture of ratio 10:3:1 was made on site and used to grout the ring in place (Figure 3-8: c). The grout filled the voids between the ring and excavated perimeter and capped the surface where coarse particles had to be removed (Figure 3-8: d). The grout was allowed to set over night prior to filling the ring with water and conducting the test. The test surface area was subsequently corrected during interpretation of the data and this interpretation is provided digitally in the Appendix. This procedure was also used for one of the fine waste rock test sites, both for comparison to a double-ring infiltrometer test and to gain an additional test location.

Figure 3-8: Single-ring infiltration test in coarse waste rock - a) intended test surface, b) final test surface excavation, c) grouted in place, d) inner grout seal

Table 3-3 summarizes the nine ring infiltrometer experiments performed on B-Dump, including the depth of installation of the rings, method used to seal the disturbance around the ring perimeter, and the test analysis type.

Table 3-3: Summary of B-Dump Ring Infiltrometer Tests

Test	Material Type	Outer Ring Depth (mm)	Inner Ring Depth (mm)	Sealant Method	Test Analysis
BD1-C-1	Fine Waste Rock	45	30	Fines/ bentonite	Constant head
BD1-C-2	Fine Waste Rock	30	15	Fines/ bentonite	Constant head
BD1-C-3	Fine Clay	54	33	Fines/ bentonite	Constant head
BD1-C-4	Coarse Clay	45	22	Fines/ bentonite	Constant head
BD1-C-5	Fine Clay	71	42	Fines/ bentonite	Constant head
BD2-C-1	Coarse Clay	50	25	Fines/ bentonite	Constant head
BD2-C-2	Fine Waste Rock	26	N/A	Grout	Falling head
BD2-C-3	Coarse Waste Rock	55	N/A	Grout	Falling head
BD2-C-4	Coarse Waste Rock	44	N/A	Grout	Falling head

3.1.2.1.2 Density

In-situ density of the soil cover materials was determined at two locations for each test site using the water replacement density method, outlined in ASTM D5030 (2004). In summary, a test pit was excavated and the mass and moisture content of the material removed was determined. The volume of the test pit was determined by adding known masses of water to fill the lined test pit. The mass per volume, or in-situ density, of the material was then determined. Typically this method is used for very coarse material (maximum particle sizes greater than 125 mm). However, other methods of determining in-situ density, such as nuclear densometer and the sand cone method, could not be conducted in this field program for various reasons, so only the water replacement method was utilized.

Wooden frames of 300 mm (12 in) square were provided for constructing the water replacement density test pits. Once the test pit site was selected, the frame was secured in place with spikes around the perimeter (Figure 3-9: a). The volume above the test pit surface was recorded by lining the surface with plastic and filling the frame up to a constant reference point with a measured mass of water (Figure 3-9: b). The test pit was then excavated and the removed material was immediately stored for mass and moisture content determination (Figure 3-9: c). The test pit was lined with plastic and filled with measured masses of water up to the same reference point (Figure 3-9: d). The volume of the test pit was calculated by subtracting the initial reference mass of water from the mass of water used to fill the test pit and the surface up to the reference point. The density of water was assumed as 1 g/cm^3. In some locations moss or lichen had grown on the surface and was scraped away prior to recording the initial surface volume.

Figure 3-9: Water replacement density test - a) secured frame, b) initial surface volume, c) excavation, d) test pit volume

ASTM (2004) recommends a minimum test pit volume of 1 cubic foot for a maximum particle size of 75 mm (3 in). An attempt was made to construct test pits in waste rock as near as possible to this volume by excavating the entire outline of the frame to a depth of 300 mm. As excavation progressed deeper into the pit, the removal of coarse particles from the test pit walls began to undermine the stability of the wooden frame. It was determined that this disturbance would yield larger inaccuracies in the calculated density than a reduced test pit size. Therefore, test pits in waste rock were dug as deep and as wide as possible without removing material from underneath the wooden frame. Typical excavations of 65 mm to 85 mm deep and as wide as the frame were achieved. This was considered sufficient to obtain a representative density sample, since the 75 mm diameter particles were not pervasive in the excavation (ASTM 2004: Appendix X1.3.1.1).

ASTM (2004) does not provide recommendations for minimum test pit volume for materials with maximum particle sizes less than 75 mm. Therefore, test pits in the clay cap material were excavated between 70 mm to 90 mm deep and to the width of the wooden frame, which was considered a sufficiently representative volume for in-situ density determinations.

3.1.2.1.3 Soil Suction

Matric suction in the B-Dump materials was measured using a pressure transducer tensiometer. Jet-fill tensiometers could not be installed in B-Dump materials.

Jet-Fill Tensiometer

Hydraulic contact with the pore stones on the jet-fill tensiometers could not be established in the B-Dump soil cover materials due to their coarse texture. Therefore, only the pressure transducer tensiometer was used to determine soil suction on B-Dump.

Pressure Transducer Tensiometer

Soil suction was measured using the UMS Infield 7 handheld read-out unit with the UMS T5 tensiometer probe. The porous ceramic tip of the device is only 5 mm in diameter and 50 mm^2 (UMS 2009), which facilitated insertion into the B-Dump materials and provided fast response times for recording soil suctions.

Soil suction was recorded after performing in-situ density measurements at each test site on B-Dump (Figure 3-10). Readings were taken as near as possible to the soil surface (10 to 30 mm depth) and at the base of the pit dug for the density tests. A small auger was used to create a hole in the fines of the material prior to inserting the probe to prevent damage of the ceramic tip. If necessary, the fines were then gently pressed around the probe to ensure hydraulic contact with the ceramic tip.

Immediately following each tensiometer reading, a thermometer was inserted into the same hole as the probe and the temperature of the soil corresponding to the suction measurement was recorded. The soil around and including the tensiometer hole was quickly sampled after the temperature measurements for moisture content determinations.

Figure 3-10: Soil suction measurement using pressure transducer tensiometer

3.1.2.1.4 Sampling

The minimum mass of test specimens recommended by the ASTM standards for the desired laboratory tests were reviewed prior to conducting the field program.

Samples of sufficient size were taken from all materials to accommodate further laboratory testing.

Bulk samples were collected from each test location following in-situ density measurements (Table 3-4). In all locations, bulk samples from the surface (0 to 100 mm depth) were collected from the area surrounding each density test pit. Additional samples for moisture content determination were taken wherever soil suction measurements were recorded.

Dry samples of the sand-cement-bentonite mixture used to seal voids and grout the ring infiltrometer in place were taken to verify its hydraulic conductivity in the laboratory program.

Table 3-4: List of Bulk Samples Collected from B-Dump Test Sites

Fine Waste Rock	Coarse Waste Rock	Fine Clay Overburden	Coarse Clay Overburden
BD1-C-1(D1) BD1-C-1(D2)	BD2-C-3(D1) BD2-C-3(D2)	BD1-C-3(D1) BD1-C-3(D2)	BD1-C-4(D1) BD1-C-4(D2)
BD1-C-2(D1) BD1-C-2(D2)	BD2-C-4(D1) BD2-C-4(D2)	BD1-C-5(D1) BD1-C-5(D2)	BD2-C-1(D1) BD2-C-1(D2)
BD2-C-2(D1) BD2-C-2(D2)			

*Note regarding sample numbers: the initial label sequence represents the test site location (Table 3-1) and is appended with (D1) and (D2), which represents the density test number where the bulk sample was taken.

3.1.2.2 Old Tailings Dam

Similar to the B-Dump procedure, areas for each individual field test on the OTD were outlined and cordoned off to prevent disturbance prior to conducting the field tests. The soil profile was established near the middle of the test site, with field tests placed adjacent to the profile area (Figure 3-11). A shovel or hand auger was used to excavate the tailings profile to depth of approximately 200 mm. Preliminary classification of the materials was recorded, along with depths of material layering and evidence of oxidation.

Figure 3-11: Example of test site layout on the Old Tailings Dam (OTD-FT-2)

3.1.2.2.1 Saturated Hydraulic Conductivity

Double-ring infiltrometer tests were used to determine the saturated hydraulic conductivity of the OTD materials at the surface. Guelph permeameter tests were used to determine the saturated hydraulic conductivity of the OTD materials at depth.

Ring Infiltrometer

Double-ring infiltrometer tests, previously described in 3.1.2.1.1, were conducted to gain K_{sat} and infiltration data on the fine tailings and hardpan materials. Due to limited time, this test could not be performed on coarse tailings. The standard practice ASTM (2009a) was followed for this test, with the exception that rings were installed to roughly half the recommended depth. The cemented surface of the hardpan material was carefully broken around the perimeter prior to driving the rings into the material. Minor disturbance was patched with a mixture of the local fines and bentonite tamped around the inner and outer ring perimeters. The constant water level in all tests was maintained using the Mariotte tube setup, with the tubes and rings being sheltered as necessary from heat, wind, and precipitation. Ring embedment depths for the OTD materials are summarized in Table 3-5, following the Guelph permeameter discussion.

Guelph Permeameter

Guelph permeameter tests were conducted in all OTD materials to gain three-dimensional infiltration data at depth (Figure 3-12). The procedure that was followed is outlined in Soilmoisture (2010). In summary, a constant head is maintained by the equipment in a bored hole and the rate of water level drop in the permeameter cylinders is recorded over time increments. This water level drop is calibrated to the cylinder volume and converted to a flow rate, from which the three dimensional field saturated hydraulic conductivity may be computed.

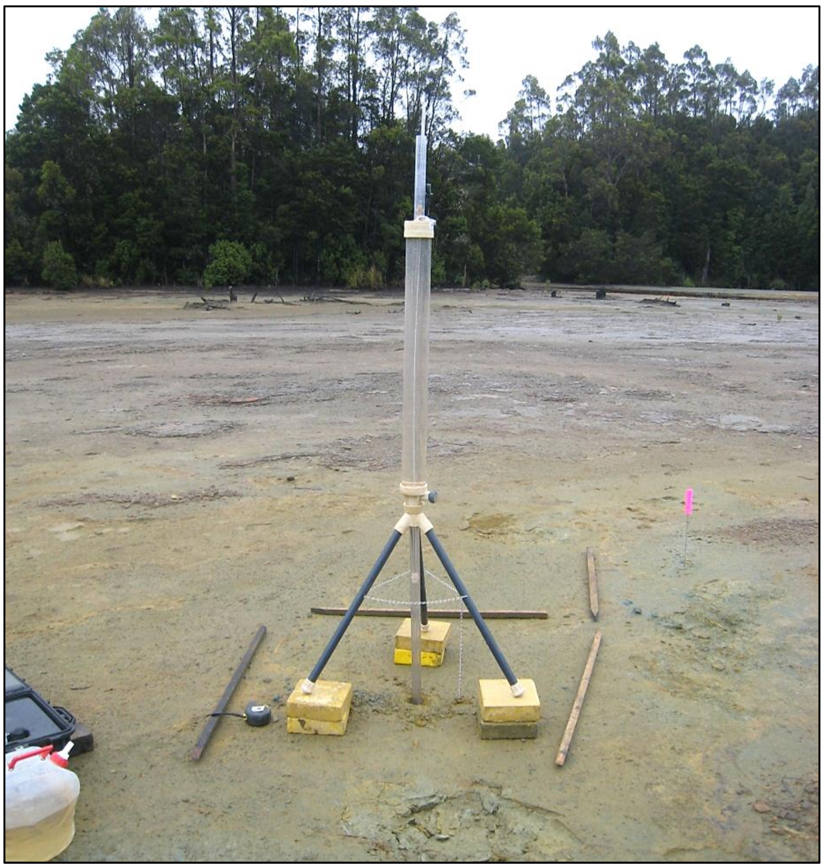

Figure 3-12: Guelph permeameter test at test site OTD-FT-2

Guelph permeameter tests were conducted at two depths for both fine tailings test sites. One test was performed on each of the hardpan sites. Only one coarse tailings location was tested due to the time constraints on the field program. Guelph permeameter test depths are summarized along with ring infiltrometer embedment depths for the OTD materials in Table 3-5.

Table 3-5: Summary of OTD Saturated Hydraulic Conductivity Tests

Test	Material Type	Ring Infiltrometer		Guelph Permeameter	
		Outer Ring Depth (mm)	Inner Ring Depth (mm)	Depth to Bottom of Test Hole 1 (mm)	Depth to Bottom of Test Hole 2 (mm)
OTD-FT-1	Fine Tailings	63	50	160	200
OTD-FT-2	Fine Tailings	78	56	130	230
OTD-HP-1	Hardpan	80	53	160	N/A
OTD-HP-2	Hardpan	59	31	160	N/A
OTD-CT-1	Coarse Tailings	N/A	N/A	14	N/A
OTD-CT-2	Coarse Tailings	N/A	N/A	N/A	N/A

3.1.2.2.2 Density

In-situ density of the tailings materials was determined at two locations at each test site using the water replacement density method, outlined in ASTM D5030 (2004), and previously described in Section 3.1.2.1.2.

Test pits in the tailings material were excavated between 60 mm to 100 mm deep and to the width of the wooden frame, which was considered sufficiently representative in volume for in-situ density determinations.

3.1.2.2.3 Soil Suction

Matric suction in the OTD materials was measured using jet-fill tensiometers and a pressure transducer tensiometer.

Jet Fill Tensiometer

Jet-fill tensiometers were used to measure soil suction at depth in the fine tailings and beneath the hardpan material. The tensiometer was installed in a bored hole of the same diameter as the probe, and twisted in place to ensure hydraulic contact. The tensiometers were then allowed to equilibrate prior to recording the soil suction reading. The temperature of the soil at depth was recorded and the area in contact with the tensiometer pore stone was sampled for moisture content determination following each suction measurement. Figure 3-11 shows the use of jet-fill tensiometers for soil suction measurements at test site OTD-FT-2.

Pressure Transducer Tensiometer

Soil suction was also measured using the UMS Infield 7 handheld read-out unit with the UMS T5 tensiometer probe, as described in 3.1.2.1.3. Measurements using the pressure transducer were taken where the jet-fill tensiometers could not be installed, such as at very shallow depths and in the coarse tailings, as well as for verification and comparison with the jet-fill tensiometer readings. Corresponding soil temperature was recorded and moisture content samples were taken for each reading.

3.1.2.2.4 Sampling

Bulk material and moisture content samples were taken from the OTD in the same manner as on B-Dump; please refer to Section 3.1.2.1.4. Table 3-6 shows the samples collected from the OTD materials.

Table 3-6: List of Bulk Samples Collected from Old Tailings Dam Test Sites

Fine Tailings	Coarse Tailings	Hardpan
OTD-FT-1(D1)	OTD-CT-1(D1)	OTD-HP-1(D1)
OTD-FT-1(D2)	OTD-CT-1(D2)	OTD-HP-1(D2)
OTD-FT-2(D1)	OTD-CT-2(D1)	OTD-HP-2(D1)
OTD-FT-2(D2)	OTD-CT-2(D2)	OTD-HP-2(D2)

*Note regarding sample numbers: the initial label sequence represents the test site location (Table 3-2) and is appended with (D1) and (D2), which represents the density test number where the bulk sample was taken.

3.2 Field Rainfall and Runoff Observations

Natural rainfall events that occurred during the field program allowed direct observation of the runoff response of the materials on B-Dump and the OTD. These observations are discussed in the following sections.

3.2.1 B-Dump Rainfall - Runoff Observations

An extended rainstorm on November 18, 2011, offered the opportunity to observe runoff formation around the B-Dump catchments and over the various materials identified. A measuring cup left out during the storm captured 17 mm of rain in approximately one hour. No rain had fallen in at least the previous 36 hours.

Rainwater began to pond on the surface of fine waste rock material within minutes of the beginning of the storm (Figure 3-13: a). The ponds visibly increased in areal extent and became interconnected within 15 minutes. The ponding depth at this point was visually estimated as less than 5 mm. The ponds continued to increase in areal extent and within five minutes of interconnecting, the surface of the fine waste rock was dominantly covered by ponded water (Figure 3-13: b). Throughout these 20 minutes, the interconnecting ponds began to converge in local low topography and formed small streams that ran downslope. The dominant runoff mechanism for this storm was considered infiltration-excess runoff or Hortonian Overland Flow, because the surface was unsaturated (no recent rainfall) and runoff formed evenly from the surface in sheet flow and minor stream flow (Figure 3-13: c).

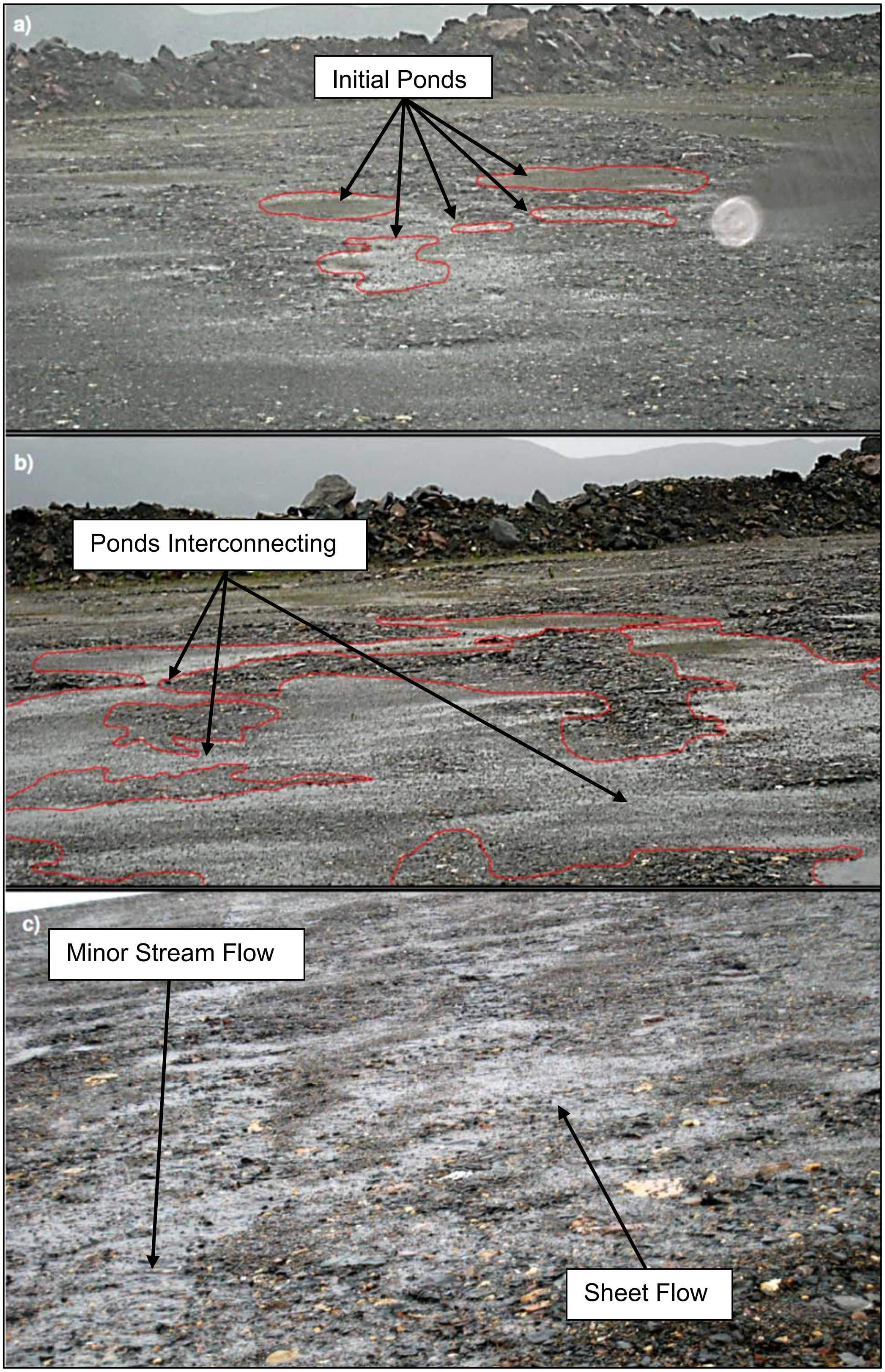

Figure 3-13: Runoff progression on fine waste rock - a) initial ponds outlined, b) interconnected ponds outlined, c) sheet flow and minor stream flow

Similar runoff was observed later in the storm on the coarse clay material (Figure 3-14). While the fine waste rock was producing runoff, surface depressions in the coarse waste rock continued to fill and overland flow was not being generated. Figure 3-15 shows ponded water on coarse waste rock in the background and overland runoff from fine waste rock in the foreground.

Figure 3-14: Runoff flowing over coarse clay overburden

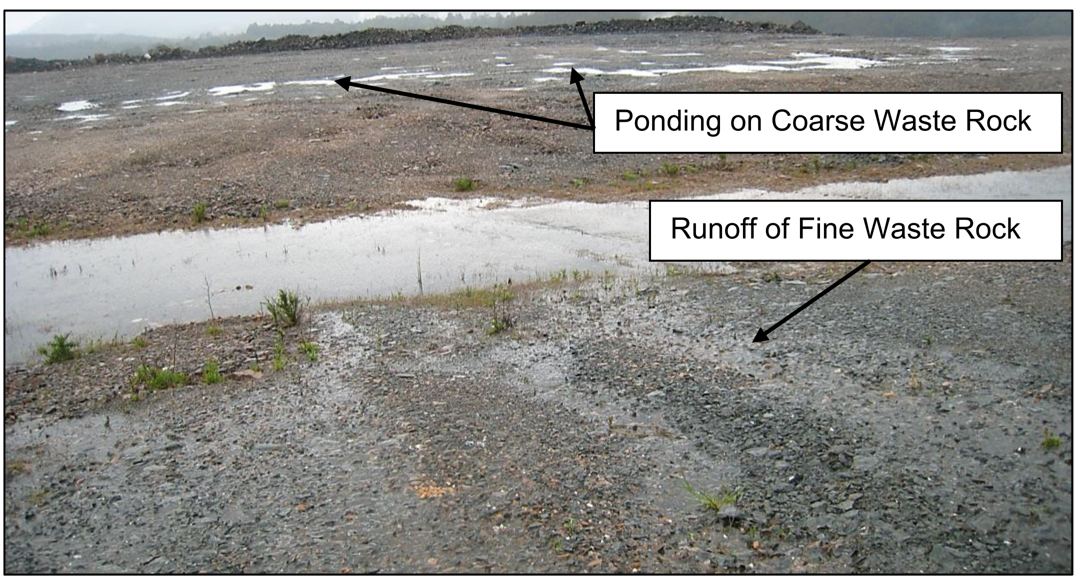

Figure 3-15: Ponded water on coarse waste rock (background) while fine waste rock (foreground) produces runoff (Nov 18, 2011)

Runoff formation was also observed during a storm on November 20, 2011. This storm began with intense driving rain that lasted for approximately 10 minutes, then the storm tapered off to intermittent less intense showers. Surface depressions in the fine clay overburden filled quickly and ponded water formed sheet and minor stream flow shortly thereafter. Visual observation of ponded water on the coarse clay material was recorded as it began to flow downslope and connect with topographically lower ponds. Once connected, the lower ponds subsequently overflowed and runoff continued downslope.

3.2.2 Old Tailings Dam Rainfall - Runoff Observations

Variations in runoff generation from the three materials on the OTD were observed during a minor rain event on November 26, 2011. Ponding occurred on the coarse tailings only in areas where the water table was near the surface. This indicates that saturation excess flow was the dominant runoff mechanism for this particular rainfall event and material. Ponded rainwater in close proximity to the main visible water table is outlined in Figure 3-16.

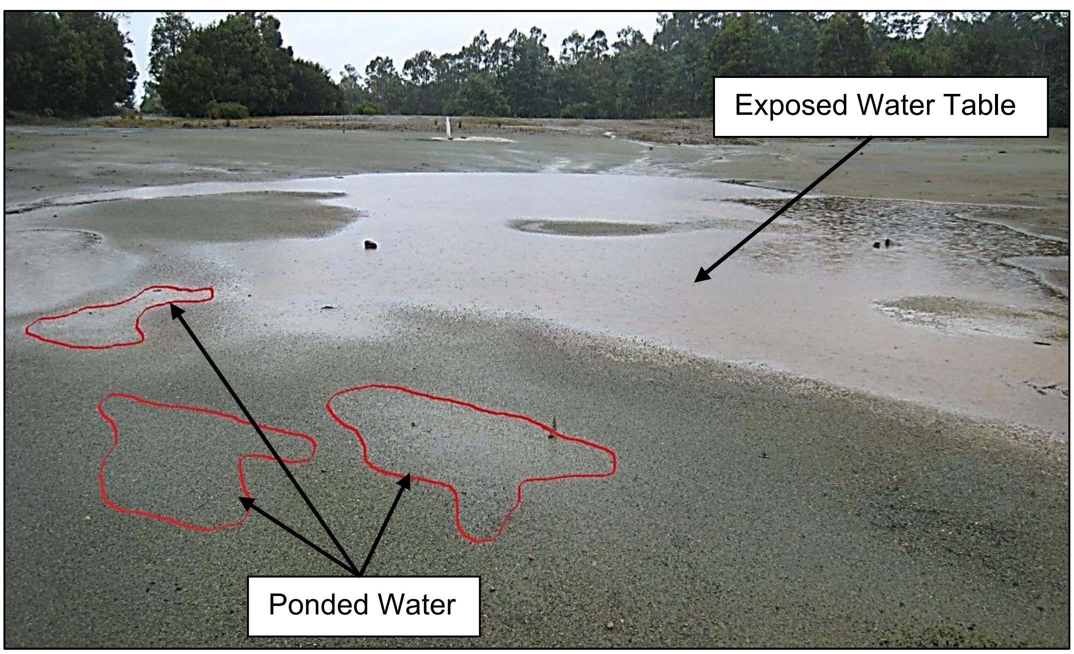

Figure 3-16: Rainwater ponding on coarse tailings near exposed water table

No water appeared to form ponds on the fine tailings during the Nov 26 rain event. Since no surface runoff was generated for this particular observed rainfall event, it indicates that the rainfall rate was lower than the infiltration capacity of the fine tailings and that the water table was below the surface. Runoff from the hardpan surface was observed during the event. Given the close proximity to the fine tailings, and the fact that the water table is not close to the fine tailings surface, the runoff mechanism for the hardpan tailings in this case was likely infiltration-excess runoff. The difference between runoff generation for the hardpan and fine tailings materials is clearly observed in Figure 3-17.

Figure 3-17: Runoff generation discrepancy between hardpan (left) and fine tailings (right) surfaces

3.3 Laboratory Testing

Bulk samples collected during the field program were shipped to the University of Alberta for further laboratory investigation. The minor samples collected for moisture content determination were taken to the geotechnical lab at the Savage River Mine and regularly processed throughout the field program. The following sub-sections outline the reasons for conducting each part of the laboratory investigation and summarize the tests performed.

3.3.1 Preliminary Laboratory Analyses

Grain-size analyses were performed on all bulk samples to verify the material types identified during the field program, and to form the basis for selecting samples for further laboratory investigation.

3.3.1.1 Sieve Analyses

Composite sieve analyses (ASTM 2009b: Method A) were performed to establish the upper grain size distribution (>75 μm) of the coarse waste rock and the coarse clay overburden. Representative specimens of a minimum dry mass of 25 kg for the waste rock and 10 kg for the coarse clay overburden were extracted from the bulk samples.

Representative specimens were manually separated into coarse (> 9.5 mm) and fine (< 9.5 mm) fractions for the composite sieve analysis. The full mass of the coarse fraction was washed through a wire sieve to remove smaller particles that may have adhered to coarser particles. A representative subsample (315 g to 785 g) of the fine fraction was washed through a mesh sieve to remove particles smaller than 75 μm. Each fraction was oven dried after washing. The coarse fraction was processed in multiple batches to avoid overloading the sieve openings. Each coarse batch was processed manually through 75, 50, and 37.5 mm openings, and then mechanically shaken for 10 minutes through sieves with mesh sizes of 37.5, 25, 19, 12.5, and 9.5 mm. The fine fraction subsample was processed in a single batch through sieves of mesh sizes 9.5, 4.75, 2.0, 0.85, 0.425, 0.25, 0.15, 0.106, and 0.075 mm using a mechanical shaker for 10 minutes. The mass of material retained on each sieve was measured for the coarse and fine fractions. The percentage of material passing each sieve was calculated by combining the coarse and fine fraction results according to their mass proportions from the original specimen.

The upper grain size distribution (>75 μm) for the fine clay overburden, fine tailings, and coarse tailings materials was established using a single sieve-set (ASTM 2009b: Method B). Representative specimens with dry masses between 280 g to 550 g were extracted from the bulk sample. The specimens were washed to remove particles smaller than 75 μm and oven dried. A mechanical shaker was used for a minimum of 10 minutes to sieve the specimens through mesh sizes of 9.5, 4.75, 2.0, 0.85, 0.425, 0.25, 0.15, 0.106, and 0.075 mm. The mass of material retained and percent passing each sieve was determined.

3.3.1.2 Hydrometer Analyses

Hydrometer analyses were performed in accordance with ASTM D422 (2007a) to determine the grain size distribution smaller than 75 µm. The hydrometer storage cylinder was filled with distilled water and 125 mL of sodium hexametaphosphate dispersing agent. The solution was left to equilibrate to room temperature prior to determining the hydrometer reading correction factor for the test. Specimens were air-dried and then soaked in 125 mL of the dispersing agent for a minimum of 16 hours. The specimen slurry was then transferred to a dispersion cup and dispersed for one minute using an electric mixer. After transferring the dispersed slurry into the sedimentation cylinder, the cylinder was filled with distilled water, capped, and agitated (turned upside down and back) for one minute.

Hydrometer readings and corresponding slurry temperature measurements were taken at 1, 2, 5, 10, 15, 30, 60, 250, and 1440 cumulative minutes, as per ASTM D422 (2007a). Additional readings were taken as frequently as possible immediately after cylinder agitation was complete. The readings were corrected using the meniscus and solution correction factors. The diameter of soil particles in suspension, based on Stoke's law for sedimentation, and the percent of soil in suspension were then calculated. The sample was washed through a 75 µm sieve, oven dried, and a sieve analysis performed on the remaining material once the hydrometer test was complete.

3.3.1.3 Sample Selection for Detailed Laboratory Testing

One bulk sample from each distinct material type was selected for detailed laboratory testing to expedite the laboratory program. Selection was primarily based on how closely the sample represented the grain size distributions of all samples of the corresponding material type. Table 3-7 lists the final samples selected for detailed testing.

Additional criteria were considered when selecting the bulk sample to represent the fine waste rock and the coarse clay overburden materials. The sample that represented the typical grain size distribution for fine waste rock was collected from the first test site of the field program, where foot-traffic disturbance of the surface was not actively avoided. The fine waste rock bulk sample ultimately selected for detailed testing was collected from an undisturbed area and was still within 2% of the typical grain size distribution. Complications during infiltration testing were encountered at the test site where the typical coarse clay overburden sample was taken. The second-closest coarse clay bulk sample, which was still within 5% of the typical grain size distribution, was selected to maintain quality infiltration data associated with detailed sample analysis.

Table 3-7: Bulk Samples Selected for Detailed Laboratory Testing

Sample Label	Material Type
BD1-C-4(D2)	Coarse clay overburden
BD1-C-5(D1)	Fine clay overburden
BD2-C-2(D2)	Fine waste rock
BD2-C-3(D1)	Coarse waste rock
OTD-FT-2(D2)	Fine tailings
OTD-CT-1(D1)	Coarse tailings
OTD-HP-2(D1)	Hardpan

3.3.2 Detailed Laboratory Testing

Detailed laboratory testing for the B-Dump and OTD materials included soil classification, specific gravity, and soil-water characteristic curve tests. These tests are discussed in the following sections.

3.3.2.1 Detailed Soil Classification

Detailed soil classification was performed on selected samples, including combined sieve and hydrometer analyses and liquid and plastic limit tests.

Detailed Grain Size Analysis

The Unified Soil Classification System (USCS) was used to describe soils in common terminology based on their particle size and plasticity characteristics (ASTM 2011). The USCS classification of each sample listed in Table 3-7 was determined based on the combined particle size distribution from hydrometer and sieve analysis and the Atterberg limits results. The classifications for the bulk samples not selected for detailed testing were inferred based on the test results from the samples that represented the average of each material (Table 3-7).

Hydrometer analyses were conducted on the first six samples listed in Table 3-7. The texture of the hardpan tailings was much finer than the other OTD and B-Dump materials; therefore, a hydrometer analysis (ASTM 2007a) was performed on all hardpan bulk samples to establish the grain size distribution. Approximately 100 g specimens extracted from the bulk sample and representing the material finer than 2.0 mm were tested using the method outlined in ASTM D422 (2007a). This process was described previously in Section 3.3.1.2. The results of the hydrometer analysis were combined with the corresponding sieve analysis to complete the particle size distribution of the first six samples in Table 3-7.

Liquid and Plastic Limits

Atterberg limit tests were conducted on the samples listed in Table 3-7 in accordance with the wet preparation method outlined in ASTM D4318 (2010a). A representative portion of the total sample was sieved through a 425 μm (No. 40) sieve to obtain approximately 200 g of material passing the sieve. The fine material was mixed with distilled water until it approached the estimated consistency of its liquid limit and then allowed to cure in a sealed container for 16 hours prior to testing. The multi-point liquid limit test was performed on all materials. The number of blows of the liquid limit device to close a groove in the material along a distance of 13 mm was recorded. The moisture content of the material was adjusted by air drying or by mixing with distilled water to achieve trials where the blow count numbered between 15 to 25, 20 to 30, and 25 to 35. The blow count was plotted with the moisture content of each trial so the liquid limit (i.e. moisture content corresponding to a blow count of 25) could be read off the graph.

The plastic limit of the material finer than 425 μm was also determined following ASTM D4318 (2010a) . The material was rolled into threads 3.2 mm in diameter, then kneaded and re-rolled until the material could no longer reach a 3.2 mm diameter thread. The moisture content of the material at this point was determined and the average of subsequent trials was taken as the plastic limit.

3.3.2.2 Specific Gravity

The specific gravity of a soil is the ratio of the density of the soil particles to the density of water. Assuming that soil particles will displace an equivalent volume of water, specific gravity is determined by finding the mass of a dry soil specimen and the mass of the same specimen in water.

Specific gravity is used with the in-situ density and moisture content obtained during the field program to determine useful mass-volume relationships. These mass-volume relations include the porosity (n), void ratio (e), and water content relations, which are valuable in unsaturated soils investigations. Specific gravity tests were conducted on the bulk samples listed in Table 3-7.

3.3.2.2.1 B-Dump Materials

The texture of the B-Dump materials was too coarse to conduct specific gravity tests using a single standard method. B-Dump materials were separated into fine and coarse test fractions based on particle sizes passing and retained on a designated sieve. The designated sieve for waste rock and clay overburden was the 4.75 mm (No. 4) sieve and the 2.0 mm (No. 10) sieve, respectively.

The average specific gravity of the full sample was computed using the mass percentage of each size fraction, as obtained from the sieve analysis. ASTM C127 (2007b) provides three ways of calculating the specific gravity – the oven dry, saturated surface dry, and apparent specific gravity methods. The in-situ condition of the material in the field is likely such that water has penetrated into the pores of the particles (absorption is satisfied), therefore the saturated surface dry calculation was deemed most appropriate.

Fine Fraction

A representative portion of the bulk sample was processed through the designated sieve to yield the fine fraction for specific gravity testing. The specific gravity for the fine fraction of the B-Dump materials was obtained using the water pycnometer method outlined in ASTM D854 (2010b). The tests were performed in 500 mL volumetric pycnometer flasks. Multiple determinations of the dry mass of the flask and mass when filled to the calibration mark with de-aired distilled water were performed, with average values used in calculations.

Moist specimens from the fine processed material were sampled to obtain representative dry masses of approximately 100 g for waste rock material or 75 g for clay material. Specimens were mixed with approximately 100 mL of distilled water and dispersed by stirring. After transferring the slurry to the pycnometer, the flask was filled to roughly 1/3 volume with de-aired distilled water. The pycnometer was attached to a vacuum and the slurry was agitated for 10 minutes to remove entrapped air. The flask was then carefully filled almost to the calibration mark with de-aired distilled water and reattached to the vacuum for a minimum of 16 hours (Figure 3-18). This period allowed the slurry temperature to equalize with room temperature and the vacuum to further remove any entrapped air. The pycnometer was filled to the calibration mark with de-aired, distilled, room-temperature water using a small pipette following the vacuum period. The mass of the pycnometer, soil, and water was determined and the temperature of the pycnometer contents was taken using a digital thermometer. The contents of the pycnometer were carefully transferred to a container, oven dried, and the final dry mass of the soil was determined.

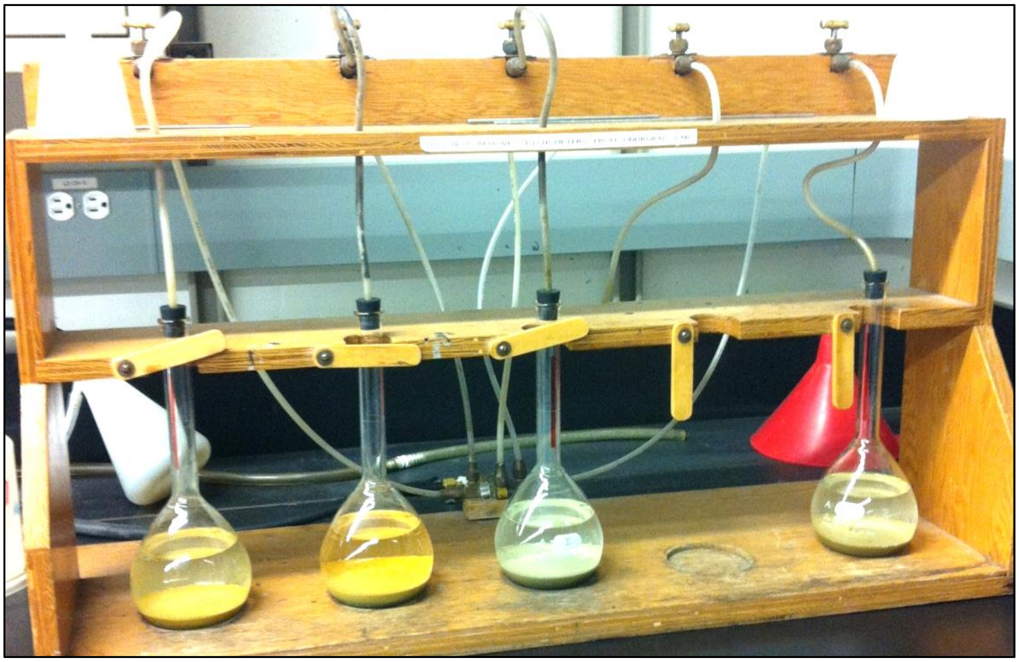

Figure 3-18: Specific gravity testing of fine materials using water pycnometer

Coarse Fraction

The coarse fraction of the B-Dump materials was tested according to ASTM C127 (2007b). In general, each test specimen was washed free of fine particles and oven dried; the details of the specimen preparation for the various materials are discussed in the following paragraphs. Once cooled, the specimen was soaked in tap water for approximately 24 hours. After the soaking period, the specimen was rolled on a towel to remove visible beads of water and the saturated-surface-dry mass was recorded. The specimen was then transferred into a wire mesh bucket, submerged in a tub of room temperature water, gently agitated to dislodge any air bubbles, and the apparent mass of specimen in water was recorded. Finally, the oven dried mass of the specimen was determined.

The specific gravity of the coarse fraction of the waste rock materials was tested in two size portions; one for particles greater than 12.5 mm, and a second for particles between 4.75 mm and 12.5 mm. Given the mass of the test sample required for the portion with particles greater than 12.5 mm, waste rock originally processed for the sieve analysis had to be utilized. This material had been previously washed free of fine material and oven dried as part of the sieve analysis procedure. The previously sieved material was processed manually through the 12.5 mm sieve and the retained particles saved for the specific gravity test portion on particles larger than 12.5 mm. A representative mass of 2 kg was pulled from the bulk waste rock sample, and then manually processed through the 12.5 mm sieve. The particles larger than 12.5 mm were discarded and the material was then washed on a 4.75 mm sieve to remove the smaller particles. The remaining material represented the 4.75 mm – 12.5 mm test portion and was oven dried to maintain a consistent preparation practice as with the >12.5 mm portion.

The specific gravity of the clay overburden coarse fraction was determined in one size portion. A 2 kg representative sample of the bulk fine clay material was processed over the 2.0 mm sieve. The larger particle size of the coarse clay fraction required a 5 kg representation of the bulk sample to be processed over the 2.0 mm sieve. The particles finer than 2.0 mm were set aside and used in testing the fine fraction with the pycnometer method (discussed above). The particles larger than 2.0 mm were thoroughly washed on the 2.0 mm sieve, with the retained material oven dried and used in the coarse portion specific gravity testing.

3.3.2.2.2 Old Tailings Dam Materials

Materials from the OTD were tested using the water pycnometer method for moist specimens (ASTM 2010b). The initial water content of the OTD materials was determined and the material sampled to yield a representative specimen with a dry mass of approximately 75 g. The tests were performed in 500 mL volumetric pycnometer flasks. The remaining process used for specific gravity testing was previously summarized in the “fine fraction” paragraphs of Section 3.3.2.2.1.

3.3.2.3 Soil-Water Characteristic Curves

The Soil-water characteristic curve (SWCC) describes the relationship between soil suction and volumetric water content for a soil (Fredlund and Xing 1994). The SWCC can be used to predict other unsaturated soil parameters including unsaturated hydraulic conductivity (Fredlund et al. 1994).

Soil-water characteristic curves were determined on the B-Dump and OTD samples listed in Table 3-7 using the Tempe cell apparatus and test procedure outlined in Fredlund and Rahardjo (1993). Plexiglas® Tempe cells (70 mm ID, 100 mm tall) with 1-bar ceramic pore stones were used for the fine clay overburden specimens from B-Dump and for all OTD specimens. Stainless steel Tempe cells (156 mm ID, 180 mm tall) with 1-bar ceramic stones were used for the fine and coarse waste rock and coarse clay overburden specimens from B-Dump. These cells are pictured in Figure 3-19. Miller et al. (2002) notes that SWCCs are dependent on compactive effort but not compaction water content, and that SWCCs determined from laboratory-compacted specimens are not significantly different from field-compacted specimens. Therefore, the in-situ dry density of each material was reproduced as best as possible in the SWCC specimen. Air dried specimens were mixed to the gravimetric water content representing the in-situ condition then manually compacted in the cell. The compacted specimen filled approximately 50% of the cell volume.

Figure 3-19: Large (left) and small (right) Tempe cells used for soil-water characteristic curve testing

Specimens were saturated in the cell at atmospheric pressure from the bottom up with distilled water, and then left at saturation for a minimum of 24 hours. Excess water was drained from the specimen, and then the initial sample height and the saturated sample plus cell mass was recorded.

The low suction portion of the SWCC for the fine and coarse waste rock, coarse tailings, and hardpan samples was defined using the hanging column method. The "zero" height of the Tempe cell discharge was measured and then the discharge tubing was lowered by 10 mm to represent 0.1 kPa of matric suction. A capillary needle was placed in the discharge tube and water draining due to the applied suction was collected in a container. The mass of the sample and cell was monitored during each increment until no further change in mass was observed. At this time, the water content of the specimen was considered to be in equilibrium with the applied matric suction, so the total mass of the sample and cell were recorded for that increment. The discharge tubing was lowered incrementally, applying higher suction pressures, and the equilibrated mass recorded for each increment. The hanging column method was used up to a maximum of 7 kPa (discharge tube 0.7 m lower than "zero" height).

Suction was initially applied using air pressure for the fine and coarse clay overburden and fine tailings samples. Air pressure, to represent matric suction, was initially applied at 0.25 PSI (1.7 kPa) increments, increasing to 2 PSI increments at higher applied pressures. The hanging column samples were transferred to air pressure gauges once the lowest discharge height was reached. Air pressure was similarly applied at higher increments and the equilibrated mass measured at each increment.

The final mass and final sample height were recorded once equilibrium was reached at the final applied pressure increment. The specimen was removed from the cell and its gravimetric water content determined. The water content of the specimen could be back-calculated for each pressure increment using the final water content and recorded changes in mass. The water content and the suction were then plotted to create the SWCC for the specimen.

3.3.3 Grout Hydraulic Conductivity

A sand-cement-bentonite grout was used to seal the voids between the steel ring infiltrometer and excavated waste rock, as previously discussed in

Section 3.1.2.1.1. The hydraulic conductivity of the cured grout mix was measured to confirm that it was lower than that of the waste rock to ensure proper interpretation of the field infiltration test results.

The cement in the dry grout mix samples taken from site appeared to have hydrated by the time grout testing commenced at the U of A, perhaps from humidity trapped within the sample bag. The dry site samples were mixed for hydraulic conductivity testing but behaved like wet sand, developing minimal cementation and virtually no strength upon curing. This behaviour was quite unlike the grout used during infiltration testing in the field program.

A similar sand-cement-bentonite mixture, with the same mix ratio of 10:3:1, was created using fresh materials available at the University of Alberta. The particle size distributions for the site and University sands were nearly identical (as shown in Figure 3-20). The cement used in both cases was typical “Portland” cement and the bentonite used in both cases was “driller mud” type bentonite. When mixed with water, the grout was consistent with the grout mixed on site and developed similar strength upon curing.

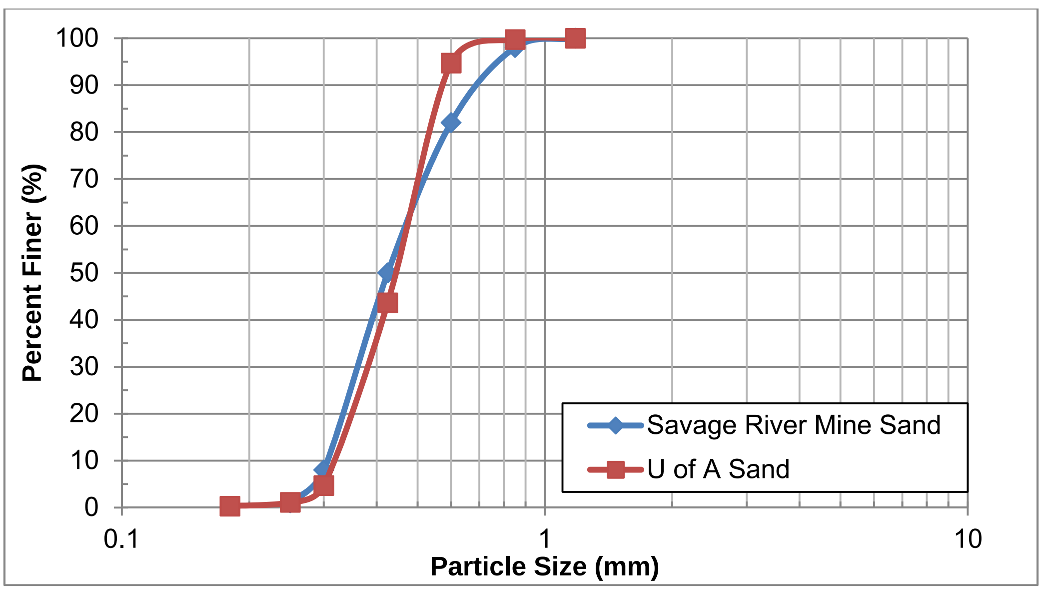

Figure 3-20: Particle size distribution of sands used in grout mixes

Constant head testing was performed, in duplicate, in the lab to verify the hydraulic conductivity of the University grout mix. The dry mix was prepared with tap water and thoroughly mixed to the same consistency achieved in the field. The grout was poured into the permeability chamber and tamped slightly to reduce air voids using a technique similar to that used in the field. The grout was allowed to cure overnight, replicating the curing time generally achieved in the field.

The maximum head applied to the grout during the field program was approximately 100 mm. Therefore a maximum field gradient of 4 was applied for an estimated minimum field grout thickness of 25 mm. The grout thickness used in the lab combined with equipment restrictions allowed a minimum gradient of 5.1 to be applied in the lab.

The cumulative flow through the specimen was recorded over time once the constant head was applied. Evaporation was prevented during the test. Measurements were taken periodically over 24 hours, after which the test was stopped. Extended testing duration was considered unnecessary since field tests were generally complete within 24 hours as well.

Chapter 4. FIELD AND LABORATORY RESULTS

The field and laboratory results for the B-Dump and OTD materials are provided in the following subsections. The areal extent of the material types and catchment areas are described. Summaries of the in-situ material properties and properties obtained from both the general and detailed laboratory tests are given. The analyses conducted on the bulk sample selected for detailed testing were considered to be representative of the remaining bulk samples. Selection of material properties used for modelling is discussed later in Section 5.1 and 5.2. The data gathered during the field and laboratory program is provided in digital format in the Appendix.

4.1 B-Dump

B-Dump is capped with fine and coarse textured alkaline waste rock and clay overburden. The perimeters of each material type and each instrumented catchment were mapped in detail. The characteristics of the mapped areas and the defined materials are discussed below.

4.1.1 Material Zones and Catchment Mapping

The areal extent of the four materials and verification points for catchment boundaries were mapped by recording GPS coordinates and a written description of each waypoint. The resolution provided by the GPS was not precise enough to exactly map the catchments and material areas, since decimal seconds could not be recorded as part of the coordinate. Therefore, the GPS waypoints were superimposed upon a scaled raster image of B-Dump to aid in the interpretation. The distance between each second recorded by the handheld GPS is a maximum of 30 m, according to the global positioning of latitude and longitude. The GPS waypoint as depicted on the image should therefore be within 15 m of its actual location on B-Dump. Material areas and were then outlined based on a combined interpretation of the waypoints and their descriptions and the B-Dump image.

B-Dump contains five catchment boundaries that are defined based on the topography of the soil cover. Runoff from Catchment 1 and Catchment 2 flows south and both these catchments have previously measured rainfall-runoff data. Runoff from Catchments 3, 4, and 5 flows north off the dump and joins natural drainage into the mine; thus it cannot be directly measured and these catchments will be omitted from further discussion. General boundaries for the catchments were provided by Grange Resources. Finalized catchment areas for the purposes of this research were interpreted using these general boundaries, GPS waypoints, the image of B-Dump, and 2010 topographic data of B-Dump. Table 4-1 shows the total area of each catchment and the area of each material zone present within the catchment.

Table 4-1: B-Dump Catchment and Material Zone Areas

Catchment 1		**Catchment 2**	
Material Type	**Area (ha)**	**Material Type**	**Area (ha)**
Fine waste rock	5.07	Fine waste rock	2.44
Coarse clay	5.32	Coarse waste rock	1.03
Fine clay	1.60	Coarse clay	1.95
Catchment 1 - Total	*11.99*	*Catchment 2 - Total*	*5.41*

Figure 3-3, previously provided, shows the catchment areas and material zones on B-Dump, along with test locations.

Generally, Catchment 1 was found to have slopes that range from 3.5% up to 8.8%. Catchment 2 had slopes that range from 0% to 4.0%. These values of slope represent the general surface area of each catchment. They do not include the slopes present on material berms, which were up to 14% in each catchment, but did not make up a significant percentage of the overall catchment areas.

4.1.2 B-Dump Material Properties

Fine and coarse run-of-mine waste rock and fine and coarse clay overburden were identified visually during the field program. The material properties determined during the field and laboratory program for each of the B-Dump materials are discussed in detail in the following sections. Average properties of the four material types are summarized in Table 4-2. Particle size distributions of the representative samples (from Table 3-7) of B-Dump materials are provided in

Figure 4-1. Soil-water characteristic curves fitted to the raw data points are shown in Figure 4-2.

Table 4-2: Summary of Average Properties of B-Dump Materials

Material Type	USCS	% Cobbles	% Gravel	%Sand	%Silt	%Clay	Dry Density (g/cm^3)	Specific Gravity	Void Ratio	Surface K_{sat}* (m/s)	Air Entry Value (kPa)	Limits LL - PL
Fine Waste Rock	GM, Silty gravel with sand	0	57	29	10	4	2.40	2.86	0.20	2.1E-07	5	non-plastic
Coarse Waste Rock	GP-GM, Poorly-graded gravel with silt, cobbles, and sand	2	64	27	6	3	2.40	2.76	0.16	1.4E-06	2	non-plastic
Fine Clay	ML, Sandy silt	0	8	46	39	20	1.35	2.60	0.93	1.6E-06	13	43 - 32
Coarse Clay	SM, Silty sand with gravel	0	45	36	14	6	2.07	2.64	0.28	5.1E-07	12	32 - 25

* NOTE: This average surface K_{sat} is the geometric mean of the measured values.

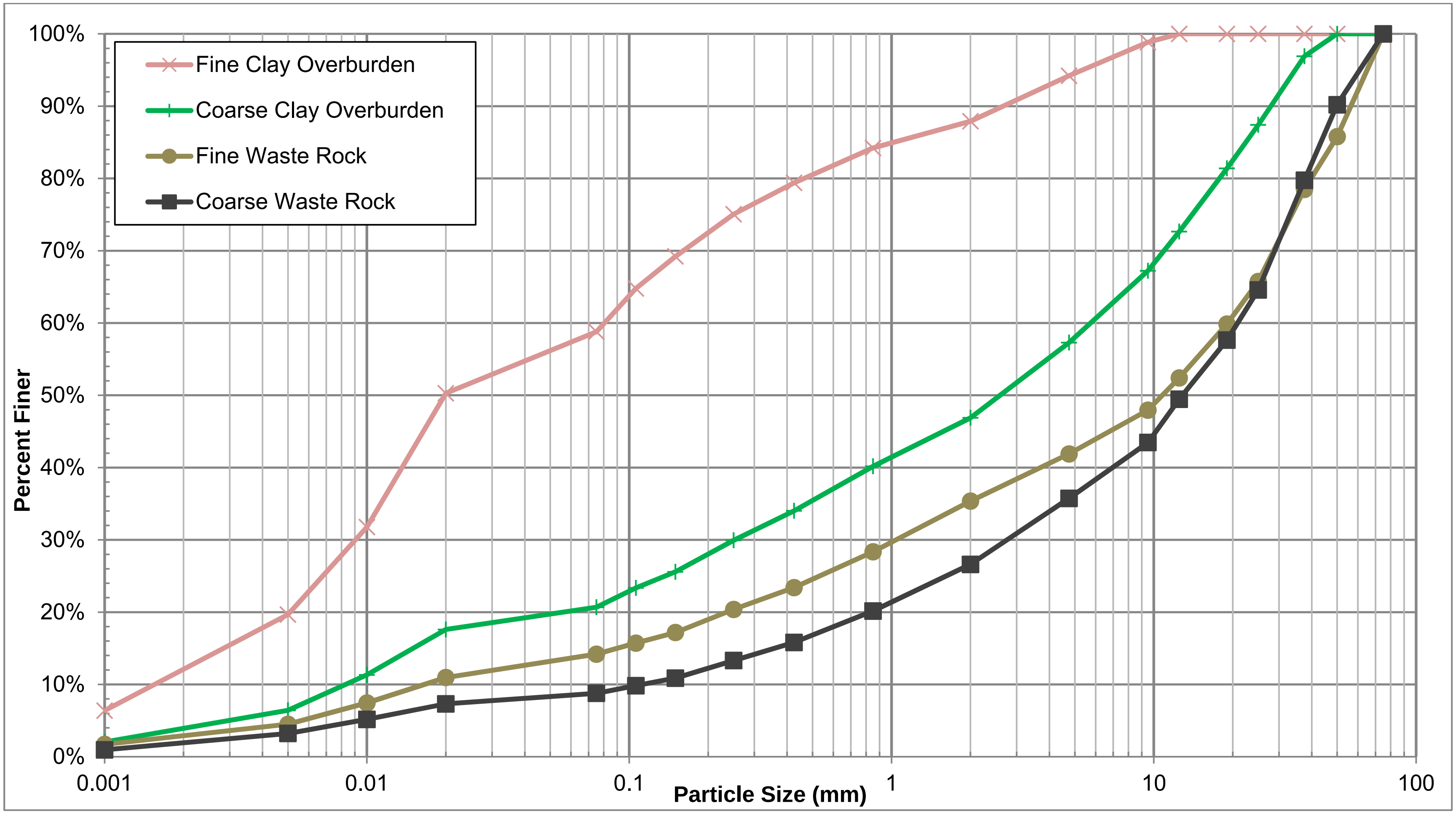

Figure 4-1: Representative particle size distributions for B-Dump materials

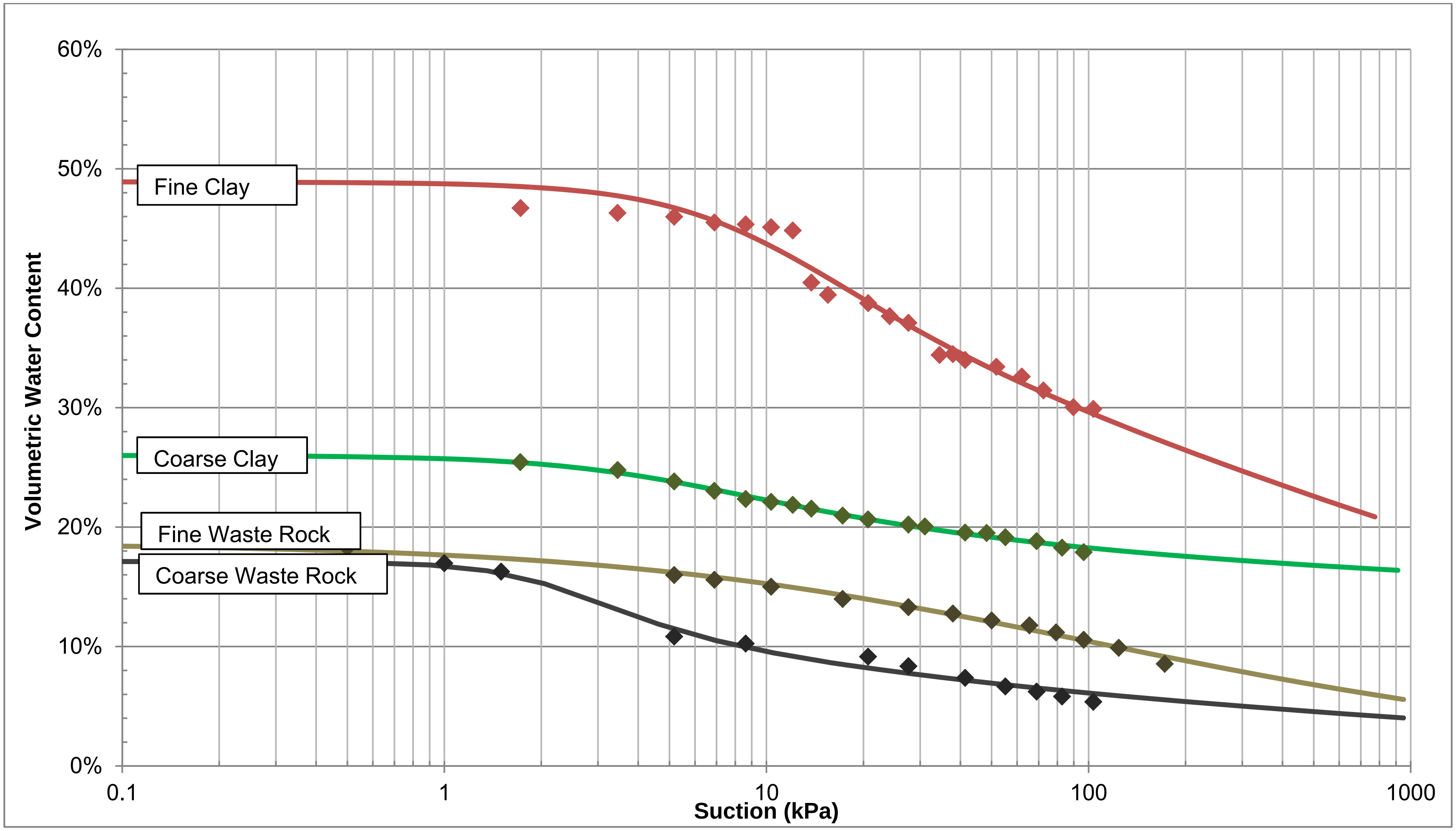

Figure 4-2: Soil-water characteristic data points with the fitted Fredlund and Xing (1994) curves for B-Dump materials

4.1.2.1 Run-of Mine Waste Rock

Fine Waste Rock

All six samples of the fine waste rock, taken from three test locations, fitted the USCS classification of silty gravel with sand (GM). The material was grey and compact in-situ, with angular particles (previously pictured in Figure 3-1:a). The particle size distribution fell within the range of 53% to 59% gravel, 28% to 33% sand, and 13% to 14% fines (<75 μm). The hydrometer analysis on the representative sample (Table 3-7) showed the material was composed of 10% silt and 4% clay. The material was generally poorly sorted and exhibited a slight gap-gradation with minimal presence of silt particles from 0.03 mm to 0.075 mm. Samples were taken from the top 100 mm of the cover and this material was exposed to runoff and wind erosion, which may have removed these fine particles causing the gap-gradation. Atterberg limits could not be determined for the fine waste rock, as the blow count would not reach 25. The fines were therefore considered non-plastic. The particle size distribution for the representative sample was provided in Figure 4-1.

The specific gravity of the fine waste rock was determined as 2.86. The in-situ dry density ranged from 2.19 to 2.55 g/cm^3, averaging 2.40 g/cm^3. The corresponding gravimetric water content ranged from 3.2% to 6.4%, averaging 4.5%. The in-situ void ratio was calculated as ranging from 0.12 to 0.31, with an average of 0.20.

Saturated hydraulic conductivity (K_{sat}) ranged from 7.7x10^{-8} to 4.1x10^{-7} m/s for the top 30 mm of material, and the geometric average was 2.1x10^{-7} m/s.

No relationship between suction and sample depth or soil temperature and depth was observed for the fine waste rock material. Suction values ranged from 7 kPa to 100 kPa and soil temperature ranged from 11 to 22.5 ^{o}C at varying points in the excavation. The gravimetric water content was fairly uniform with depth, ranging from 2.9% to 7.5%.

The SWCC for fine waste rock showed the material desaturated immediately and gradually with increasing suction. The fine waste rock had an air entry value

(AEV) of 5 kPa, which corresponded to a volumetric water content of 16% and a gravimetric water content of 7%. Curve fitting of the experimental data using the Fredlund and Xing (1994) method in the Soilvision (2010) computer program suggested a residual volumetric water content of approximately 5%. The experimental data and the fitted SWCC for fine waste rock were provided in Figure 4-2.

Coarse Waste Rock

The four samples of coarse waste rock, from two test locations, had USCS classification GP-GM, and range from poorly-graded gravel with silt and sand to poorly-graded gravel with cobbles, silt, and sand. The material was grey with very angular particles that interlocked (previously pictured in Figure 3-1:b). The particle size distribution fell within the range of 0% to 3% cobbles, 62% to 65% gravel, 25% to 29% sand, and 7% to 9% fines (<75 μm). The hydrometer analysis on the representative sample (Table 3-7) showed the material was composed of up to 6% silt and 3% clay. The material exhibits a slight gap-gradation where silt particles from 0.03 mm to 0.075 mm diameter are minimal, similar to the fine waste rock. The material was considered non-plastic since Atterberg limits could not be determined. The particle size distribution for the representative sample was previously provided in Figure 4-1.

The specific gravity of the coarse waste rock was 2.76. The in-situ dry density ranged from 2.24 to 2.56 g/cm^3, and averaged 2.39 g/cm^3. The corresponding gravimetric water content ranged from 1.7% to 6.2%, and averaged 4.3%. The in-situ void ratio ranged from 0.08 to 0.23, with an average of 0.16.

The K_{sat} ranged from 1.1x10^{-6} to 1.7x10^{-6} m/s for the top 50 mm of material, with a geometric average of 1.4x10^{-6} m/s.

The measured suction decreased by approximately 4 kPa over the 125 mm testing depth in the coarse waste rock. Soil temperature averaged 23.5 ^{o}C at 15 mm depth and 19 ^{o}C between 50 and 125mm depths. Gravimetric water content at the surface (15 mm depth) averaged 6.2% and 4.5% between 50 and 125 mm depths.

The AEV for the coarse waste rock was approximately 2 kPa, which corresponded to a volumetric water content of 15% and a gravimetric water content of 7%. Curve fitting of the experimental data using the Fredlund and Xing (1994) method in the Soilvision (2010) computer program suggested a residual volumetric water content of approximately 7.5%. The experimental data and the fitted SWCC for coarse waste rock were previously provided in Figure 4-2.

4.1.2.2 Clay Cap from Overburden

Fine Clay Overburden

The four samples of fine clay, collected from two test locations, varied in texture from USCS classification ML to SM. The material ranged from sandy silt to silty sand to silty sand with gravel. The material was “rusty” red in color and contained traces of weathered stones that flaked or crumbled with moderate effort (pictured in Figure 3-2:a). The gravel content ranged from 5% to 7% for three samples and one sample contained 15% gravel. The sand content was either 55% or 37%, and the fines (<75 μm) content was either 33% or 57%, for the four samples collected. The hydrometer analysis on the representative sample (Table 3-7) showed the material contained up to 39% silt and 20% clay. Minor gap-gradation was found for silt particles 0.03 mm to 0.075 mm in diameter. The material had a liquid limit of 43, a plastic limit of 32, and a plasticity index of 11. The particle size distribution for the representative sample was previously provided in Figure 4-1.

The specific gravity of the fine clay overburden was 2.60. The in-situ dry density ranged from 1.24 to 1.49 g/cm^3, averaging 1.35 g/cm^3. The corresponding gravimetric water content ranged from 24% to 36%, and averaged 31%. The in-situ void ratio was calculated as ranging from 0.75 to 1.1, with an average of 0.93.

The K_{sat} ranged from $7.6\text{x}10^{-7}$ to $3.1\text{x}10^{-6}$ m/s for the top 50 mm of material, with a geometric average of $1.6\text{x}10^{-6}$ m/s.

Suction ranged from 13 to 15 kPa over the 110 mm testing depth, decreasing slightly as depth increased. Soil temperature was uniform (9 to 10 ^{o}C) or decreased (18 to 12 ^{o}C) with depth, depending on test location. The gravimetric water content was fairly uniform with depth, averaging approximately 33%.

The fine clay has an AEV of 13 kPa, which corresponded to a volumetric water content of 42% and a gravimetric water content of 36%. Curve fitting of the experimental data using the Fredlund and Xing (1994) method in the Soilvision (2010) computer program suggested a residual volumetric water content of approximately 30%. The experimental data and fitted SWCC for fine clay were previously provided in Figure 4-2.

Coarse Clay Overburden

The clay cover material was sourced from weathered clayey overburden removed from the mine's south expansion area. The current clay overburden cap on B-Dump was sourced from the same area and placed using similar methods as the material directly tested by Thompson and Brett (2002), which was subsequently covered or significantly disturbed by additional construction on B-Dump. The properties obtained by Thompson and Brett (2002), discussed in Section 2.4, are comparable to those determined by this research for the coarse clay material.

The four samples of coarse clay, collected from two test locations, varied in texture from USCS classification SM to GM. The material ranged from silty sand with gravel to silty gravel with sand. Similar to the fine clay, the material was "rusty" red in color and contained some weathered stones that broke apart or flaked with moderate effort (pictured in Figure 3-2:b). The particle size distribution ranged from 42% to 51% gravel, 33% to 37% sand, and 16% to 21% fines (<75 μm). The hydrometer analysis on the representative sample (Table 3-7) showed the material was composed of 14% silt and 6% clay. Silt particles from 0.03 mm to 0.075 mm in diameter were also minimal in the coarse clay particle size distribution. The material had a liquid limit of 32, a plastic limit of 25, and a plasticity index of 7. The particle size distribution for the representative sample was previously provided in Figure 4-1.

The specific gravity of the coarse clay overburden was 2.64. The in-situ dry density ranged from 2.00 to 2.15 g/cm^3, and was 2.07 g/cm^3 on average. The corresponding gravimetric moisture content ranged from 11% to 14%, and was 13% on average. The in-situ void ratio was calculated as ranging from 0.23 to 0.32, with an average of 0.28.

The K_{sat} ranged from 2.9x10^{-7} to 9.4x10^{-7} m/s for the top 50 mm of material, with geometric average of 5.1x10^{-7} m/s.

Soil suction of the coarse clay overburden ranged between 1 to 6 kPa at varying points in the 80 mm testing depth. Soil temperature varied between 9 and 17 ^{o}C, but no trend was apparent between temperature and depth. The gravimetric water content decreased slightly with depth, from an average of 16% at 15 mm depth to 14% between 55 to 80 mm depth.

The SWCC for coarse clay showed gradual desaturation and an AEV of approximately 12 kPa. This AEV corresponded to a volumetric water content of 22% and a gravimetric water content of 12%. Curve fitting of the experimental data using the Fredlund and Xing (1994) method in the Soilvision (2010) computer program suggested a residual volumetric water content of approximately 10%. The experimental data and the fitted SWCC for coarse clay were previously provided in Figure 4-2.

4.1.2.3 Grout Mix

The results of the constant head test on the two University of Alberta grout samples are shown in Figure 4-3. The cumulative permeability of the grout decreased considerably within the first two hours of testing, dropping to 34 - 44% of the initial permeability. The permeability of the grout tended toward a constant value between 19 - 23% of the initial permeability by the end of the test. The initial permeability was between 1.8x10^{-8} to 4.2x10^{-8} m/s. And the final permeability reached was between 3.6x10^{-9} to 9.5x10^{-9} m/s.

The initial grout permeability was between 10 to 22 times less than the fine waste rock K_{sat} and the final grout permeability was between 43 to 115 times less The initial grout permeability was between 26 to 60 times less than the K_{sat} of the coarse waste rock material and the final grout permeability was between 116 to 310 times less. These results are conservative, given that 1) the gradient applied in the lab was higher than that applied in the field and 2) the grout thickness in the field was likely greater than estimated minimum of 25 mm in most areas. The surface area covered by the grout during the infiltration test was also minimal compared to the exposed waste rock surface being tested. Therefore, it was considered that this grout mix provided a satisfactory seal and infiltration through the grout would have a negligible impact on the saturated hydraulic conductivity results for the grouted waste rock infiltration tests.

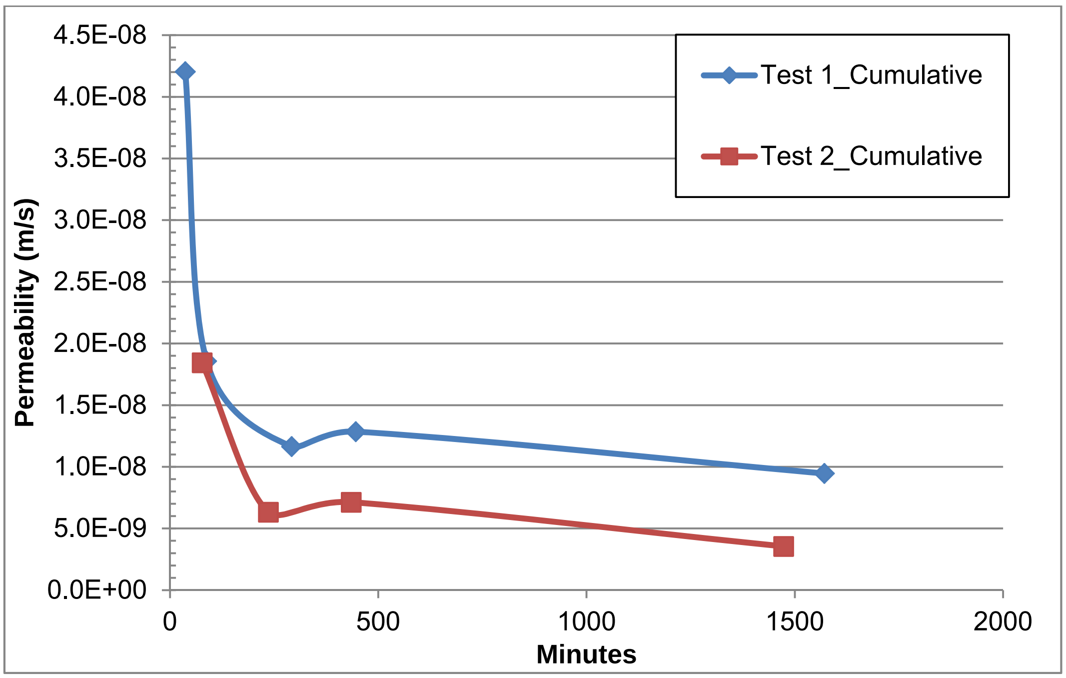

Figure 4-3: Cumulative grout permeability with time

4.2 Old Tailings Dam

The OTD is comprised of two catchments that were manually defined and instrumented for this research. Three material types, including fine tailings, coarse tailings, and hardpan tailings are present at the OTD. However, only two materials (fine and hardpan tailings) are present within the defined catchments. The catchment and material properties at the OTD are discussed below. Data gathered for the coarse tailings is presented for comparison only.

4.2.1 Material Zones and Catchment Mapping

Two catchments on the OTD were defined and instrumented specially for this research. The two catchments were manually outlined during the field program on the basis of the tailings surface topography, visual identification of the materials present, and observed runoff directions. Catchment A contains both fine tailings and hardpan materials while Catchment B contains only fine tailings. Small berms around the outlined catchments were created in January 2012 from the local tailings by a small rubber-tired excavator (Hutchison 2012). The catchments were each instrumented with a V-notch weir. The berms serve to direct surface runoff from beyond the catchments away from the weir measurement locations. One gauge was installed near the weirs to record rainfall for both catchments. The weirs, berms, and catchments are pictured in Figure 4-4, the rain gauge is to the left of Weir A just left of the photo frame.

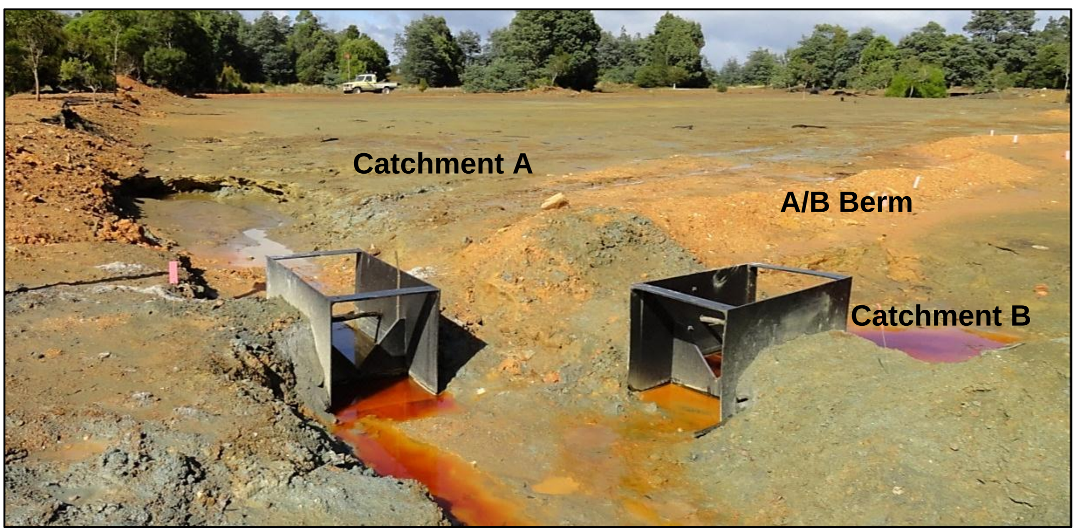

Figure 4-4: OTD v-notch weirs and berm

The berms outlining each catchment were surveyed. The material zones of fine tailings and hardpan material were delineated by Grange Resources based on field inspection and survey, and supplemented by interpretation of photos taken during rainfall events. These zones, along with the test locations discussed in Section 3.1.1.2, were shown on Figure 3-5. The surface area of each material in the OTD catchments is provided in Table 4-3.

Table 4-3: Old Tailings Dam Catchment and Material Zone Areas

Catchment A	
Material Type	**Area (ha)**
Fine tailings	0.217
Hardpan	0.202
Catchment A - Total	*0.419*

Catchment B	
Material Type	**Area (ha)**
Fine tailings	0.122
Catchment B - Total	0.122

4.2.2 OTD Material Properties

Fine, coarse, and hardpan tailings were identified visually during the field program. The material properties determined during the field and laboratory program for each of the OTD materials are discussed in detail in the following sections. The average properties of each material are summarized in Table 4-4. Particle size distributions of the representative samples (from Table 3-7) of the OTD materials are provided in Figure 4-5. Soil-water characteristic curves were fitted to the raw data using the Fredlund and Xing (1994) method in the SoilVision (2010) computer program and are shown in Figure 4-6.

Table 4-4: Summary of Average Properties of OTD Materials

Material Type	USCS	% Cobbles	% Gravel	%Sand	%Silt	%Clay	Dry Density (g/cm^3)	Specific Gravity	Void Ratio	Surface K_{sat*} (m/s)	Air Entry Value (kPa)	Limits LL - PL
Fine Tailings	SM, Silty sand	0	0	69	38	5	1.44	2.98	1.11	9.4E-06	13	Non-plastic
Coarse Tailings	SM, Silty sand	0	4	85	9	5	1.82	3.05	0.67	--	3	Non-plastic
Hardpan	ML, Silt with sand	0	0	15	54	31	1.30	2.93	1.26	4.3E-07	8	Non-plastic

* NOTE: This average surface K_{sat} is the geometric mean of the measured values.

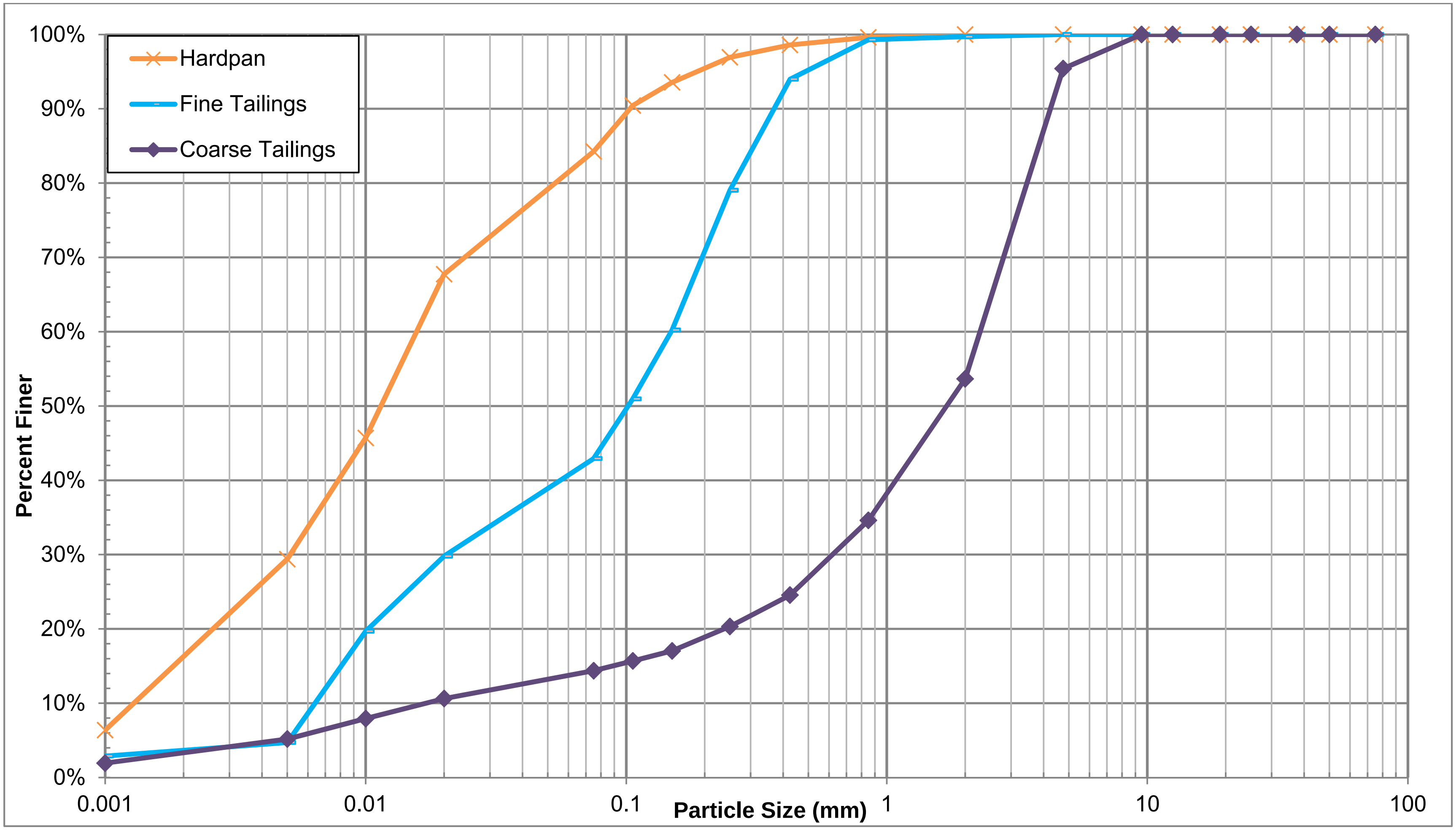

Figure 4-5: Particle size distributions for representative Old Tailings Dam materials

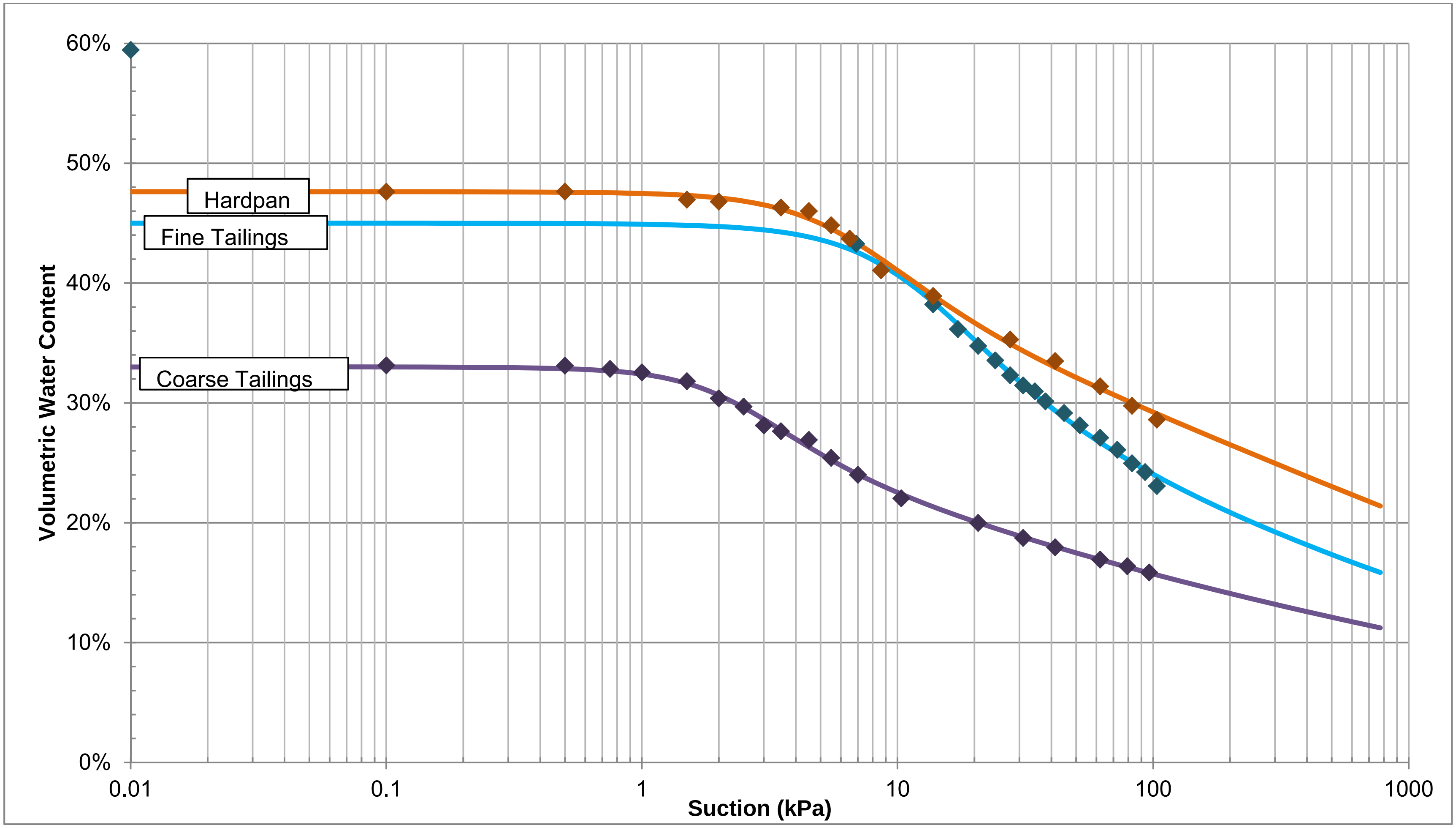

Figure 4-6: Soil-water characteristic data points and fitted Fredlund and Xing (1995) curves for OTD materials

4.2.2.1 Fine Tailings

The four samples of fine tailings, collected from two test locations, fitted USCS classification SM for silty sand. The upper 50 to 80 mm of the profile consisted of oxidized, “rusty” red colored fine tailings (pictured in Figure 3-4:a). Beneath the oxidized layer were unoxidized, grey fine tailings. The gravel content was less than 1%. The sand content was either 55% or 84%, and the fines (<75 μm) content was either 46% or 15%, for the four samples collected. The hydrometer analysis on the representative sample (Table 3-7) showed the material was composed of 38% silt and 5% clay. Atterberg limits could not be determined for the fine tailings, therefore the material was considered non-plastic. The particle size distribution for the representative sample was previously provided in Figure 4-5.

The specific gravity of the fine tailings was 2.98. The in-situ dry density ranged from 1.19 to 1.74 g/cm^3, and averaged 1.44 g/cm^3. The corresponding gravimetric water content ranged from 11% to 33%, and averaged 23%. The calculated in-situ void ratio ranged from 0.71 to 1.5, with an average of 1.1.

The surface K_{sat} ranged from 4.9×10^{-6} to 1.8×10^{-5} m/s for the top 60 mm of material, and averaged 9.4×10^{-6} m/s. Two measurements of K_{sat} at depth were taken using the Guelph permeameter at each test location. The upper test, on average 145 mm deep, yielded an average K_{sat} of 2.2×10^{-5} m/s. The lower test, on average 215 mm deep, yielded an average K_{sat} of 8.5×10^{-6} m/s. The K_{sat} of the fine tailings appeared to decrease with depth, as the upper test yielded a permeability 2.6 times greater than the lower test.

Soil suction remained relatively uniform with depth in the fine tailings material, averaging 4.9 kPa or 5.6 kPa, depending on the test location. Similarly, soil temperature ranged from 14.5 to 19 ^{o}C at various test points, but no trend was apparent with depth. The gravimetric water content decreased with depth, averaging 24% in the upper 75 mm to 18% between 105 to 235 mm depth.

The SWCC for fine clay showed an AEV of 13 kPa matric suction followed by constant desaturation with increasing suction. This AEV corresponded to a volumetric water content of 38% and a gravimetric water content of 30%. Curve fitting of the experimental data using the Fredlund and Xing (1994) method in the SoilVision (2010) computer program suggested a residual volumetric water content of approximately 23%. The experimental data and the Fredlund and Xing fitted SWCC for fine tailings were previously provided in Figure 4-6.

4.2.2.2 Coarse Tailings

The four samples of coarse tailings, collected from two test locations, varied in texture from USCS classification SM, to SW, to SW-SM. The material ranged from silty sand, to well-graded sand, to well-graded sand with silt. The upper 100 to 180 mm of the profile consisted of oxidized, "rusty" red colored coarse tailings (pictured in Figure 3-4:b). The oxidation was either constant in the upper profile or banded with ~40 mm unoxidized grey-brown coarse tailings. Unoxidized, grey fine tailings were beneath the upper layer. The particle size ranged from 3% to 5% gravel and 76% to 92% sand. The fines (<75 μm) content was either 5% or 17% for the four samples collected. The hydrometer analysis on the representative sample (Table 3-7) showed the material was composed of 9% silt and 5% clay. Atterberg limits could not be determined for the coarse tailings, as the blow count would not reach 25. The fines were therefore considered non-plastic and no liquid or plastic limit was found. The particle size distribution for the representative sample was previously provided in Figure 4-5.

The specific gravity of the coarse tailings was 3.05. The in-situ dry density ranged from 1.78 to 1.87 g/cm^3, and averaged 1.82 g/cm^3. The corresponding gravimetric water content ranged from 8% to 10%, with an average of 9%. The in-situ void ratio ranged from 0.63 to 0.71, with an average of 0.67.

The surface K_{sat} was not determined using the double ring infiltrometer. One measurement of K_{sat} at 140 mm depth was taken using the Guelph permeameter. This single test yielded a K_{sat} at depth of $1.2\text{x}10^{-7}$ m/s.

Both suction and soil temperature were observed to decrease with depth for the coarse tailings material. Suction decreased from 10.5 kPa at 15 mm depth to 5.6 kPa at 180 mm depth, and decreased from 3.7 kPa at 15 mm depth to 1.2 kPa at 250 mm depth in the first and second coarse tailings test location, respectively.

Soil temperature decreased from an average of 23 ^{o}C at the surface (15 mm depth) to 19 ^{o}C between 100 mm and 250 mm depth. Gravimetric water content of the coarse tailings ranged from 8% to 14%, with no apparent trend with depth.

The SWCC for fine clay showed the material remained saturated up to an AEV of 3 kPa matric suction, then gradually desaturated with increasing suction. This AEV corresponded to a volumetric water content of 28% and a gravimetric water content of 14%. Curve fitting of the experimental data using the Fredlund and Xing (1994) method in the SoilVision (2010) computer program suggested a residual volumetric water content of approximately 19%. The experimental data and the fitted SWCC for coarse tailings were previously provided in Figure 4-6.

4.2.2.3 Hardpan

The hardpan tailings were characterized by a 5 mm thick crust at the surface (pictured in Figure 3-4:c). Approximately 100 mm of interbedded oxidized and unoxidized silty layers, which resembled fine tailings, was beneath this crust. The oxidized layers were “rusty” red in color and the unoxidized layers were grey-blue in color. Unoxidized very fine sand to silt, which also resembled fine tailings, was below 120 mm depth. The following description of the hardpan tailings pertains to the upper 100 mm of material, not including the crust, unless otherwise noted.

Four hardpan tailings samples were collected from two test locations. The material was classified as USCS group ML, and varied in texture from silt to silt with sand. The particle sizes ranged from 12% to 20% sand and 80% to 88% fines (<75 μm). The hydrometer analyses showed the material was composed of 46% to 64% silt and 17% and 42% clay. Atterberg limits could not be determined for the representative sample of hardpan tailings (Table 3-7), as the blow count would not reach 25. The fines were therefore considered non-plastic. The particle size distribution for the representative sample was previously provided in Figure 4-5.

The specific gravity of the hardpan tailings was 2.93. The in-situ dry density ranged from 1.26 to 1.39 g/cm^3, and averaged 1.30 g/cm^3. The corresponding gravimetric water content ranged from 31% to 39%, and averaged 36%. The in-situ void ratio was from 1.1 to 1.3, and averaged 1.26.

The K_{sat} of the surface crust was determined using the double-ring infiltrometer test. Values ranged from 2.1×10^{-7} to 9.0×10^{-7} m/s, with a geometric average of 4.3×10^{-7} m/s. Two measurements of K_{sat} at 160 mm depth were taken using the Guelph permeameter, which averaged 4.6×10^{-6} m/s.

Suction measurements decreased from 17 kPa at 15 mm depth to 2 kPa at 215 mm depth in the hardpan test locations. Soil temperature was seen to decrease as well from 23 ^{o}C at the surface to as low as 16.5 ^{o}C at 270 mm depth. Similarly, gravimetric water content decreased with depth from an average of 40% in the upper 80 mm to 33% at depths between 110 to 270 mm.

The AEV for the hardpan tailings was 8 kPa, which corresponded to a volumetric water content of 42% and a gravimetric water content of 36%. Curve fitting of the experimental data using the Fredlund and Xing (1994) method in the SoilVision (2010) computer program suggested a residual volumetric water content of approximately 30%. The experimental data and the fitted SWCC for the hardpan were previously provided in Figure 4-6.

Chapter 5. RAINFALL RUNOFF PREDICTION

Rainfall runoff was predicted using two one-dimensional models. The following sections: 1) describe the models used, including the input parameters for each model, 2) present the runoff predictions resulting from the modelled scenarios, and 3) compare the predictions to the measured rainfall runoff response.

5.1 Proposed Rainfall Runoff Model

The physical basis and rationale for the proposed rainfall runoff model, and its input parameters are described in the following section. The proposed model is referred to as the Savage River Runoff Model, or SRR Model, in the remainder of the thesis.

5.1.1 Proposed SRR Model Description

The physical basis for the SRR model is the fundamental understanding that the immediate soil surface will be saturated during periods of surface runoff generation (Smith 2002), for both the infiltration-excess and saturation-excess runoff mechanisms. Although factors such as antecedent moisture content and subsurface soil characteristics are considered in infiltration analyses, the SRR Model inherently omits these influences in its runoff prediction equations.

Rates of runoff generation were predicted by comparing real-time rainfall intensity to the measured surface K_{sat} of the soil cover material (after Wilson (2006)), as follows:

$$Material\,runoff\ \ rate\ = Rainfall\,intensity\ -\ Material\,K_{sat}$$

If the rainfall intensity did not exceed K_{sat}, a runoff rate of zero was applied. This method allows for rainfall to infiltrate the soil profile at the rate of K_{sat} or rainfall intensity, whichever is smaller, as depicted in Figure 5-1.

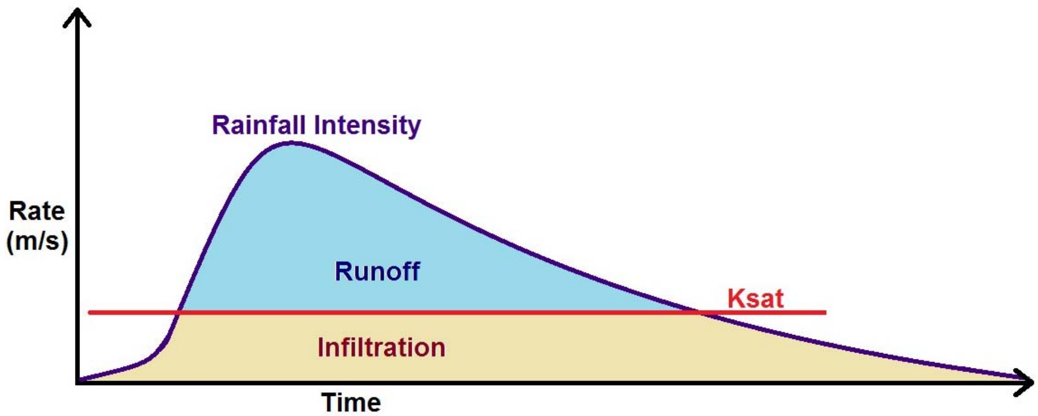

Figure 5-1: Runoff prediction using the SRR Model for a typical rainfall event, after Wilson (2006)

Runoff volumes were separately predicted for each material, then converted to catchment runoff volumes as follows:

$$Material\ runoff\ volume\ within\ catchment$$
$$= (Material\ runoff\ rate)(Material\ area\ in\ catchment)(time\ increment)$$

$$Catchment\ runoff\ volume\ = \sum Material\ runoff\ volumes\ within\ catchment$$

5.1.2 Proposed SRR Model Parameter Selection

Two main parameters were used as input for the SRR Model: 1) rainfall and 2) the measured surface K_{sat} of the materials investigated during the field program.

5.1.2.1 Measured Rainfall

Rainfall data was collected at B-Dump in a tipping bucket rain gauge in 15-minute increments over the period of March 29 to June 20, 2007. The rainfall volume collected in the increment was then converted to a 15-minute rainfall intensity. Calculated 15-minute rainfall intensities ranged from $2.2x10^{-7}$ m/s to $7.8x10^{-6}$m/s. The most frequent rainfall intensity, which accounted for approximately half of rainfall readings, was $2.2x10^{-7}$ m/s and corresponded to the minimum volume of rain detectable by the rain gauge (0.2 mm in 15 minutes).

The event-averaged rainfall intensity was also calculated to provide a comparison between runoff predictions and model rainfall resolution. The duration and total rainfall from the storm event was defined each day from the raw data. An average rainfall intensity for the storm event was calculated based on the total rainfall and the duration of the storm. Daily rainfall events ranged from 0.25 hours to 24 hours in duration and lasted 10 hours on average. The event-averaged intensity was 3.2×10^{-7} m/s.

Measured runoff on B-Dump generally followed the same pattern as the measured rainfall. This pattern (for example, Figure 5-2) illustrates that when rainfall was recorded runoff accumulated shortly thereafter, and when the rain event finished runoff soon dissipated.

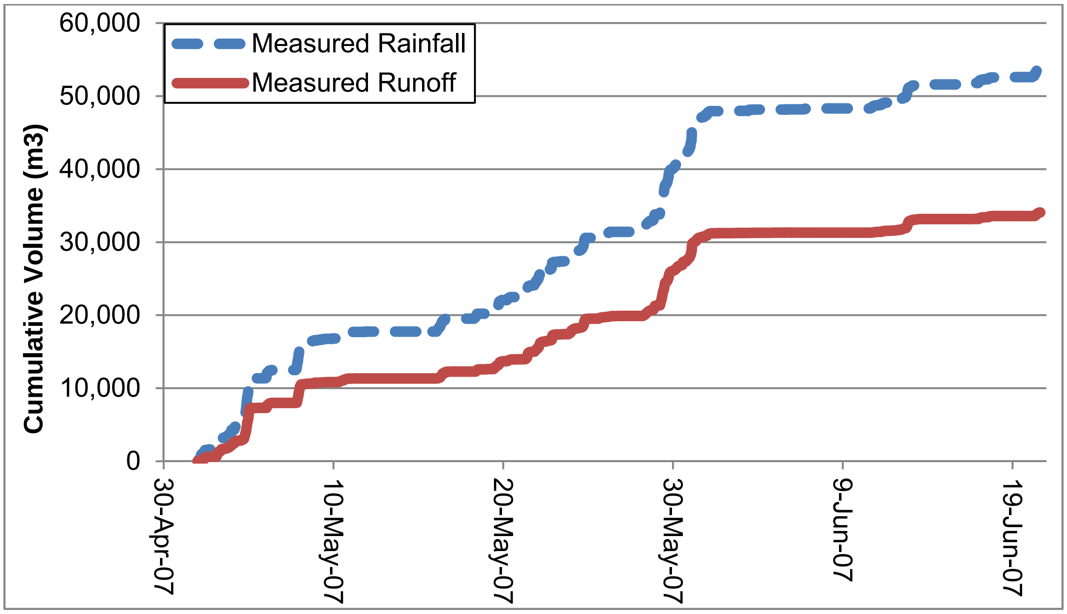

Figure 5-2: Typical pattern of measured rainfall and measured runoff for B-Dump

A deviation from this pattern was observed from mid-April to early May, as shown in Figure 5-3. Upon further examination of both the measured rainfall and runoff raw data it was found that from April 6 to May 1, inclusive, significant runoff was being recorded but rainfall measurements were intermittent. In all other periods there was consistent correlation between measured rainfall and runoff. Therefore the rainfall measurements from April 6 to May 1 at B-Dump were considered to be unreliable.

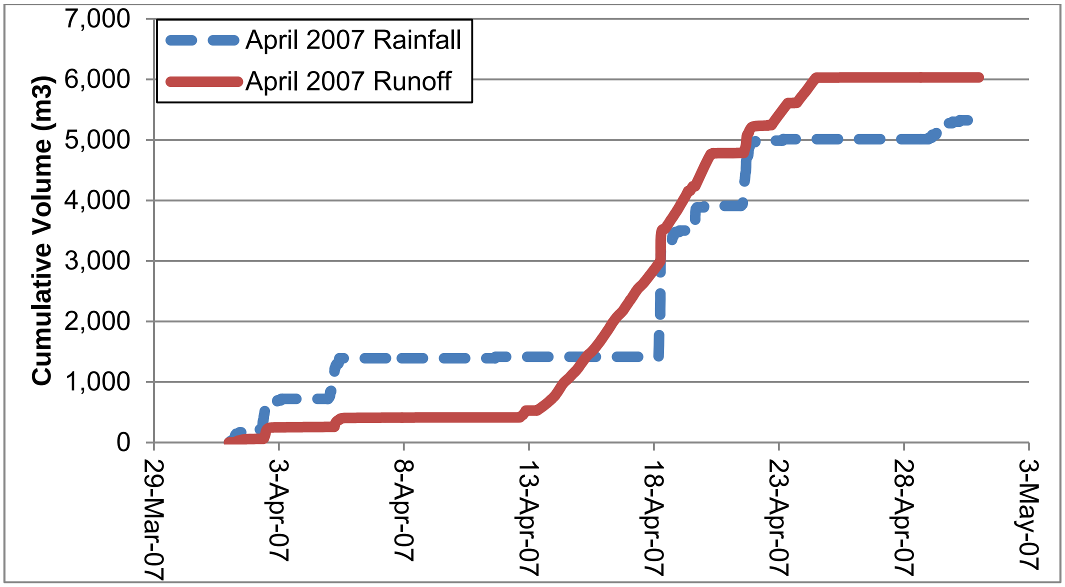

Figure 5-3: Deviation from the typical pattern of measured rainfall and runoff for B-Dump

Runoff predictions using the SRR Model depend on measured rainfall values. The inconsistent rainfall recorded at B-Dump from April 6 to May 1 would introduce errors in the cumulative runoff predictions following this period. Therefore, runoff predictions were evaluated using only data from the continuous period of May 2 through June 20, 2007, which showed a reliable and longer-term measured rainfall-runoff correlation.

Separate rainfall data was not available for the OTD location, therefore the data collected at B-Dump from May 2 to June 20, 2007 was also used for the OTD predictions.

5.1.2.2 Saturated Hydraulic Conductivity of the Surface, K_{sat}

The infiltration tests yielded a range of surface K_{sat} for each of the materials on B-Dump and the OTD. This range was used to facilitate modelling and to evaluate the potential variation in predicted runoff volumes within actual measured limits. The lowest measured, average, and highest measured K_{sat} values that were used for each material are shown in Table 5-1. In all cases, no more than a half-order-of-magnitude separated the highest and lowest measured K_{sat} values.

Table 5-1: Measured K_{sat} Values Used in Runoff Modelling

Material	Low K_{sat} (m/s)	Average K_{sat} (m/s)	High K_{sat} (m/s)
B-Dump Materials			
Fine Waste Rock	7.72 x10^{-8}	2.14 x10^{-7}	4.10 x10^{-7}
Coarse Waste Rock	1.09 x10^{-6}	1.36 x10^{-6}	1.70 x10^{-6}
Fine Overburden	7.60 x10^{-7}	1.57 x10^{-6}	3.10 x10^{-6}
Coarse Overburden	2.92 x10^{-7}	5.10 x10^{-7}	9.35 x10^{-7}
Old Tailings Dam Materials			
Fine Tailings	4.90 x10^{-6}	9.41 x10^{-6}	1.83 x10^{-5}
Hardpan	2.08 x10^{-7}	4.27 x10^{-7}	9.03 x10^{-7}

As previously described, runoff from each material was predicted separately then summed according to the material areas to find the total runoff for the catchment. To provide further comparison, the area-weighted average K_{sat} is provided for each catchment in Table 5-2.

Table 5-2: Area Weighted Average K_{sat} for Modelled Catchments

K_{sat} Range	Area Weighted K_{sat} (m/s)			
	B-Dump		Old Tailings Dam	
	Catchment 1	Catchment 2	Catchment A	Catchment B
Lowest	1.9 x10^{-7}	2.1 x10^{-7}	1.1 x10^{-6}	4.9 x10^{-6}
Average	4.1 x10^{-7}	4.2 x10^{-7}	2.1 x10^{-6}	9.4 x10^{-6}
Highest	7.7 x10^{-7}	7.2 x10^{-7}	4.3 x10^{-6}	1.8 x10^{-5}

5.2 SoilCover One Dimensional Analysis

SoilCover is a one-dimensional finite element modelling software that uses a physically based method to predict the exchange of water and energy between the atmosphere and the soil surface (Unsaturated Soils Group 2000). The model can accommodate a variety of scenarios including vegetation influences, detailed or reduced climatic inputs, freeze-thaw modelling, and numerous detailed soil parameter inputs that may be user defined or suggested by Soil Cover.

SoilCover calculates runoff with each iteration and for every time step as follows:

1) If the surface is not saturated, precipitation minus internally calculated actual evaporation is applied at the top node as a liquid flux boundary condition.

2) If the surface is saturated, runoff equals precipitation minus actual evaporation minus Darcy flux infiltration.

3) If the calculated runoff is negative, this means the top node is passing enough infiltration to desaturate the surface and the calculation reverts to step 1).

5.2.1 Parameter Selection

A number of parameters are required for input into the SoilCover software model. These include several soil and climate parameters, as well as model specific input, such as initial and boundary conditions. The following sections describe the parameters used to set up the SoilCover model.

5.2.1.1 Soil Parameters

The soil properties, including input details and source information, used in the model are provided in Table 5-3.

Table 5-3: Soil Parameter Inputs for SoilCover Model

Parameter	Input Details	Source
K_{sat}	Three cases of lowest, average, and highest measured saturated hydraulic conductivity input for each material. Refer to Table 5-1.	Field program results.
Gs	Measured specific gravity input for each material.	Laboratory program results
SWCC	Measured SWCC curve data input as matric suction versus volumetric water content. Curve fit generated using SoilCover subroutine, which uses Fredlund and Xing (1994).	
Porosity	Volumetric water content at zero suction from SWCC data was input as soil porosity. This avoided discontinuity in the model.	
Mv	Coefficient of volume change (1/kPa) was input based on curve generated by Soil Vision SVFlux software to fit measured SWCC data.	(SoilVision 2010)
K_{unsat} Function	Unsaturated permeability function (matric suction versus relative permeability) was generated using SoilCover subroutine that uses Fredlund et al. (1994)	SoilCover (2000)
Thermal Conductivity Function	Gravimetric water content versus thermal conductivity function generated using SoilCover subroutine. Quartz content estimated based on SoilCover (2000) suggestions.	
Volumetric Specific Heat Function	Gravimetric water content versus volumetric specific heat function generated using SoilCover subroutine, which uses de Vries (1963)	

5.2.1.2 Climate Parameters

The reduced data option for climatic parameter input was selected for the models, since detailed daily data for net radiation and wind speed was unavailable. The climatic parameters listed in Table 5-4 were used in the models for B-Dump and the OTD. Table 5-4 also describes the input details of each parameter and the source of the data.

Table 5-4: Climate Parameter Inputs for SoilCover Model

Parameter	**Input Details**	**Source**
Precipitation	Daily input, intensity was manipulated by adding the start/end time of rainfall. Applied for the period of May 2 to June 20, 2007. Input daily data in mm.	GHD (2009)
Minimum / maximum relative humidity	Mean 9AM and 3PM relative humidity each month (averaged over the years 1969 – 1989). Minimum relative humidity input was the 3PM value; maximum relative humidity input was 9AM value. Percentage input as a decimal for months of May and June.	Commonwealth of Australia (2012)
Minimum / maximum daily air temperature	Mean daily minimum and maximum air temperatures available for each month (averaged over the years 1966 – 1989). Input in Celsius for months of May and June.	
Pan Evaporation	Mean daily evaporation available for each month (averaged over the years 1966-1983). Input as a negative flux value in mm/day for months of May and June.	
Latitude	The latitude of Savage River Mine: 41^{O} 30' S. Input as negative 41.5.	Field program GPS coordinates

Two cases using the precipitation parameter were evaluated. The 15-minute rainfall data resolution that was used in the SRR Model is too high of a resolution to be used as input in SoilCover. Therefore, the first SoilCover case modelled the event-averaged intensity of the applied rainfall; this corresponds to the second case of the SRR Model. The second case modelled in SoilCover used the total daily precipitation as if it fell over the entire 24 hour period. This provides comparison between SoilCover simulations using higher and lower resolution rainfall.

5.2.1.3 Model Details

Simplified analyses were performed by using the reduced climate parameter option and by omitting vegetation influences and freeze/thaw scenarios. Model convergence and time step parameters were left at the SoilCover default values. For each material, a soil profile consisting of a single material of 1 m and 0.6 m thickness was modelled for B-Dump and the OTD, respectively. The minimum and maximum finite element node spacing was 10 mm and 2 mm, respectively, and a node spacing expansion factor of 1.1 was applied.

Initial conditions applied to the top and bottom nodes of the profile were gravimetric water content and soil temperature. The top and bottom nodes were set at the average gravimetric water content measured from the bulk samples collected for each material during the field program. The soil temperature of the upper node was set at the average temperature found from suction/temperature measurements within 50 mm of the surface for each material. The soil temperature of the base node was set at the lowest measured temperature found at depth from suction/temperature measurements taken during the field program.

In all cases, the daily top moisture boundary condition type was precipitation, input in mm/day (Table 5-4). The bottom moisture boundary condition, discussed above, was set each day as the average gravimetric water content of the material modelled.

5.3 Results and Discussion

The SRR Model and SoilCover analyses were used to predict runoff from materials found on B-Dump and the OTD. The modelling results discussed below are also provided in digital format in the Appendix.

Measured rainfall from B-Dump for the period of May 2 to June 20, 2007 was applied for the B-Dump and OTD models. Measured rainfall-runoff data from the OTD was not available. OTD runoff was modelled using B-Dump rainfall measurements and an estimate of reasonable runoff is proposed based on the conclusions from the B-Dump comparisons. Rainfall and runoff volumes were found based on the material and catchment areas[2] found during this research.

Cumulative volumes of measured rainfall, measured runoff, and predicted runoff are compared for each catchment on B-Dump and the OTD in the following sections. For convenient reference, Figure 5-4 to Figure 5-15 in the following sections contain a legend sequence that represents the line order from top to bottom in that chart. Measured rainfall is represented by the dashed bold blue line. Measured runoff is shown by the bold red line. The three narrow lines represent the predicted runoff volumes. The runoff predicted by the lowest, average, and highest measured K_{sat} values are represented by the green, orange, and purple narrow lines, respectively.

5.3.1 B-Dump

Runoff from B-Dump was predicted using both the SRR Model and SoilCover analyses. The predictions are compared to amended measurements of runoff from B-Dump for the period of May 2 to June 20, 2007 (discussed previously in Section 2.4.4). First, the results are presented and discussed for the SRR Model in Section 5.3.1.1. The results and discussion of the SoilCover analyses are provided in Section 5.3.1.2. The SoilCover results are also compared with the SRR Model predictions within the Section 5.3.1.2 discussion.

5.3.1.1 Proposed SRR Model Runoff Predictions

15-Minute Rainfall Intensity

The cumulative volumes of measured rainfall and runoff, as well as runoff predicted with the SRR Model using the 15-minute rainfall intensity are shown for B-Dump Catchment 1 and Catchment 2 in Figure 5-4 and Figure 5-5, respectively.

[2] B-Dump catchment areas reported by GHD (2009) are slightly smaller than those reported in this research. Accordingly, GHD (2009) measurements were factored to represent the catchment areas reported by this research (Section 4.1.1).

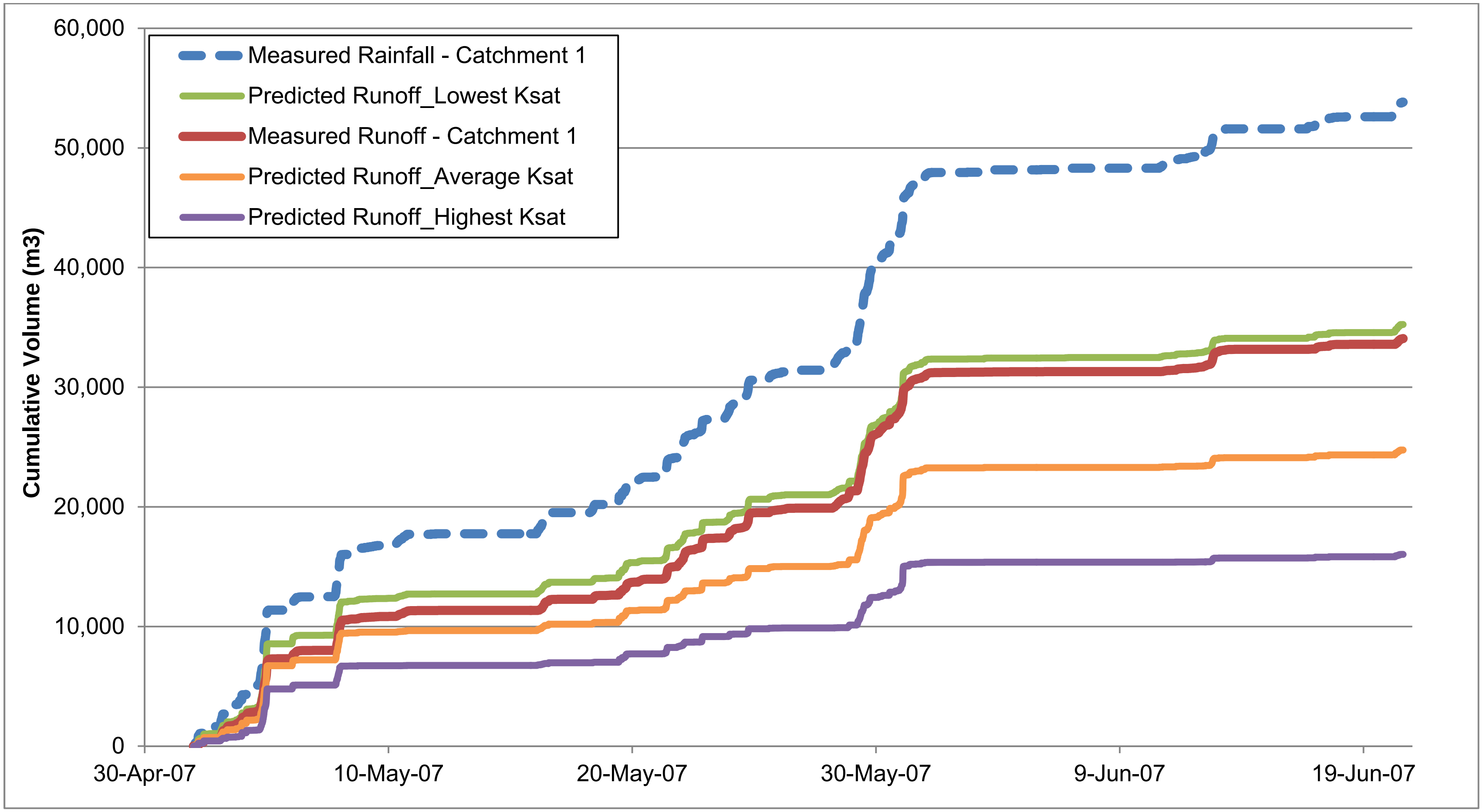

Figure 5-4: Comparison of measured rainfall and runoff to SRR Model predicted runoff using 15-minute rainfall intensity - B-Dump Catchment 1

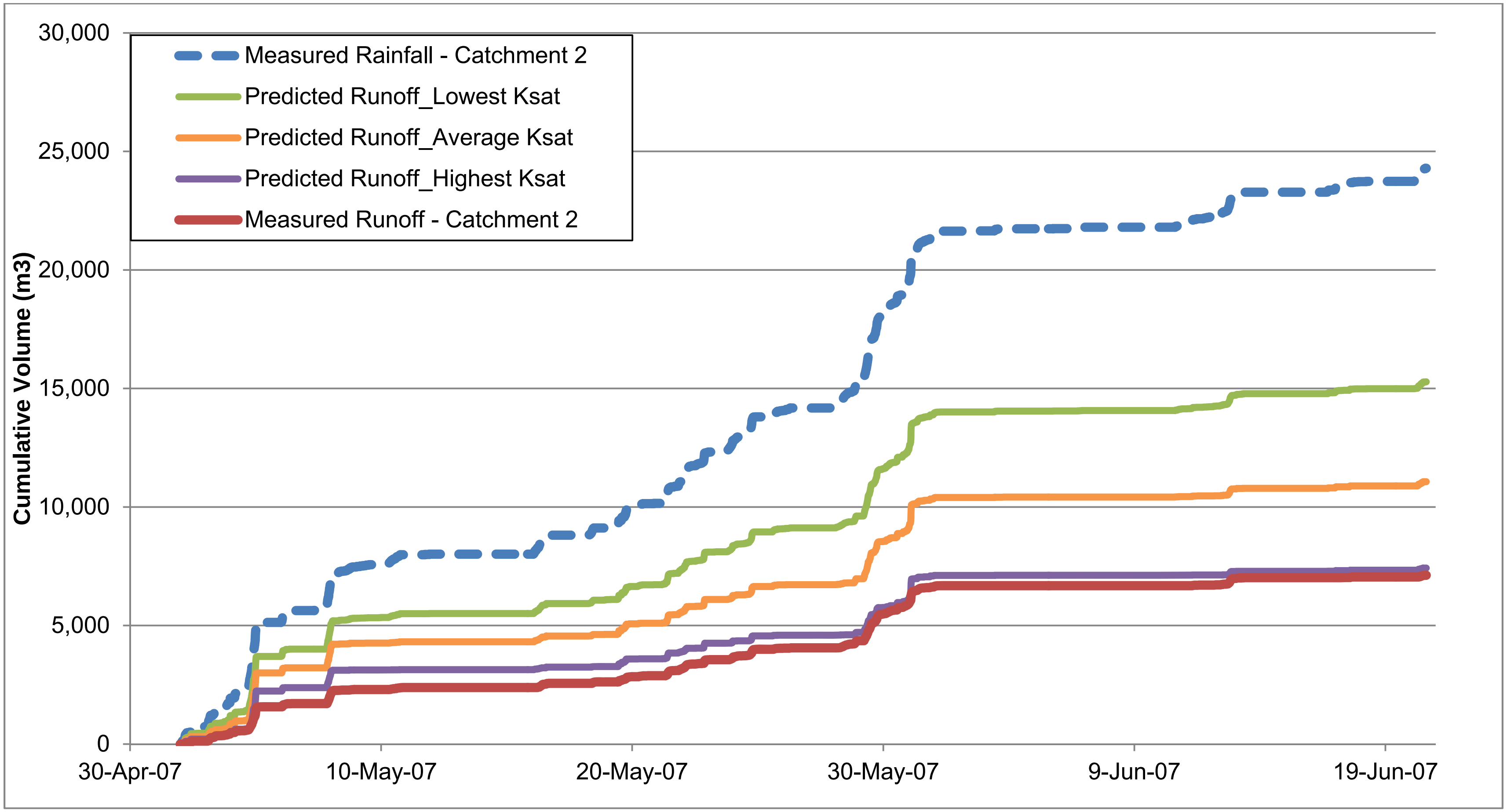

Figure 5-5: Comparison of measured rainfall and runoff to SRR Model predicted runoff using 15-minute rainfall intensity - B-Dump Catchment 2

Runoff was predicted using the lowest, average, and highest K_{sat} values measured for each material (previously provided in Table 5-1). Figure 5-4 shows that the best runoff prediction for B-Dump Catchment 1 is achieved by using the lowest measured K_{sat} for each material. In this case, the final cumulative runoff volume is overpredicted by 3.4%.

The area averaged K_{sat} that would produce runoff predictions that match the final measured cumulative runoff was back-analyzed and found to be 2.2×10^{-7} m/s. As expected, this value is within the range of area averaged K_{sat} provided for Catchment 1 in Table 5-2. This indicates that runoff can be predicted based on rainfall intensities and actual surface K_{sat} measurements without introducing calibration factors into the model.

Figure 5-5 shows that the best runoff prediction for B-Dump Catchment 2 is achieved by using the highest measured K_{sat} for each material. The final cumulative runoff volume is overpredicted by 4.3% using this highest K_{sat} value. The area averaged K_{sat} that would produce a cumulative runoff prediction that matched measured runoff is 7.3×10^{-7} m/s. This value is less than 1.5% beyond the range of weighted K_{sat} noted for Catchment 2 in Table 5-2.

The cumulative runoff volumes predicted by the SRR Model are compared to measured runoff for both catchments and the range of K_{sat} input in Table 5-5.

Table 5-5: Percent Difference between Final Cumulative Runoff Volume Predicted using SRR Model and Measured Runoff – 15 Minute Rainfall Intensity

K_{sat} Range	% Difference (Final Cumulative Runoff Volume)	
	Catchment 1	Catchment 2
Lowest Measured	3.44%	115%
Average	-27.4%	55.4%
Highest Measured	-53.0%	4.25%

The same measured rainfall data was used to predict runoff from both catchments, differing only in the magnitude of area applied to calculate the cumulative volumes. Furthermore, Catchment 1 and Catchment 2 are characterized by very similar area weighted average K_{sat} values, as previously shown in Table 5-2. Given the large variation in prediction accuracy between catchments, shown in Table 5-5, another factor must be influencing the actual measured runoff from these catchments.

Intuitively, a greater slope should enhance runoff. Mechanistically, whenever the rainfall intensity exceeds the ability of the soil to accept water at the surface, the excess water will begin to fill surface depressions and form ponds. A hydraulic head is introduced if the surface is flat, which promotes infiltration. A sloped surface will direct ponded water downslope by gravity flow, increasing surface runoff and limiting the quantity of water available for infiltration. As discussed in Section 4.1.1, the surface slope of Catchment 1 was found to be between 3.4% - 8.8%, and between 0% - 4.0% in Catchment 2.

The SRR Model is one-dimensional and does not account for the slope of the surface. Given that a sloped surface will limit infiltration, as described above, a slope could be simulated in a one-dimensional model by reducing the surface permeability. Figure 5-4 shows that runoff predicted by the SRR Model is more accurate using a lower K_{sat} value for Catchment 1, which has a greater slope. By comparison, Figure 5-5 shows that the SRR Model predicts runoff with greater accuracy using a higher K_{sat} value for Catchment 2, which has low to no slope. Therefore, the results of the SRR Model are consistent with both the physical runoff mechanisms and the limitations imposed by the one-dimensional model itself. In addition, if the slope of the catchment is considered when selecting K_{sat} input for the SRR Model, measured runoff volumes can be predicted within 4%.

Event-Averaged Rainfall Intensity

Figure 5-6 and Figure 5-7 illustrate the runoff predicted by the SRR Model if the average intensity for the rainfall event is used for Catchment 1 and 2, respectively.

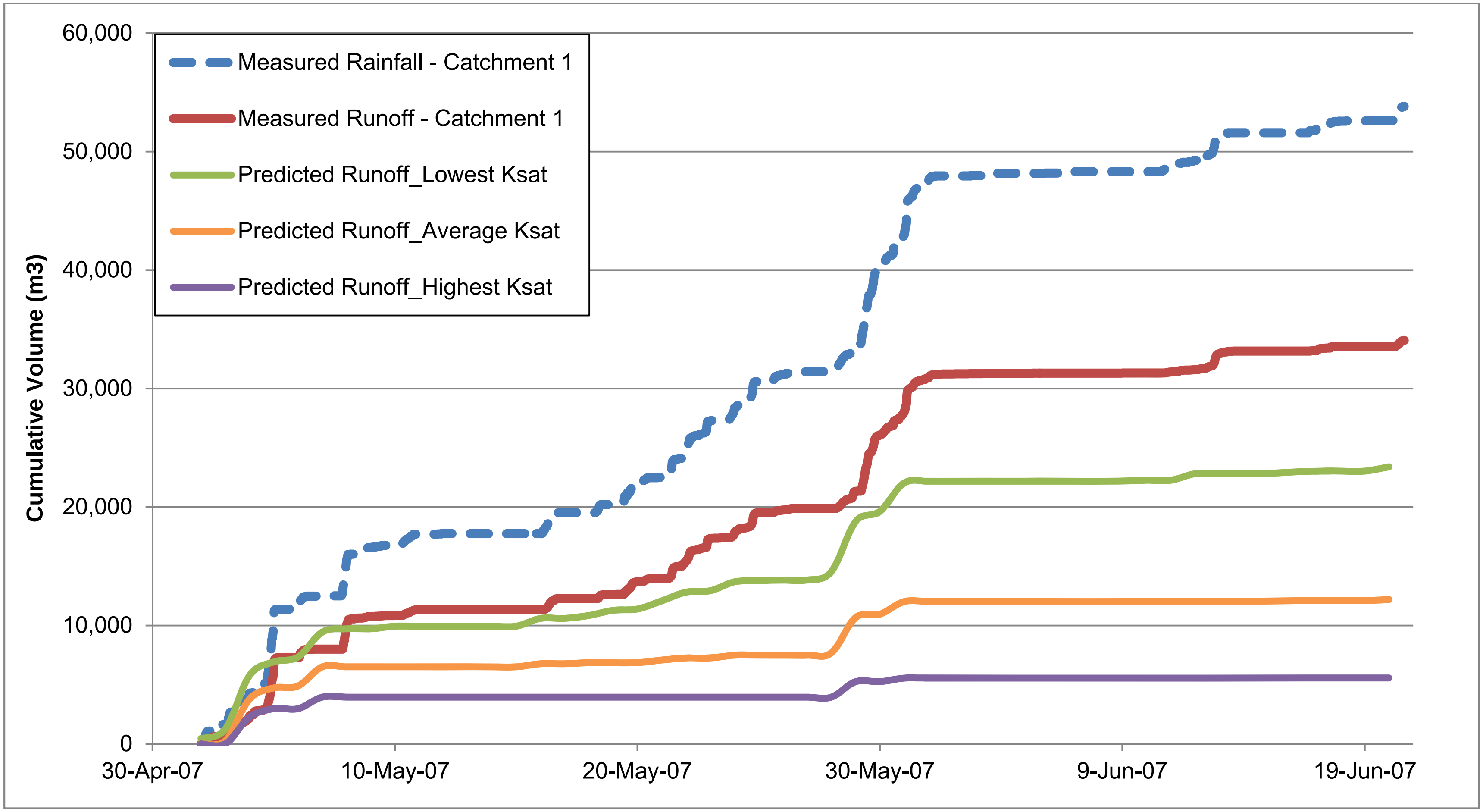

Figure 5-6: Comparison of measured rainfall and runoff to SRR Model predicted runoff using event-averaged rainfall intensity - B-Dump Catchment 1

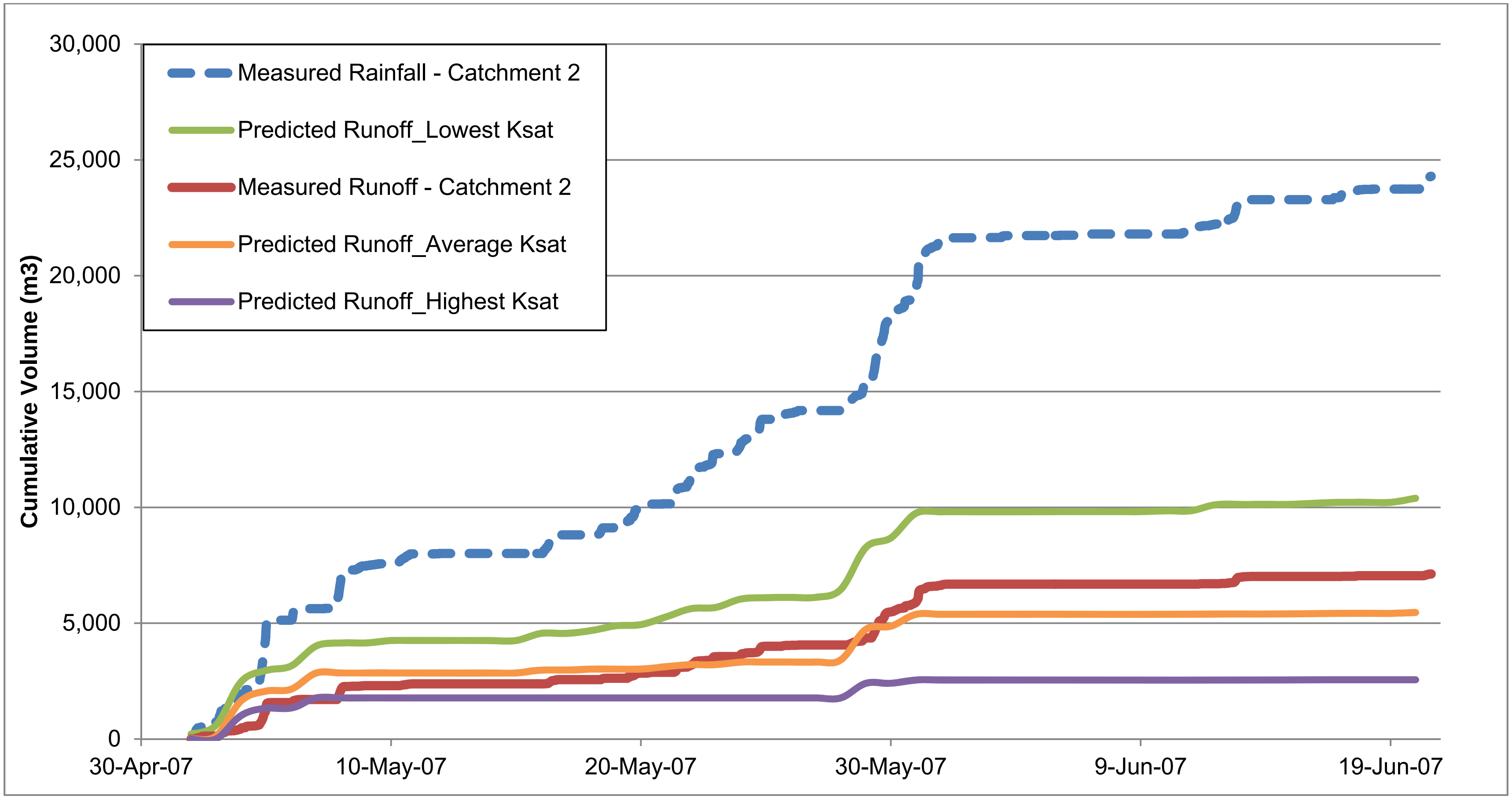

Figure 5-7: Comparison of measured rainfall and runoff to SRR Model predicted runoff using event-averaged rainfall intensity - B-Dump Catchment 2

Comparing Figure 5-4 through Figure 5-7, it is apparent that runoff predictions using the SRR Model are highly sensitive to the rainfall intensity used as input. In both catchments and for the entire range of K_{sat} evaluated, runoff predictions were reduced by 33% to 190% by using the event-averaged rainfall intensity as compared to the 15-minute rainfall intensity. The percent differences between measured and predicted runoff volumes for each catchment using the event-averaged intensity are shown in Table 5-6. Much better agreement between final predicted and measured runoff volumes is achieved using the 15-minute rainfall intensity (Table 5-5) compared to the event-averaged intensity (Table 5-6).

Table 5-6: Percent Difference between Final Cumulative Runoff Volume Predicted using SRR Model and Measured Runoff – Event-Average Rainfall Intensity

K_{sat} Range	% Difference (Final Cumulative Runoff Volume)	
	Catchment 1	Catchment 2
Lowest Measured	-31.3%	45.9%
Average	-64.2%	-23.3%
Highest Measured	-83.6%	-64.1%

The actual measured runoff for Catchment 2 is found within the bounds of runoff predictions using the event-averaged rainfall intensity. The average measured K_{sat} property produces the closest runoff prediction, but still under-predicts the quantity by more than 23%. This may indicate that when high resolution rainfall data is unavailable, average soil properties should be used for the best runoff predictions when both the model and the simulated surface are one-dimensional (recall, Catchment 2 is relatively flat).

As previously discussed, no more than a half-order-of-magnitude separated the highest and lowest measured K_{sat} values. Still, this relatively narrow range of K_{sat} values produced significantly different runoff predictions, regardless of rainfall intensity resolution. The K_{sat} used in the SRR Model inherently becomes a threshold where any rainfall intensity below this value no longer generates runoff. When high resolution rainfall data is used as input, rainfall intensities naturally vary above and below the threshold K_{sat}. An artificial factor is introduced when using low resolution or event-averaged rainfall data, which does not represent the natural rainfall process. These results show that the use of real-time or high resolution rainfall will produce the most accurate predictions using the SRR Model.

Overall, the SRR Model is capable of predicting runoff within 4% using only rainfall intensities and measured surface K_{sat} properties. The accuracy of runoff predictions, however, can vary widely with the resolution of rainfall data available. The best possible runoff predictions generally required the use of high resolution rainfall data, which may not always be available at site. Runoff predictions can also vary within the natural range of measured K_{sat} values. If the selection of the K_{sat} to be used in the model is based on knowledge of both the catchment slope characteristics and one-dimensional model limitations, runoff predictions can be significantly improved, even with lower resolution rainfall data.

5.3.1.2 SoilCover Runoff Predictions

Event-Averaged Rainfall Intensity

The cumulative volumes of measured rainfall and runoff, as well as runoff predicted with SoilCover using event-averaged rainfall intensities are shown for B-Dump Catchment 1 and Catchment 2 in Figure 5-8 and Figure 5-9, respectively.

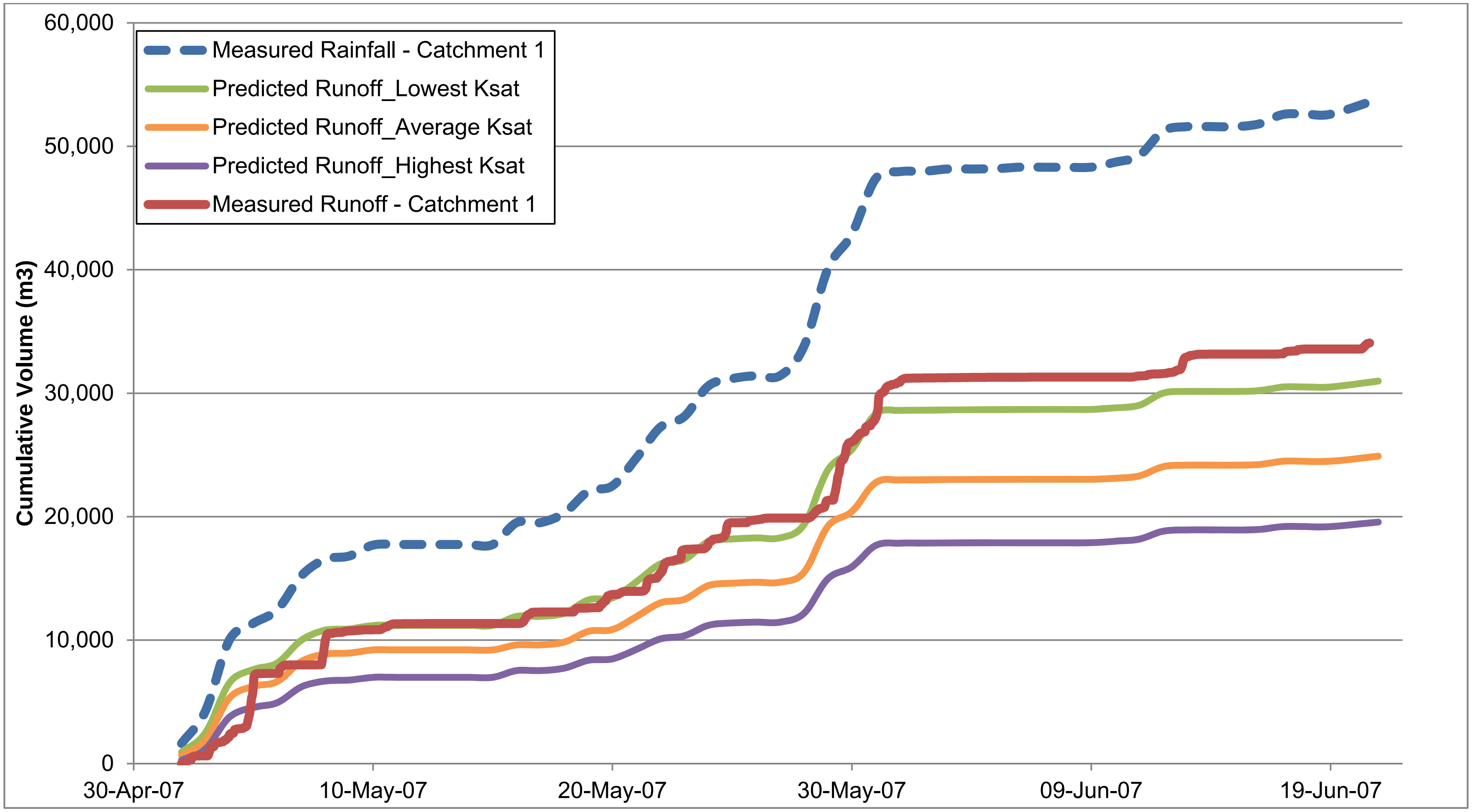

Figure 5-8: Comparison of measured rainfall and runoff to SoilCover predicted runoff using event-averaged rainfall intensity - B-Dump Catchment 1

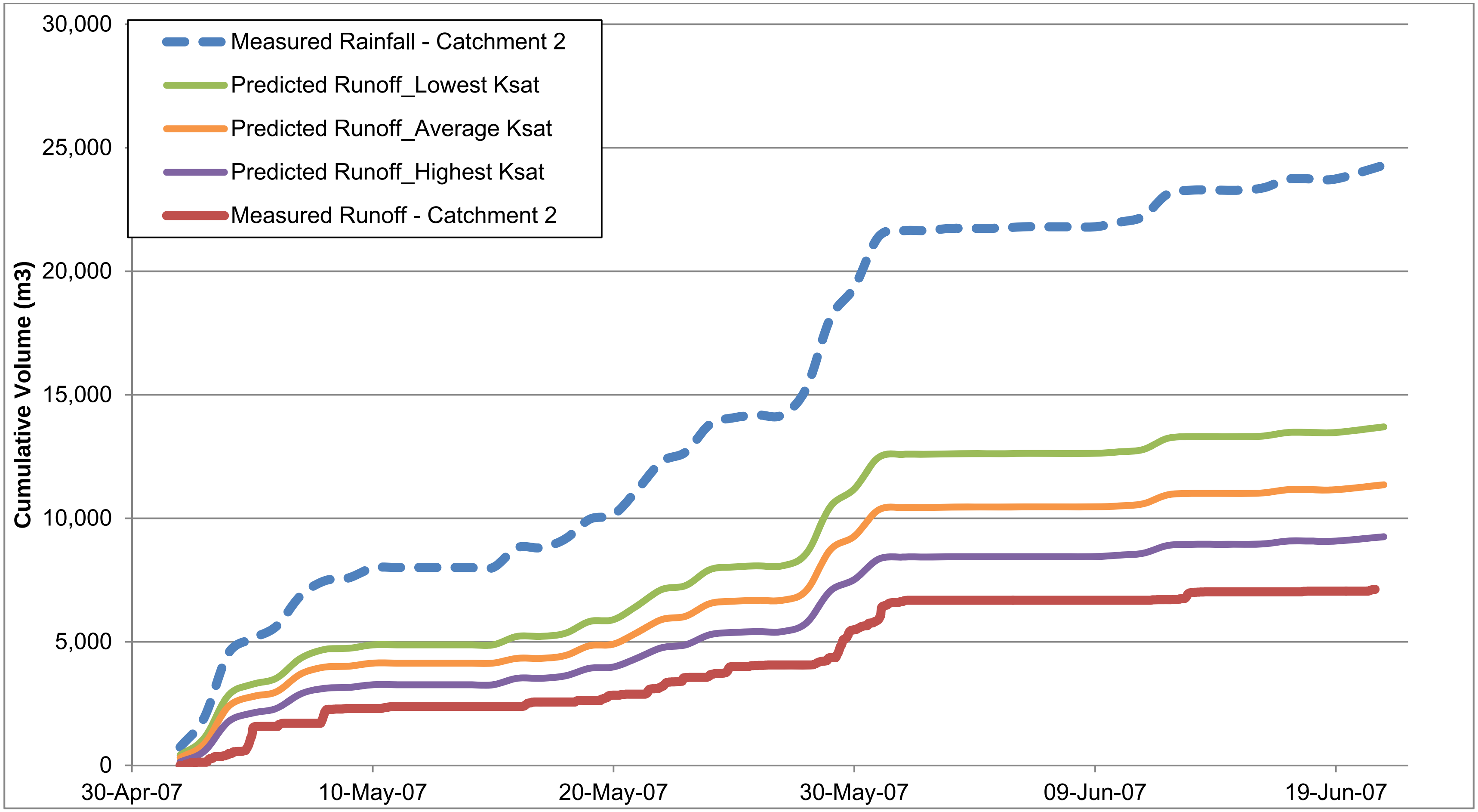

Figure 5-9: Comparison of measured rainfall and runoff to SoilCover predicted runoff using event-averaged rainfall intensity - B-Dump Catchment 2

Runoff was predicted using the lowest, average, and highest K_{sat} values measured for each material. With SoilCover, the best runoff prediction for Catchment 1 is achieved using the lowest measured K_{sat} value, as seen in Figure 5-8. By contrast, the best runoff prediction for Catchment 2 was achieved using the highest measured K_{sat} value, as seen in Figure 5-9. This pattern was also observed with the predictions using the SRR Model and is likely due to the slope of each catchment influencing the actual measured runoff (discussed in Section 5.3.1.1). The percent differences between predicted runoff using event-averaged rainfall intensity in SoilCover and measured runoff for Catchment 1 and 2 are shown in Table 5-7.

Table 5-7: Percent Difference between Final Cumulative Runoff Volume Predicted using SoilCover and Measured Runoff – Event-Averaged Rainfall Intensity

K_{sat} Range	% Difference (Final Cumulative Runoff Volume)	
	Catchment 1	Catchment 2
Lowest Measured	-9.06%	92.4%
Average	-26.9%	59.4%
Highest Measured	-42.6%	29.9%

The event-averaged intensity case must be examined in order compare the runoff predictions from the SRR Model and the SoilCover analyses. The results of the two models can be compared through Table 5-6 and Table 5-7. When the event-averaged rainfall intensity is used, SoilCover will generally produce more accurate runoff predictions compared to those from the SRR Model. However, it is interesting to note that measured runoff for Catchment 2 was within the bounds of runoff predictions using the SRR Model (Table 5-6), but the SoilCover analyses overpredicted runoff in all K_{sat} cases.

24-Hour Rainfall

The resolution of rainfall was adjusted and input over 24 hours in the second analysis case using SoilCover. The runoff predictions using the three K_{sat} cases are plotted along with measured rainfall and runoff for Catchments 1 and 2 in Figure 5-10 and Figure 5-11, respectively.

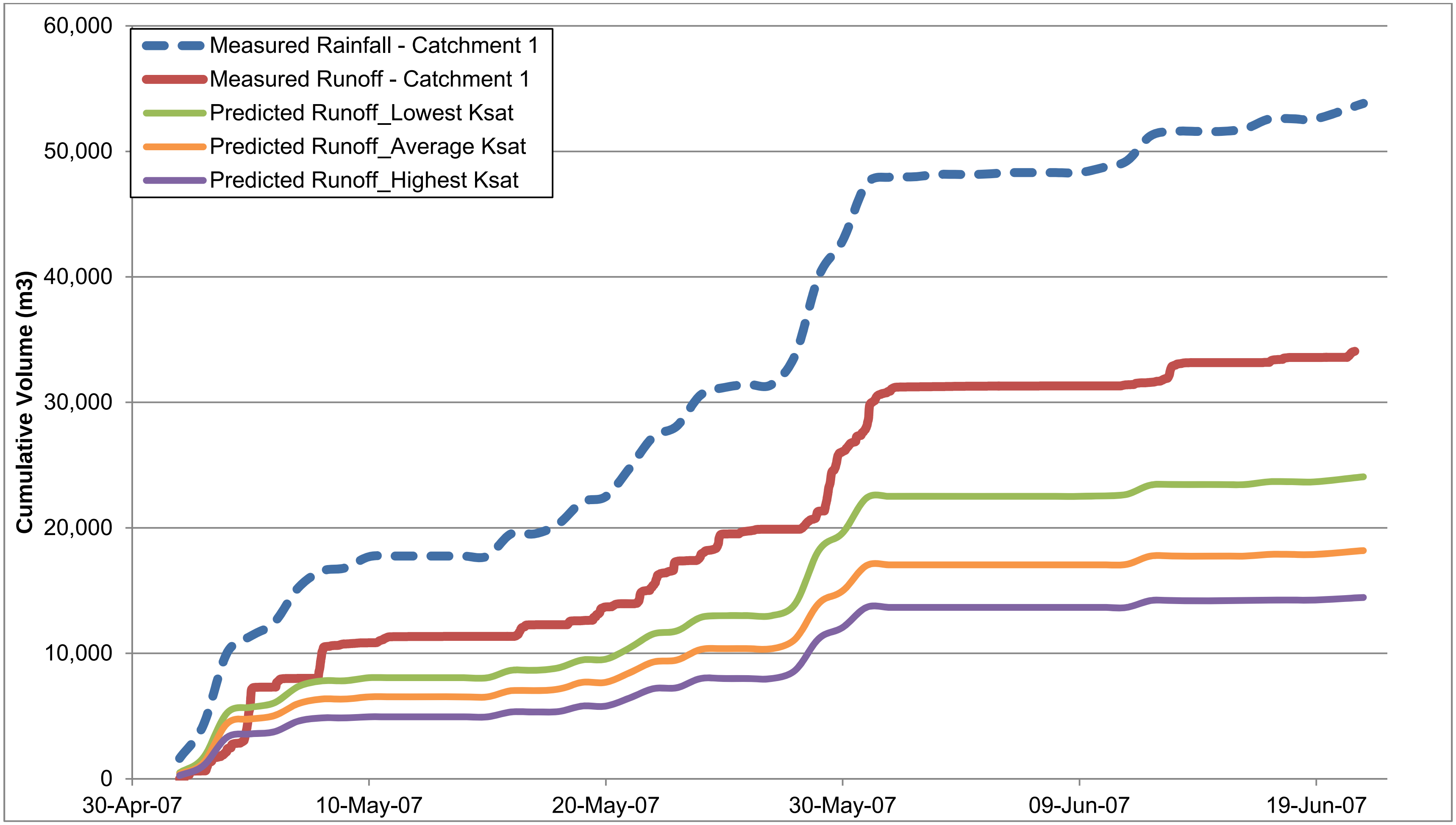

Figure 5-10: Comparison of measured rainfall and runoff to SoilCover predicted runoff using 24-hour rainfall - B-Dump Catchment 1

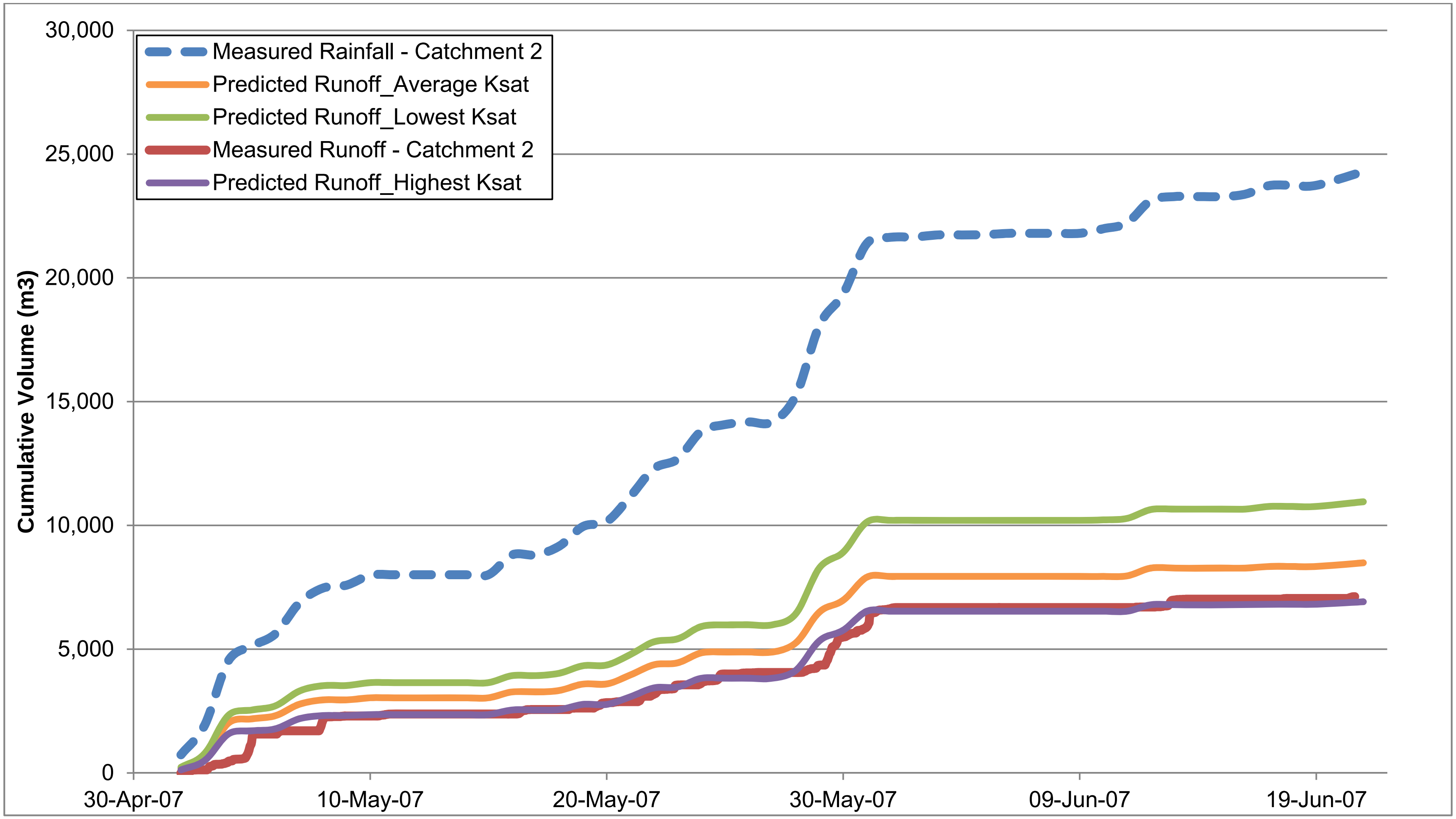

Figure 5-11: Comparison of measured rainfall and runoff to SoilCover predicted runoff using 24-hour rainfall - B-Dump Catchment 2

The percent differences between predicted runoff using a 24-hour rainfall simulation in SoilCover and measured runoff for Catchment 1 and 2 are shown in Table 5-8.

Table 5-8: Percent Difference between Final Cumulative Runoff Volume Predicted using SoilCover and Measured Runoff – 24 hour Rainfall

K_{sat} Range	% Difference (Final Cumulative Runoff Volume)	
	Catchment 1	**Catchment 2**
Lowest Measured	-29.4%	53.8%
Average	-46.6%	19.2%
Highest Measured	-57.6%	-2.90%

Figure 5-8 and Figure 5-10 show that using the event-averaged rainfall intensity improves the accuracy of SoilCover runoff predictions for Catchment 1. In both cases, the lowest measured K_{sat} provides the most accurate runoff prediction. Given that SoilCover is a one-dimensional model, the lower K_{sat} value is simulating a sloping surface within the model and is representative of Catchment 1, as previously discussed. SoilCover is more likely to calculate runoff from higher rainfall intensities, as noted in Section 5.2. The event-averaged intensity produces more accurate predictions in Catchment 1 than the 24-hour rainfall because of both the higher rainfall resolution (better simulating a natural event) and the fact that a sloping surface is a characteristic of Catchment 1.

On the other hand, the use of 24-hour rainfall in SoilCover predicts runoff with very good agreement in Catchment 2 (shown in Figure 5-11), compared to overprediction using the event-averaged rainfall intensity (shown in Figure 5-9). Similar to other modelled cases, the highest measured K_{sat} again produces the best runoff predictions for Catchment 2. As mentioned above, SoilCover calculates more runoff with higher rainfall intensities. Therefore, using a low resolution rainfall in a model makes sense for a surface that is relatively flat and not expected to produce as much surface runoff.

Overall, SoilCover provides the most accurate predictions of runoff when the input is adjusted based on both the expectations of runoff and the characteristics of the surface being modelled. As with the SRR Model, the accuracy of SoilCover runoff predictions can vary widely with both the resolution of rainfall and K_{sat} used as input. In contrast to the SRR Model, some notion of the expected runoff may be necessary in order to adjust the SoilCover input to achieve accurate runoff predictions. Previous results showed the best runoff predictions were achieved using a combination of 1) the highest resolution of rainfall data available and 2) the selection of K_{sat} that best represented the surface slope for a one-dimensional model. However, runoff from Catchment 2 was most accurately predicted by SoilCover using low resolution rainfall and the highest measured K_{sat} property. Given the previous results, this model input combination for Catchment 2 might only be selected based on expected runoff quantities. At the same time, very accurate runoff predictions could be achieved in this case if expected runoff was considered during the selection of model input.

5.3.2 Old Tailings Dam

High resolution rainfall-runoff measurements were not available for the OTD. Therefore, the rainfall data available from B-Dump was used in combination with the soil properties gathered from the OTD to produce runoff predictions. Both the SRR Model and SoilCover were used to produce runoff estimates for the OTD. The best estimate of runoff for the OTD is then selected based on the assessment of the most accurate runoff predictions from the various modelled cases from B-Dump.

The estimated runoff results are presented and compared within each OTD catchment in the sections below. The 15-minute and event-averaged rainfall intensity cases were modelled using the SRR Model. The event-averaged rainfall intensity and 24-hour rainfall cases were modelled using SoilCover. The lowest, average, and highest measured K_{sat} properties for the OTD materials were also modelled in each simulation.

5.3.2.1 OTD Catchment A – Combined Hardpan and Fine Tailings Surface

The final cumulative runoff volume estimated from Catchment A using both the SRR Model and SoilCover is provided in Table 5-9, along with the estimated runoff as a percent of measured rainfall, for all rainfall intensity and K_{sat} cases simulated. Runoff estimates for Catchment A using the SRR Model are shown in Figure 5-12 for both the 15-minute and event-averaged rainfall intensity cases. Estimates using SoilCover are provided in Figure 5-13 for the event-averaged and 24-hour rainfall cases. For both models, the runoff estimates using the higher resolution rainfall data are shown in solid lines and the lower rainfall resolution estimates are shown in dash-dotted lines for all three K_{sat} cases. For additional clarity, the legend provides the line order from top to bottom in the chart.

Table 5-9: Estimated Percent Runoff for OTD Catchment A

K_{sat} Range	Estimated Final Runoff Volumes (m^3) (Runoff as Percent of Measured Rainfall)			
	SRR Model		SoilCover	
	15-Min	Event-Averaged	Event-Averaged	24-Hour
Lowest Measured	592 (31%)	350 (19%)	448 (24%)	236 (13%)
Average	404 (22%)	169 (9.0%)	198 (11%)	83.2 (4.4%)
Highest Measured	210 (11%)	47.3 (2.5%)	31.9 (1.7%)	0.252 (0.01%)

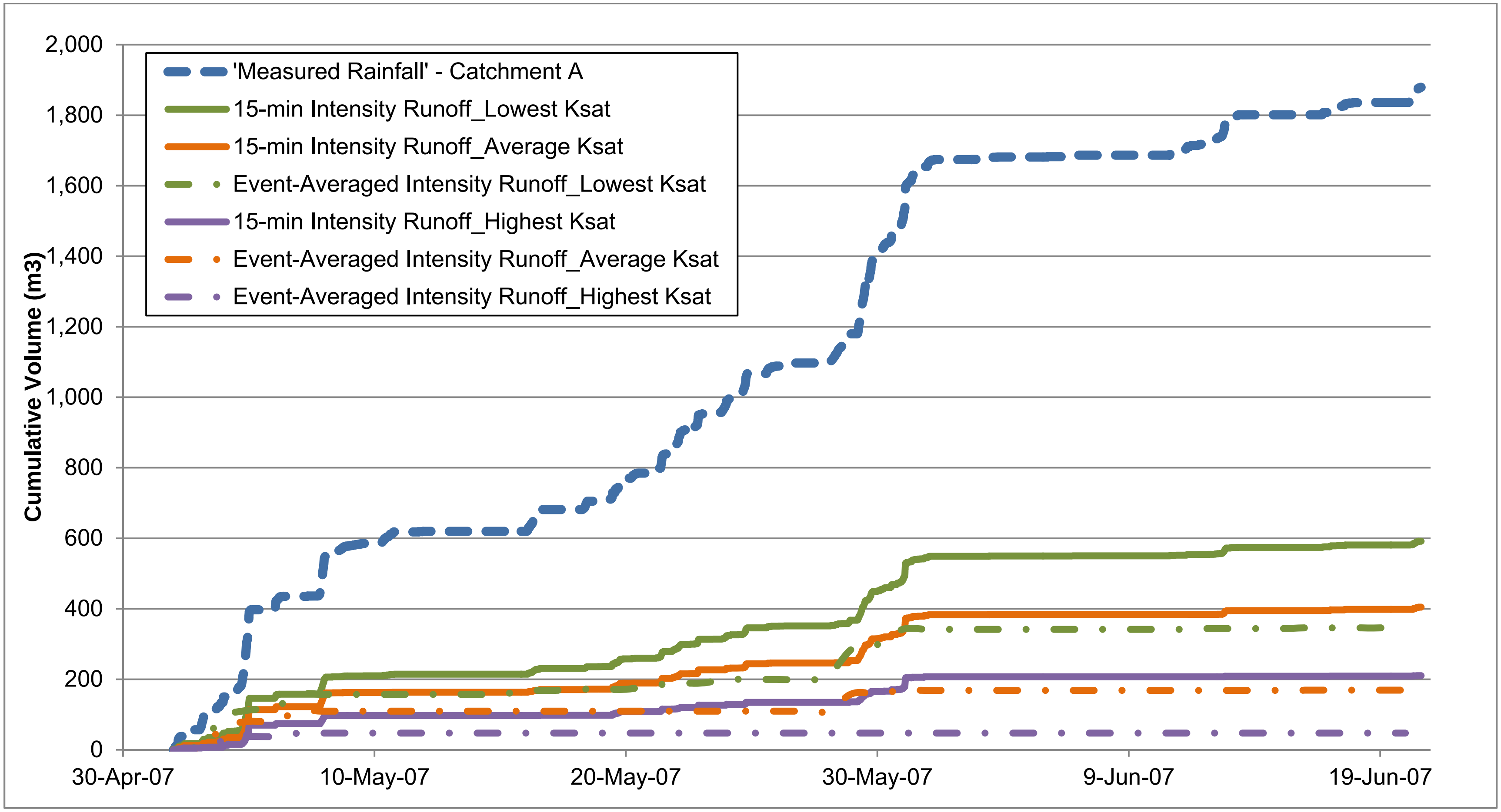

Figure 5-12: Comparison of 'measured rainfall' to SRR Model predicted runoff using 15-minute and event-averaged rainfall intensity-OTD Catchment A

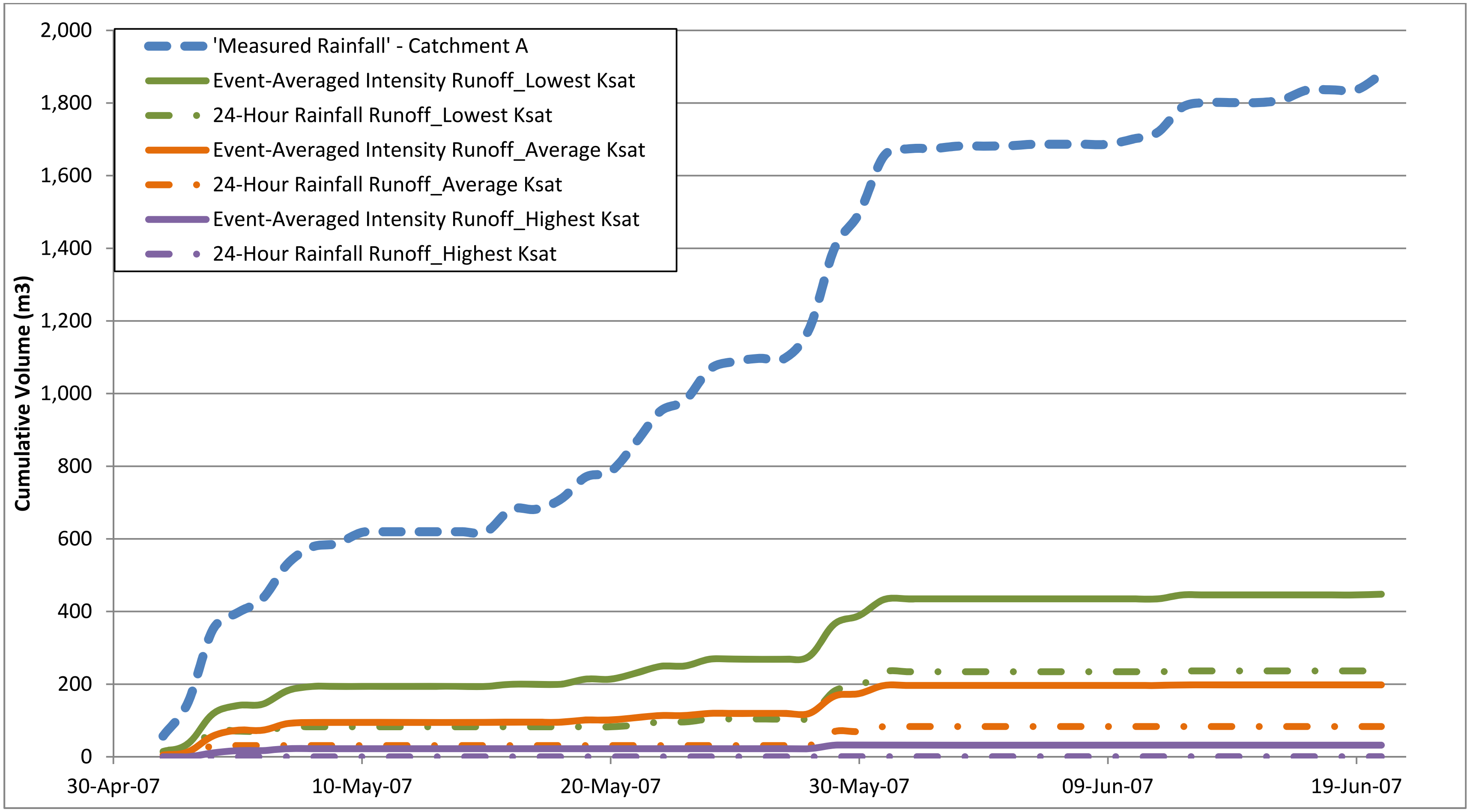

Figure 5-13: Comparison of ‘measured rainfall’ to SoilCover predicted runoff using event-averaged intensity and 24-hour rainfall - OTD Catchment A

As expected, the runoff estimates vary considerably between the two models, selected rainfall resolutions, and three K_{sat} cases. Without actual runoff measurements for comparison, the question becomes: which runoff estimate is reasonable, given the surface characteristics, expected runoff, and model limitations?

Using the results of the B-Dump analysis, the rainfall resolution and slope-K_{sat} interdependency should be considered when selecting an appropriate OTD runoff scenario. Catchment A has a relatively flat slope, similar to B-Dump Catchment 2. The best Catchment 2 runoff predictions were achieved with the 15-minute and high K_{sat} SRR Model; the event-averaged intensity and average K_{sat} SRR Model; and the 24-hour and high K_{sat} SoilCover model. If this comparison were to directly transfer to OTD Catchment A, then estimated runoff could be between 0.3 m^3 to 210 m^3, or up to 11% of measured rainfall.

Further analysis of the modelled data indicates that runoff is dominantly produced from the hardpan material, which covers approximately 50% of the surface of Catchment A. Greater than 98% of the runoff estimated by the SRR Model and greater than 89% of the runoff estimated by SoilCover was generated by the hardpan material. Given this observation, the estimated runoff quantities will be highly dependent on the surface area of the hardpan, which was partially obtained by interpreting photographs. Runoff predictions could be improved by surveying the hardpan material during a rainfall event when the surface runoff is clearly visible (recall Figure 3-17).

5.3.2.2 OTD Catchment B – Fine Tailings Surface

The final cumulative runoff volume estimated from Catchment B is provided in Table 5-10, along with the runoff as a percent of measured rainfall, for all rainfall intensity and K_{sat} cases simulated in both models. Runoff estimates for Catchment B using the SRR Model are shown in Figure 5-14 for both the 15-minute and event-averaged rainfall intensity cases. Estimates using SoilCover are provided in Figure 5-15 for the event-averaged and 24-hour rainfall cases. For both models, the runoff estimates using the higher resolution rainfall data are shown in solid lines and the lower rainfall resolution estimates are shown in dash-dotted lines for all three K_{sat} cases. For additional clarity, the legend provides the line order from top to bottom in the chart and the runoff estimates are shown relative to the right-hand secondary axis.

Table 5-10: Estimated Runoff Volumes for OTD Catchment B

K_{sat} Range	Estimated Final Runoff Volumes (m^3) (Runoff as Percent of Measured Rainfall)			
	SRR Model		SoilCover	
	15-Min	Event-Averaged	Event-Averaged	24-Hour
Lowest Measured	3.65 (0.7%)	0 (0%)	26.7 (4.9%)	2.42 (0.4%)
Average	0 (0%)	0 (0%)	0.729 (0.1%)	0 (0%)
Highest Measured	0 (0%)	0 (0%)	.002 (0%)	0 (0%)

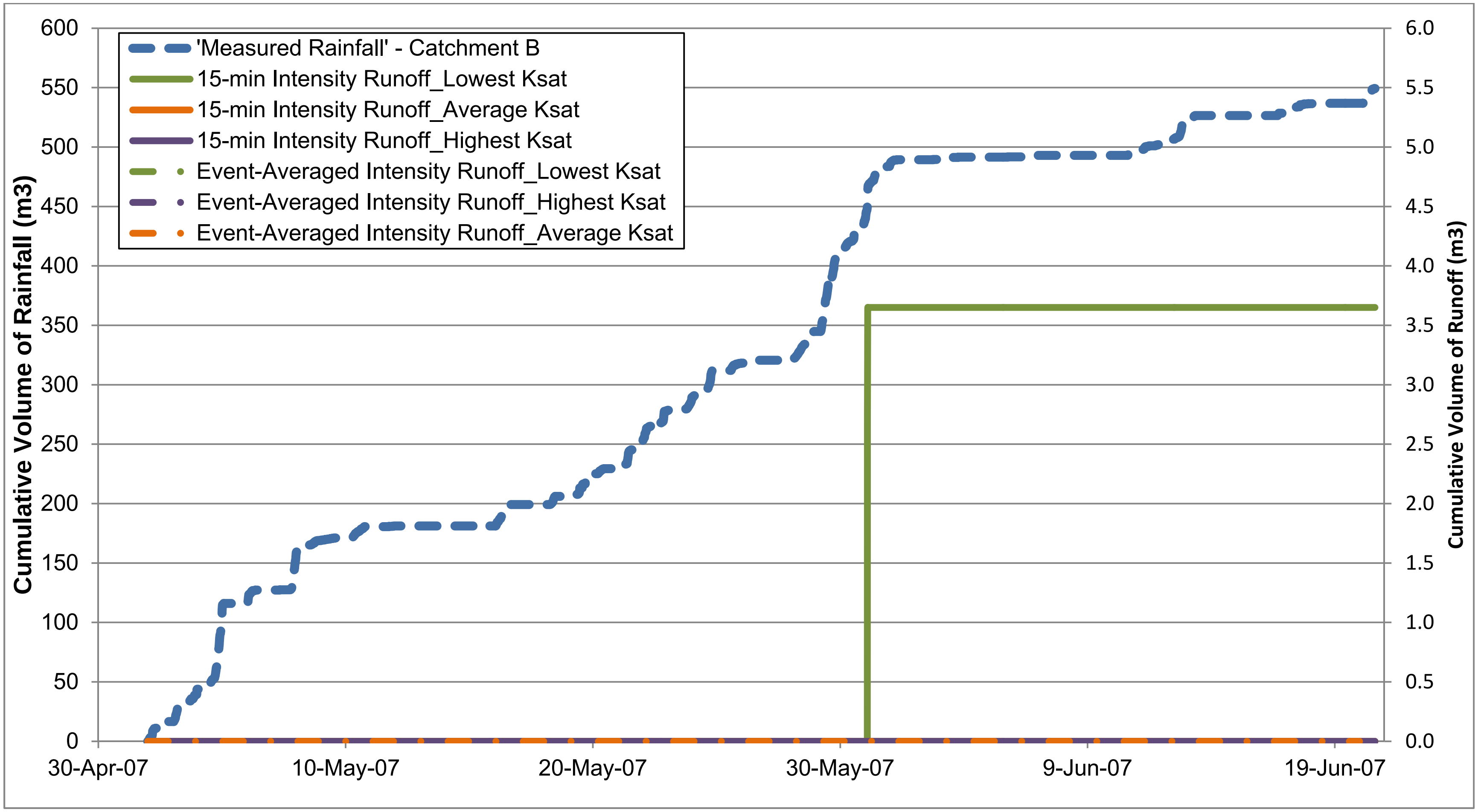

Figure 5-14: Comparison of 'measured rainfall' to SRR Model predicted runoff using 15-minute and event-averaged rainfall intensity-OTD Catchment B

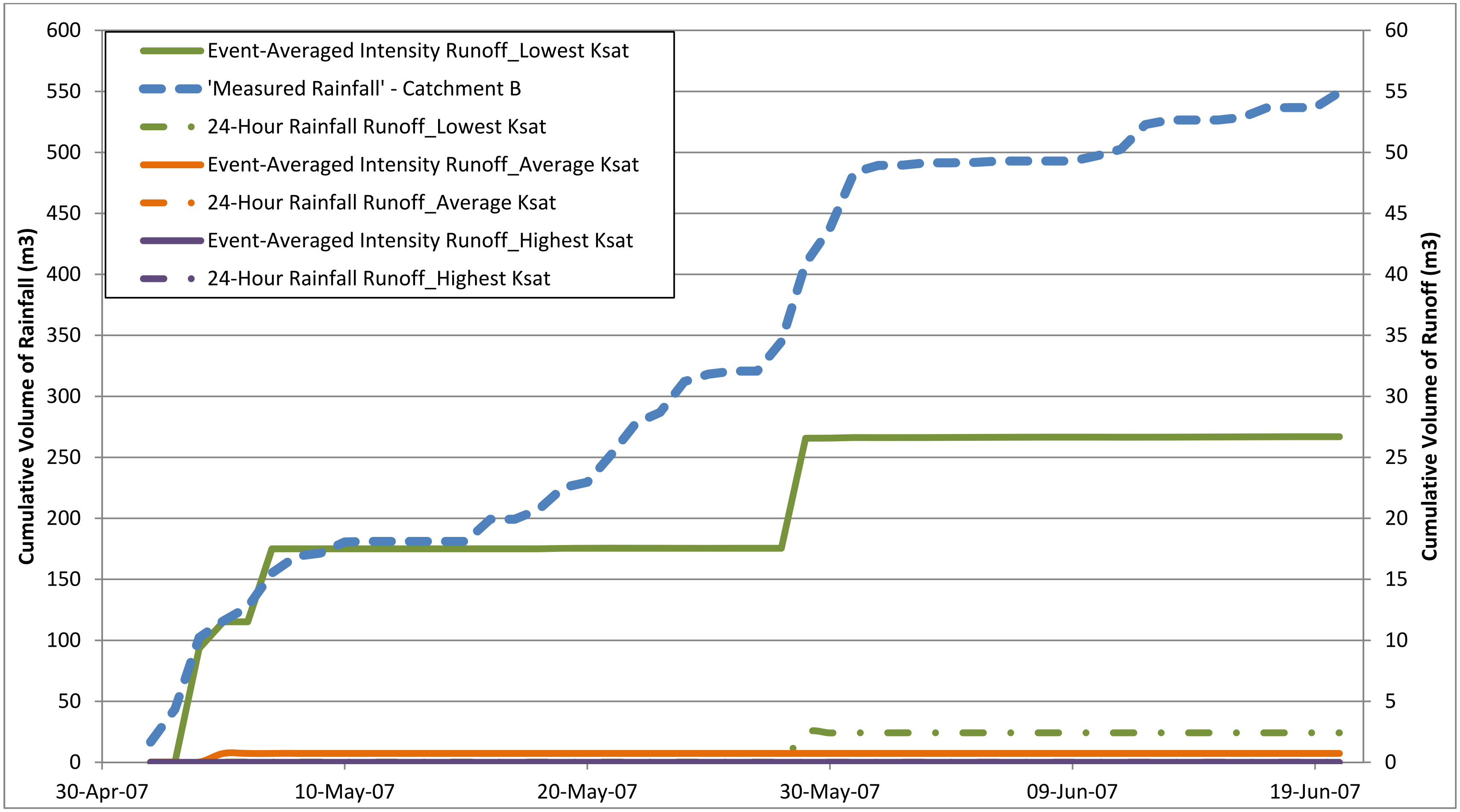

Figure 5-15: Comparison of 'measured rainfall' to SoilCover predicted runoff using event-averaged intensity and 24hour rainfall- OTD Catchment B

Catchment B consists of only fine tailings material, which was seen to contribute minimal volumes of runoff in the Catchment A analysis. Low runoff estimates were therefore expected from OTD Catchment B. Catchment B runoff estimates do vary between models, selected rainfall resolutions, and three K_{sat} cases; however not to the same degree as found from Catchment A.

Recall from Table 5-1 and Table 5-2 that the lowest, average, and highest K_{sat} for fine tailings was 4.9×10^{-6} m/s, 9.4×10^{-6}m/s and 1.8×10^{-5} m/s, respectively. Table 5-10 and Figure 5-14 show that the SRR Model predicts runoff in only the lowest measured K_{sat}, high resolution rainfall case. This runoff is produced over only one half-hour period where rainfall intensity exceeds the surface K_{sat} of the fine tailings. The SoilCover analyses, however, calculate some runoff in half the cases (shown in both Table 5-10 and Figure 5-15). The SoilCover analyses may be more appropriate for predicting runoff from high surface permeability low-slope surfaces, such as Catchment B. Factors such as moisture migration through the soil profile and fluxes at the soil-atmosphere boundary are a significant part of runoff calculations for high permeability surfaces, compared to low permeable and sloping surfaces, and these factors are not reflected by the SRR Model. This considered, the highest runoff volume predicted by SoilCover for Catchment B is only up to 4.8% of total rainfall. If the fine tailings in Catchment B were to be considered for an engineered soil cover, a runoff prediction between 0% and 5% of rainfall would likely be a suitable range for design.

Chapter 6. SUMMARY AND CONCLUSIONS

Net infiltration of water is a critical factor governing the design of an engineered soil cover. Surface runoff can be the single largest factor that immediately reduces the quantity of precipitation that may turn into infiltration. From the literature review, it was concluded that there did not appear to be any proven reliable procedure for predicting surface runoff based on measurable properties at the soil surface. In this thesis, two models were used to predict runoff using measured rainfall and soil properties and the predictions were compared to measured runoff volumes.

The surface of B-Dump at the Savage River Mine is capped with a compacted waste rock and overburden soil cover. Corresponding rainfall and runoff was recorded at 15-minute intervals from May 2 to June 20, 2007, for the two main B-Dump catchments. Measurements from Catchment 1 showed that up to 63% of rainfall was converted into runoff. Catchment 2 measurements showed that up to 29% rainfall was converted into runoff. The research objective was to develop a model that could predict the measured rainfall-runoff response based on measured properties of the soil cover surface. The objective was accomplished by 1) conducting a field and laboratory investigation to characterize the hydraulic properties of the materials comprising the B-Dump soil cover, and 2) developing a proposed model and utilizing existing SoilCover software to predict runoff based on the field and laboratory measurements and measured rainfall data. The discrepancy between runoff measurements on the two B-Dump catchments formed the basis of comparison for runoff predictions using the two models.

The field program identified and mapped the areal extent of four different materials making up the B-Dump soil cover. The materials were characterized by: i) conducting double ring infiltrometer tests to gain the saturated hydraulic conductivity of the surface (K_{sat}); ii) water-replacement in-situ density tests; iii) soil temperature and suction measurements; and iv) collecting samples for laboratory testing. The laboratory program included USCS soil classification, specific gravity testing, and soil-water characteristic curve tests.

The measured rainfall data was used in conjunction with field and laboratory properties of the B-Dump soil cover to predict runoff using two different one-dimensional models, as follows:

1. The proposed SRR Model - used rainfall intensity and the saturated hydraulic conductivity (K_{sat}) of the soil cover surface, and
2. SoilCover software – used basic site climate data and detailed soil hydraulic properties

Resulting runoff predictions from the two models were compared to each other and the measured rainfall runoff response. For both models, the accuracy of runoff predictions varied widely with the resolution of rainfall data used as input. Runoff predictions also varied within the natural range of measured K_{sat} values. Depending on the selected rainfall resolution and K_{sat} scenario, the accuracy of runoff predictions from the SRR Model varied between 3.4% to -84% for Catchment 1 and between 115% to -64% for Catchment 2. Similarly, the accuracy of runoff predictions using the SoilCover model varied between -9.1% to -58% for Catchment 1 and between 92% and -2.9% for Catchment 2, depending on the rainfall resolution and K_{sat} selected.

Results showed the best runoff predictions were achieved using a combination of 1) the highest resolution of rainfall data available and 2) the selection of K_{sat} that best represented the surface slope for input into a one-dimensional model. It was found that if model input was selected based on the catchment slope characteristics, runoff predictions could be significantly improved from both models, even with lower resolution rainfall data. The range of accuracy of runoff predictions for Catchment 1 was reduced to between 3.4% to -31% for the SRR Model and to between -9.1% to -29% for the SoilCover model when the lowest measured K_{sat} for each material was used. The range of accuracy of runoff predictions for Catchment 2 was reduced to between 4.3% to -64% for the SRR Model and to between 30% to -2.9% for the SoilCover model when the highest measured K_{sat} for each material was used. The best possible runoff predictions (between 3.4% to -9.1% for the SRR Model and between 4.3% to -2.9% for the SoilCover model) also required the use of high resolution rainfall data. Using the lowest and highest measured K_{sat} values in the one-dimensional models effectively simulated the slope of Catchment 1 (which ranged between 3.5% to 8.8%) and Catchment 2 (which ranged between 0% to 4.0%), respectively.

The SRR Model is capable of predicting runoff within 4% using only rainfall intensities and measured K_{sat} properties at the surface. However, for the SoilCover model, some notion of the expected runoff may be necessary in order to adjust the SoilCover input to achieve the most accurate runoff predictions. Runoff predicted by SoilCover was within 3% of measured runoff when the low resolution – high K_{sat} case for Catchment 2 was selected. Given that high resolution rainfall generally produced the best predictions, this particular modelling scenario would only be selected if expected runoff quantities were considered during the selection of input.

The need for runoff models that do not need to be calibrated to produce results that match field observations was identified in the literature review. However, only limited success had recently been achieved using an uncalibrated model to predict runoff. Given the results of this research, very good agreement between predicted and measured runoff can be achieved using measurable soil properties and rainfall intensities in both the SRR Model and SoilCover software. Both models used in this research are one-dimensional and it was found that better agreement between predicted and measured runoff could be achieved by adjusting the K_{sat} input to simulate a slope (or no slope). To some, this could be considered “calibration” of the model. However, the K_{sat} factor was adjusted only within the range of actual measured values. Additionally, the adjustment was consistent with the physical runoff and infiltration mechanisms and considered the limitation of simulating actual slope characteristics in a one-dimensional model. Runoff generation in reality is a four-dimensional process (X, Y, Z, time), so achieving runoff predictions within 4% of measured runoff from physically representative one-dimensional simulations is considered a great success for soil cover models.

The SRR Model developed during this research has shown that very good agreement can be achieved between predicted and measured runoff using minimal measured soil data and rainfall intensity as input. The model was proven for the B-Dump soil cover, which is predominately non-vegetated and its surface is smooth and compact with little variation in the micro-topography. The following are recommendations to verify the applicability of the SRR Model in other soil cover modelling scenarios:

1. The basis for the SRR Model is that the immediate soil surface will be saturated during periods of surface runoff generation, thus K_{sat} is the only soil property required for input. The study of soil covers of various size, material composition, and surface characteristics in a variety of climatic conditions would improve confidence in the inherent assumption of SRR Model that the inclusion of antecedent and subsurface soil characteristics is not necessary for accurate runoff prediction.
2. The analysis on the high permeability OTD material predicted very limited runoff. Although this result was consistent with expectations, the estimates could not be compared with actual measurements of runoff. The SRR Model should be verified using corresponding rainfall and runoff measurements from a soil cover with generally higher surface K_{sat}, such as a “store-and-release” cover system.
3. Further investigation into the applicability of the SRR Model on soil covers with varying slopes could be performed. This would provide additional confidence in the engineering judgment used if adjusting measured soil properties to better simulate a slope in the one-dimensional model.
4. The SRR Model was shown to be highly sensitive to the rainfall intensity used as input. A detailed sensitivity analysis is recommended to determine the variation of modelled runoff accuracy with levels of rainfall resolution. The result of this analysis could then be combined with the economics of data collection and interpretation to provide suggestions for reasonable rainfall data collection increments.

REFERENCES

ABM. 2006. SRRP B-dump water shedding cover construction report. Australian Bulk Minerals, Tasmania, AUS.

Albright, W.H., Benson, C.H., and Apiwantragoon, P. 2012. Field hydrology of landfill final covers with composite barrier layers (accepted manuscript), Journal of Geotechnical and Geoenvironmental Engineering, .

Albright, W.H., Benson, C.H., Gee, G.W., Abichou, T., McDonald, E.V., Tyler, S.W., and Rock, S.A. 2006. Field performance of a compacted clay landfill final cover at a humid site, Journal of Geotechnical and Geoenvironmental Engineering, **132**(11): 1393-1403.

Albright, W.H., Benson, C.H., Gee, G.W., Roesler, A.C., Abichou, T., Apiwantragoon, P., Lyles, B.F., and Rock, S.A. 2004. Field water balance of landfill final covers, Journal of Environmental Quality, **33**(6): 2317-2332.

ASTM. 2011. D2487-11: Standard practice for classification of soils for engineering purposes (unified soil classification system). ASTM International, USA.

ASTM. 2010a. D4318-10: Standard test methods liquid limit, plastic limit, and plasticity index of soils. ASTM International, USA.

ASTM. 2010b. D854-10: Standard test methods for specific gravity of soil solids by water pycnometer. ASTM International, USA.

ASTM. 2009a. D3385-09: Standard test method for infiltration rate of soils in field using double-ring infiltrometer. ASTM International, USA.

ASTM. 2009b. D6913-04: Standard test methods for particle-size distribution (gradation) of soils using sieve analysis. ASTM International, USA.

ASTM. 2007a. D422-63: Standard test method for particle-size analysis of soils. ASTM International, USA.

ASTM. 2007b. C127-07: Standard test method for density, relative density (specific gravity), and absorption of coarse aggregate. ASTM International, USA.

ASTM. 2004. D5030-04: Standard test method for density of soil and rock in place by the water replacement method in a test pit. ASTM International, USA.

Benson, C.H. 2010. Prediction in geoenvironmental engineering: Recommendations for reliable predictive modeling. *In* GeoFlorida 2010: Advances in Analysis, Modeling and Design, Reston, VA, USA., pp. 1-14.

Benson, C.H., Sawangsuriya, A., Trzebiatowski, B., and Albright, W.H. 2007. Postconstruction changes in the hydraulic properties of water balance cover soils, Journal of Geotechnical and Geoenvironmental Engineering, **133**(4): 349-359.

Benson, C.H., Bohnhoff, G.L., Ogorzalek, A.S., Shackelford, C.D., Apiwantragoon, P., and Albright, W.H. 2005. Field data and model predictions for a monolithic alternative cover. *In* Geo-Frontiers, pp. 3569-3584.

Benson, C.H., Bohnhoff, G.L., Apiwantragoon, P., Ogorzalek, A.S., Shackelford, C.D., and Albright, W.H. 2004. Comparison of model predictions and field data for an ET cover, Proceedings, Tailings and Mine Waste '04, : 137-142.

Beven, K.J. 2012. Rainfall-runoff modelling: The primer (2nd. ed). Jon Wiley & Sons Ltd., Oxford, UK.

Bohnhoff, G.L., Ogorzalek, A.S., Benson, C.H., Shackelford, C.D., and Apiwantragoon, P. 2009. Field data and water-balance predictions for a monolithic cover in a semiarid climate, Journal of Geotechnical and Geoenvironmental Engineering, **135**(3): 333-348.

Bronstert, A. and Bardossy, A. 2003. Uncertainty of runoff modelling at the hillslope scale due to temporal variations of rainfall intensity, Physics and Chemistry of the Earth, **28**: 283-288.

Commonwealth of Australia, Bureau of Meteorology (BOM). 2012. Climate data online - savage river mine [online]. Available from http://www.bom.gov.au/climate/data/index.shtml [cited 07/17 2012].

de Vries, D.A. 1963. Thermal properties of soils. *In* Physics of Plant Environment *Edited by* W.R. Van Wihk. North Holland Pub. Co., Amsterdam, pp. 210-235.

Dunne, T. and Black, R.D. 1970. An experimental investigation of runoff production in permeable soils, Water Resources Research, **6**(2): 478-490.

Dunne, T., Zhang, W., and Aubry, B.F. 1991. Effects of rainfall, vegetation, and microtopography on infiltration and runoff, Water Resources Research, **27**(9): 2271-2285.

Fayer, M.J., Rockhold, M.L., and Campbell, M.D. 1992. Hydrologic modeling of protective barriers: Comparison of field data and simulation results, Soil Science Society of America Journal, **56**(3): 690-700.

Fredlund, D.G. and Wilson, G.W. 2006. Are we doing it right? Geotechnical News, (March): 43-48.

Fredlund, D.G. and Xing, A. 1994. Equations for the soil-water characteristic curve, Canadian Geotechnical Journal, **31**(4): 521-532.

Fredlund, D.G. and Rahardjo, H. 1993. Soil mechanics for unsaturated soils. John Wiley & Sons Inc., USA.

Fredlund, D.G., Xing, A., and Huang, S. 1994. Predicting the permeability function for unsaturated soils using the soil-water characteristic curve, Canadian Geotechnical Journal, **31**(4): 533-546.

GHD. 2009. Report for B-dump cap: Report on flow monitoring. Rev 1, January 2009, Australian Bulk Minerals, Hobart, AUS.

Grange Resources. 2012a. Savage river - location [online]. Available from http://www.grangeresources.com.au/php/page.php?grangeS+11 [cited 05/28 2012].

Grange Resources. 2012b. Savage river - environment [online]. Available from http://www.grangeresources.com.au/php/page.php?grangeS+14 [cited 05/28 2012].

Grange Resources. 2012c. ASX release. 29 February 2012, Grange Resources Limited, Australia.

Hawkins, R.H. 1982. Interpretations of source area variability in rainfall-runoff relations. *In* Rainfall-Runoff Relationship *Edited by* V.P. Singh. Water Resources Publications, Littleton, CO, pp. 303-324.

Hearman, A.J. and Hinz, C. 2007. Sensitivity of point scale surface runoff predictions to rainfall resolution, Hydrology and Earth System Sciences, **11**(2): 965-982.

Hewlett, J.D. and Hibbert, A.R. 1967. Factors affecting the response of small watersheds to precipitation in humid areas. *In* Forest Hydrology *Edited by* W.E. Sopper and H.W. Lull. Pergamon Press, New York, pp. 275-290.

Hopp, L., McDonnell, J.J., and Condon, P. 2011. Lateral subsurface flow in a soil cover over waste rock in a humid temperate environment, Vadose Zone Journal, **10**(1): 332-344.

Horton, R.E. 1940. An approach toward a physical interpretation of infiltration capacity, Soil Science Society of America Proceedings, **5**: 399-417.

Horton, R.E. 1933. The role of infiltration in the hydrologic cycle, Transactions of the American Geophysical Union, **14**: 445-460.

Hursh, C.R. 1944. Appendix B - report of sub-committee on subsurface-flow, Transactions of the American Geophysical Union, **25**: 743-746.

Hutchison, B. 2012. OTD runoff trial bunding. Grange Resources, Burnie, AUS.

Janeau, J.L., Mauchamp, A., and Tarin, G. 1999. The soil surface characteristics of vegetation stripes in northern mexico and their influences on the system hydrodynamics. an experimental approach, Catena, **37**(1-2): 165-173.

Langhans, C., Govers, G., Diels, J., Leys, A., Clymans, W., Van den Putte, A., and Valckx, J. 2011. Experimental rainfall-runoff data: Reconsidering the concept of infiltration capacity, Journal of Hydrology, **399**(3-4): 255-262.

Loague, K.M. 1988. Impact of rainfall and soil hydraulic property information on runoff predictions at the hillslope scale, Water Resources Research, **24**(9): 1501-1510.

Mein, R.G. and Larson, C.L. 1973. Modeling infiltration during a steady rain, Water Resources Research, **9**(2): 384-394.

Miller, C.J., Yesiller, N., Yaldo, K., and Merayyan, S. 2002. Impact of soil type and compaction conditions on soil water characteristic, Journal of Geotechnical and Geoenvironmental Engineering, **128**(9): 733-742.

Miskolczi, J. 2007. Performance evaluation of cover systems constructed of paste rock material. M.Sc., University of British Columbia, Canada.

Ogorzalek, A.S., Bohnhoff, G.L., Shackelford, C.D., Benson, C.H., and Apiwantragoon, P. 2008. Comparison of field data and water-balance predictions for a capillary barrier cover, Journal of Geotechnical and Geoenvironmental Engineering, **134**(4): 470-486.

O'Kane, M. and Wels, C. 2003. Mine waste cover system design - linking predicted performance to groundwater and surface water impacts. *In* Sixth International Conference on Acid Rock Drainage, Cairns, QLD, pp. 341-349.

Philip, J.R. 1957. The theory of infiltration: 1. the infiltration equation and its solution. Soil Science, **83**: 345-357.

Rahardjo, H., Lee, T.T., Leong, E.C., and Rezaur, R.B. 2005. Response of a residual soil slope to rainfall, Canadian Geotechnical Journal, **42**(2): 340-351.

Roesler, A.C., Benson, C.H., and Albright, W.H. 2002. Field hydrology and model predictions for final covers in the alternative assessment program. Geo Engineering Report No. 02-08, University of Wisconsin-Madison, USA.

Sajid, A. 2009. Investigation of rainfall-runoff process in relation to soil physical and hydraulic properties. Ph.D., University of Guelph, Canada.

Scanlon, B.R., Reedy, R.C., Keese, K.E., and Dwyer, S.F. 2005. Evaluation of evapotranspirative covers for waste containment in arid and semiarid regions of southwestern USA, Vadose Zone Journal, **4**: 55-71.

Scanlon, B.R., Christman, M., Reedy, R.C., Porro, I., Simunek, J., and Flerchinger, G.N. 2002. Intercode comparisons for simulating water balance of surficial sediments in semiarid regions, Water Resources Research, **38**(12): 1323-1339.

Scherrer, S. and Naef, F. 2003. A decision scheme to indicate dominant hydrological flow processes on temperate grassland, Hydrological Processes, **17**(2): 391-401.

Scherrer, S., Naef, F., Faeh, A.O., and Cordery, I. 2007. Formation of runoff at the hillslope scale during intense precipitation, Hydrology and Earth System Sciences, **11**(2): 907-922.

Schmocker-Fackel, P., Naef, F., and Scherrer, S. 2007. Identifying runoff processes on the plot and catchment scale, Hydrology and Earth System Sciences, **11**: 891-906.

Sherman, L.K. 1932. The relation of hydrographs of runoff to size and character of drainage basins. Transactions of the American Geophysical Union, **13**: 332-339.

Smith, R.E. 2002. Infiltration theory for hydrologic applications. American Geophysical Union, Washington, DC.

Soilmoisture. 2010. Operating instructions: Model 2800K1 guelph permeameter. Soilmoisture Equipment Corp., Santa Barbara, USA.

SoilVision. 2010. SV office 2009. SoilVision Systems Ltd., .

SRK Consulting. 2010. Savage river - old tailings dam phase I investigations: Geochemical assessment of near-surface tailings. DEP002, Department of Environment, Parks, Heritage and Arts, Sydney, AUS.

Stone, J., Renard, K.G., and Lane, L.J. 1996. Runoff estimation on agricultural fields. *In* Soil erosion, conservation, and rehabilitation *Edited by* M. Agassi. Marcel Dekker Inc., New York, pp. 203-238.

Stone, J.J., Paige, G.B., and Hawkins, R.H. 2008. Rainfall intensity-dependent infiltration rates on rangeland rainfall simulator plots, Transactions of the ASABE, **51**(1): 45-53.

Stothoff, S.A. 1997. Sensitivity of long-term bare soil infiltration simulations to hydraulic properties in an arid environment, Water Resources Research, **33**(4): 547-558.

Swanson, D.A., Barbour, S.L., Wilson, G.W., and O'Kane, M. 2003. Soil-atmosphere modelling of an engineered soil cover for acid generating mine waste in a humid, alpine climate, Canadian Geotechnical Journal, **40**(2): 276-292.

The International Network for Acid Prevention (INAP). 2009. Global acid rock drainage guide (GARD guide) [online]. Available from http://www.gardguide.com/ [cited 07 2012].

Thompson and Brett Pty Ltd. 2002. Preliminary report on B-dump capping. Australian Bulk Minerals, Australia.

UMS. 2009. User manual for T5/T5x pressure transducer tensiometer. UMS-GmbH, Munich.

Unsaturated Soils Group. 2000. SoilCover. Department of Civil Engineering, University of Saskatchewan, Saskatoon, SK, Canada.

USDA. 2004. Chapter 10 - estimation of direct runoff from storm rainfall. Part 630 Hydrology, National Engineering Handbook, Natural Resources Conservation Service.

Wainwright, J. and Parsons, A.J. 2002. The effect of temporal variations in rainfall on scale dependency in runoff coefficients, Water Resources Research, **38**(12): 1271-1281.

Weiler, M. 2011. Field-based observation of hydrological processes . *In* Treatise on Water Science *Edited by* P. Wilderer. Elsevier, Oxford, pp. 339-350.

Weyman, D.R. 1970. Throughflow on hillslopes and its relation to the stream hydrograph, Bulletin of the International Association of Scientific Hydrology, XV, **2**(6): 25-33.

Wilson, G.W. 2006. The application of cover systems for mine closure - are we doing it right? *In* First International Seminar on Mine Closure, Perth, Australia, pp. 31-42.

Wilson, G.W., Miskolczi, J., Dagenais, A., Levesque, I., Smith, Q., Lanteigne, L., Hulett, L., and Landriault, D. 2006. The application fo blended waste rock and tailings for cover systems in mine waste management. *In* Seventh International Conference on Acid Rock Drainage, St. Louis, US., pp. 2424-2438.

Yin, J. 2008. Spatiotemporal variation in soil moisture and hydraulic properties and their impacts on rainfall-runoff and infiltration processes. Ph.D., University of Nevada, United States.

Zhan, T.L.T., Ng, C.W.W., and Fredlund, D.G. 2007. Field study of rainfall infiltration into a grassed unsaturated expansive soil slope, Canadian Geotechnical Journal, **44**(4): 392-408.

APPENDIX – DATA CD

Files Included in Appendix – Data CD

Field Program (Folder)

- Double-Ring Infiltrometer_RAW DATA (Excel Spreadsheet)
- Field Density, Moisture, Suction (Excel Spreadsheet)
- Guelph Permeameter_SUMMARY_Final Rate (Excel Spreadsheet)
- *Infiltrometer Area Correction (Folder)*
    - BD1-C-3_Inner Correction (AutoCAD Drawing)
    - BD2-C-2_Waste Rock_UofA Outer Correction (AutoCAD Drawing)
    - BD2-C-3_Coarse_SRM Outer Correction (AutoCAD Drawing)
    - BD2-C-4_Coarse_SRM Outer Correction (AutoCAD Drawing)

Laboratory (Folder)

- Particle Size Analyses (Excel Spreadsheet)
- Soil-Water Characteristic Curves_RAW DATA (Excel Spreadsheet)
- Specific Gravity (Excel Spreadsheet)

Model (Folder)

- Catchment and Material Areas (Excel Spreadsheet)
- B-Dump 29 march to 20 June 07_ORIGINAL (Excel Spreadsheet)
- Runoff Data_AMENDED (Excel Spreadsheet)
- SRR Model (Excel Spreadsheet)
- *SoilCover (Folder)*
    - *Event-Averaged (Folder)*

      Contains event-averaged rainfall SoilCover ".XLP" files for BDump. Three files per material for lowest measured, average, and highest measured K_{sat}.
    - *24-Hour (Folder)*

      Contains 24-hour rainfall SoilCover ".XLP" files for BDump. Three files per material for lowest measured, average, and highest measured K_{sat}.